UNIVERSITY OF CALIFORNIA,
IRVINE

Circadian Amplification of Alpha Factors, Energy Intensity and Indirect Greenhouse Gas Emissions in Aerated Processes for Water Resource Recovery Facilities

DISSERTATION

submitted in partial satisfaction of the requirements
for the degree of

DOCTOR OF PHILOSOPHY

in Civil Engineering

by

Nasir Emami

Dissertation Committee:
Professor Diego Rosso, Chair
Professor Soroosh Sorooshian
Professor Sunny C. Jiang

2018

DEDICATION

To

my family and Professor Rosso who their constant encouragement kept me on track

and

the anonymous taxi driver in southern Iran who inspired me to strive for the excellence for the betterment of humanity

The highest goal in life is to inquire and to create; to search the riches of the past; … carry the quest … help people how to learn on their own; it's you the learner; it's up to you what you will master.

Noam Chomsky

TABLE OF CONTENTS

LIST OF FIGURES

LIST OF TABLES

ACKNOWLEDGMENTS

I would like to acknowledge with gratitude, the support and love of my parents, Sedigheh and Masoud; my brothers, Nima and Kaveh and my fiancée, Maryam. They all kept me going with their constant encouragement.

I am especially grateful to my advisor as well as committee chair, Professor Diego Rosso. I am forever indebted to him for his enthusiasm, guidance, and unremitting support throughout this research.

A special word of gratitude is due to Professor Soroosh Sorooshian and Professor Sunny Jiang who served as both my dissertation and candidacy committee members, offering their support, insight, and commitment.

I would like to acknowledge Professor Brett Sanders, Dr. Reza Sobhani, and Dr. Manel Garrido-Baserba who helped me in my research Projects.

Lastly, I thank the City of Los Angeles, Bureau of Sanitation (LASAN). This dissertation would not have been possible without the financial support provided by LASAN.

CURRICULUM VITAE

Nasir Emami

1995	B.S. in Chemical Engineering, Sistan & Baluchestan University, Iran
2001-04	CH2M HILL, Southern California Office, USA Staff Process Engineer (Water and Wastewater Processes)
2004-06	City of Los Angeles, Bureau of Sanitation, Watershed Protection Division
2006	M.S. in Engineering, Department of Chemical Engineering, California State University, Long Beach
2006-14	City of Los Angeles, Bureau of Sanitation, Wastewater Engineering Services Division
2014-18	City of Los Angeles, Bureau of Sanitation, Hyperion Water Reclamation Plant
2010–18	Graduate Student Researcher (PIs: B. Sanders; D. Rosso), Department of Civil and Environmental Engineering, University of California, Irvine
2018	Ph.D. in Civil Engineering with an emphasis in Hydrology/Water Resources, University of California, Irvine

FIELD OF STUDY

Energy footprint and greenhouse gas emissions in water resource recovery facilities

PUBLICATIONS

Diurnal Variations of the Energy Intensity and Associated Greenhouse Gas Emissions for Activated Sludge Processes, **Nasir Emami**, Reza Sobhani, Diego Rosso. *Water Science and Technology* (in press).

WE&RF Carbon Capture and Management Strategies: Role of Extracellular Polymeric Substances (EPS) on Oxygen Transfer and Secondary Settling, Manel Garrido-Baserba, **Nasir Emami**, José Jimenez, Haydee De Clippeleir, Ahmed Al-Omari, Diego Rosso. Abstract was submitted to Water Environment Federation Technical Exhibition and Conference (WEFTEC) 2018 Annual Conference.

Effects of Flow Equalization on BNR's Energy and Carbon Footprint, **Nasir Emami**, Roshanak Aflaki, David Bianchi, Reza Sobhani, and Diego Rosso. California Water Environment Association (CWEA) Annual Conference, Santa Clara, CA, April 2016.

Circadian Amplification of Energy Consumption, its Associated Costs, and GHG Emissions in Aeration Processes, **Nasir Emami**, Reza Sobhani, and Diego Rosso. Water Environment Federation Technical Exhibition and Conference (WEFTEC) Annual Conference, New Orleans, LA, September 2016.

ABSTRACT OF THE DISSERTATION

Circadian Amplification of Alpha Factors, Energy Intensity and Indirect Greenhouse Gas Emissions in Aerated Processes for Water Resource Recovery Facilities

By

Nasir Emami

Doctor of Philosophy in Civil Engineering

University of California, Irvine, 2018

Professor Diego Rosso, Chair

The primary objective of this research is to test the hypothesis that the compounding peaking of process dynamics input and process variables results in much amplified greenhouse gas emissions associated with process power demand in water resource recovery facilities. We developed a simplified equilibrium biokinetic model to study the effects of circadian variations in influent flow and carbonaceous/nitrogenous constituent concentration on the air requirement and the associated energy consumption, energy costs, and carbon emissions. The ultimate goal is to demonstrate the significance of integrating appropriate aeration submodels into the activated sludge model (ASM) family biokinetic models in developing predictive dynamic models for the activated sludge process (ASP).

A model was developed for a water resources recovery facility (WRRF) ASP operating in the Modified Ludzack-Ettinger (MLE) configuration, commonly used for water reclamation. The amplification of air requirements and the associated energy consumption were observed as a result of concurrent circadian variations in ASP influent flow and

carbonaceous/nitrogenous constituent concentrations. The indirect carbon emissions associated with the ASP aeration were further amplified due to the simultaneous variations in carbon emissions intensity [$kgCO_{2,eq}(kWh)^{-1}$] and electricity consumption (kWh). The ratio of peak to minimum increased to 3.4 (for flow), 4.2 (for air flow and energy consumption), and 5.2 (for indirect $CO_{2,eq}$ emission), which is indicative of strong amplification. Similarly, the energy costs for ASP aeration were further increased due to the concurrency of peak energy consumption and power demand with time-of-use (TOU) electricity rates. A comparison between the results of the equilibrium model and observed data from the benchmark WRRF demonstrated the occurrence of under- and over-aeration attributed to the circadian variation in air requirements and limitations associated with the aeration system specification and design. Our results not only test the research hypothesis but offer practical recommendations for operations and design/retrofit.

CHAPTER 1: INTRODUCTION

Municipal water resource recovery facilities (WRRF) typically utilize the activated sludge process (ASP) to reduce organic carbon and nitrogen from influent wastewater. It is an energy intensive process and is associated with the direct and indirect release of greenhouse gases (GHG). (Monteith et al., 2005; de Haas et al., 2008; Kampschreur et al. 2009; Ahn et al., 2010; Foley et al., 2010; Park et al., 2010; Flores-Alsina et al. 2011; Corominas et al. 2012; Law et al., 2012).

The indirect marginal emissions of electrical demand vary spatially and temporally across the United States (Zivin et al., 2014). It should be noted that the direct CO_2 emissions from WRRF ASP are considered short-cycle and do not represent a net flux to the atmosphere. ASP direct CO_2 emissions are of biogenic origin and are not accounted in the Intergovernmental Panel on Climate Change (IPCC) Guidelines (IPCC 2006).

Electrical energy consumption to treat and transport water and wastewater accounts for 2-3% of the world's energy and 1-18% of the electrical energy consumption in urban areas (Olsson, 2012a). Energy systems are strongly influenced by consumption patterns. Demand side management (DSM) includes a portfolio of measures such as smart energy tariffs to improve energy efficiencies in ASP. While there is plenty of experience in optimizing energy generation and distribution, it is the demand side that is receiving increasing attention by research and industry (Palensky and Dietrich, 2011; Aymerich 2015).

Energy costs are site-specific and depend on local energy tariff structures applied at various water reclamation facilities (Aymerich et al., 2015). The ASP energy costs are strongly influenced by time-of-use (TOU) charges and peak power demand penalties. Using average energy prices may lead to biased conclusions (Rieger et al., 2015).

The aeration blowers are the core of energy requirements in ASP. The ASP aeration typically accounts for 45 to 75 percent of the overall plant energy costs (Reardon, 1995; Rosso and Stenstrom, 2005; Rosso et al., 2008; WEF, 2009).

The aeration/energy requirements, their associated costs, and GHG emissions are influenced by circadian variations in flow rates and carbonaceous/nitrogenous constituent composition and fractionation factors in the influent (Gori et al., 2011; Mannina et al., 2016b).

Due to general human activities, the variations in chemical oxygen demand (COD) and total suspended solids (TSS) follow the pattern of flow rate variations (Metcalf, & Eddy, Inc, 2014). The ASP requires higher rates of aeration during the peak flow and peak carbonaceous/nitrogenous constituent loadings to be able to maintain the dissolved oxygen (DO) set-points, and to meet the effluent water quality limits.

As air flow increases, larger bubbles are formed. It lowers the surface to volume ratio and increases the bubble rise velocity. The net effect reduces the oxygen transfer rates from gas to liquid phase (Rosso et al., 2005). The high concentrations of surfactants, and biodegradable COD (bCOD) decrease the α factor and depress the oxygen transfer efficiency (OTE) in the aeration tanks (Rosso and Stenstrom, 2006b, Leu et al 2009).

Sobhani et al. (2013) shows how those variations amplify the energy consumption during the peak hours, and consequently cause higher energy costs and carbon emissions.

Extracellular polymeric substances (EPS) are crucial constituent of activated sludge and may account for 60–80% of the total biomass (Liu and Fang, 2003; Zhang et al., 2015). The effects of EPS characteristics on oxygen transfer efficiency are being slowly understood. A plethora of studies have consistently shown that increasing solid retention time (SRT) improves aeration efficiency (Kaliman et al., 2008; Rosso et al., 2008, 2005).

EPS and DO play essential roles in activated sludge aeration and sludge settling in ASP, governing the efficiency and the overall operational performance. It has been observed that the EPS characteristics that promote improved oxygen transfer efficiency differ from those required for enhanced sludge settling properties. A thorough analysis and understanding of the EPS and DO roles and the best balance to achieve the benefits of both cases are of the upmost importance to optimize WRRFs operations.

The inherent variations of the influent flow and carbonaceous/nitrogenous constituents' concentrations in the wastewater treatment plants can be dampened by utilizing flow equalization basins. Significant savings can be realized if the plant flow is shifted to diurnal periods associated with lower power rates or an operating strategy of limiting peak flows (Leu et al., 2009).

Even though ASP has typically been investigated and presented in literature in its steady-state condition, the dynamics of this process have been of interest since the introduction of dynamic simulations. ASP dynamic modelling has been widely applied since the introduction of activated sludge model (ASM) family by International Water

Association (IWA) task group. The ASM model family includes a set of standardized basis models frequently used in the core of most ASP dynamic models (Henze et al., 1987, 2000). Dynamic simulation of ASP provides detailed insight into the bacterial growth, substrates degradation, and oxygen requirements.

The required oxygen can be supplied by means of various aeration systems aiming to achieve high oxygen transfer efficiencies while minimizing the associated energy demand. Fine bubble diffusers are commonly used in ASP to maximize the effective contact area between gas-liquid interfaces and oxygen transfer efficiencies. Aeration models are external submodels to biokinetic ASM family models to predict air requirements for ASP.

Aeration models are external submodels to biokinetic ASM family models to predict air requirements for ASP. The aeration system design for the ASP must be adequate to satisfy the oxygen demand for the biological oxidation of the bCOD, endogenous respiration of the biomass, and biological nitrification in the influent wastewater. Additionally, the aeration system design must be able to provide adequate mixing, and maintain the desired DO concentration throughout the aeration tank (Metcalf, & Eddy, Inc, 2014).

Coupling supervisory control and data acquisition (SCADA) systems and ASM family biokinetic models allows for conducting optimization strategies and implementing complex computational algorithms to enhance system design, and control strategy to improve aeration efficiency and the associated energy requirements (Karpinska et al., 2015; Åmand and Carlsson, 2012).

The primary objective of this research is to develop a simplified equilibrium biokinetic model to study the effects of circadian variations in influent flow and carbonaceous/nitrogenous constituent concentration on the air requirement and the associated energy consumption, energy costs, and carbon emissions. The ultimate goal is to demonstrate the significance of integrating appropriate aeration submodels into the ASM family biokinetic models in developing predictive dynamic models for the ASP.

CHAPTER 2: LITERATURE REVIEW

2.1 Introduction to Dynamics of ASP

Due to general human activities, the variations in COD and TSS follow the pattern of flow rate variations (Metcalf, & Eddy, Inc, 2014). The ASP requires higher rates of aeration during the peak flow and peak carbonaceous/nitrogenous constituent loadings to be able to maintain the DO set-points, and to meet the effluent water quality limits.

As air flow increases, larger bubbles are formed. It lowers the surface to volume ratio and increases the bubble rise velocity. The net effect reduces the oxygen transfer rates from gas to liquid phase (Rosso et al., 2005). The high concentrations of surfactants, and bCOD decrease the α factor and depress the oxygen transfer efficiency in the aeration tanks (Rosso and Stenstrom, 2006b, Leu et al 2009). Sobhani et al. (2013) shows how those variations amplify the energy consumption during the peak hours, and consequently cause higher energy costs and carbon emissions.

2.2 Activated Sludge Process Biokinetic Modelling

2.2.1 Background

Even though ASP has typically been investigated and presented in literature in its steady-state condition, the dynamics of this process have been of interest since the introduction of dynamic simulations.

ASP dynamic modelling has been widely applied since the introduction of ASM family by IWA task group. The ASM family includes a set of standardized basis models

frequently used in the core of most ASP biokinetic dynamic models (Henze et al., 1987, 2000).

Quantification of different sources of GHG emissions and evaluation of control strategies using dynamic modelling offer sustainable solutions to reduce the overall GHG emissions, improve effluent water quality, and reduce operational costs (Flores- Alsina et al., 2011; Corominas et al., 2012; Guo et al., 2012; Flores- Alsina et al., 2014). Plant-wide mechanistic dynamic models are essential tools to optimize design and operation of WRRF and to develop strategies aimed at reducing energy consumption and GHG emissions (Gori et al., 2013; Flores-Alsina et al. 2014; Caniani et al., 2015; Mannina et al., 2016a).

Dynamic simulation of WRRF provides detailed insight into the ASP behavior. Biokinetic models are robust tools for process design, operational optimization, performance assessment, controller design, and model-based process control to respond effectively to these variations.

2.2.2 Oxygen Requirements Calculation

Using simplified equilibrium biokinetic model, the oxygen required for the biodegradation of carbonaceous and nitrogenous substrates is determined from a mass balance using the bCOD concentration of the wastewater treated and the amount of the biomass wasted from the system per day (Metcalf, & Eddy, Inc, 2014). Conducting a mass balance the required oxygen for a suspended growth process is the following:

$$R_0 = Q\,(S_0\text{-}S) - 1.42P_{x,\,bio} \qquad (2\text{-}1)$$

Where:

R_0 = Oxygen Requirements

Q = influent flowrate, m^3d^{-1}

S_0 = influent soluble substrate concentration, gm^{-3}

S = Effluent soluble substrate concentration, gm^{-3}

$$S = \frac{K_s[1+b_H(SRT)]}{(SRT)(\mu_{max,T} - b_{H,T})-1} \quad (2\text{-}2)$$

SRT = Solids retention time, d

$\mu_{max,T}$ = maximum specific bacterial growth rate at temperature T (^oC), g new cells/ g cells.d

$$\mu_{max,T} = (\mu_{m,20})\ \theta^{(T-20)} \quad (2\text{-}3)$$

$\mu_{m,20}$ = 6.0 g/g.d (Adapted from Henze et al. (1995); Barker and Dold (1997)

θ = Temperature Coefficient (1.07) (Adapted from Henze et al. (1995); Barker and Dold (1997)

$b_{H,T}$ = endogenous decay coefficient at temperature T (oC), g VSS/g VSS.d

$$b_{H,T} = (b_{H,20})\ \theta^{(T-20)} \quad (2\text{-}4)$$

$b_{H,20}$ = 0.12 g/g.d (Adapted from Henze et al. (1995); Barker and Dold (1997)

θ = Temperature Coefficient (1.04) (Adapted from Henze et al. (1995); Barker and Dold (1997)

Ks = half-velocity constant, substrate concentration at one-half the maximum specific substrate utilization rate, gm^{-3}

$P_{x,bio}$ = biomass as VSS wasted, gd^{-1}

$$P_{x,bio} = \frac{QY_H(S_0-S)(1\ kg/10^3g)}{1+ b_{H,T}(SRT)} + \frac{Q(f_d)(b_H)Y_H(S_0-S)(SRT)(1\ kg/10^3g)}{1+b_{H,T}(SRT)} + \frac{QY_n(NO_x)(1\ kg/10^3g)}{1+ b_{n,T}(SRT)} \quad (2\text{-}5)$$

Where:

NO_x = concentration of NH_4-N in the influent flow that is nitrified, mgl^{-1}

b_n = endogenous decay coefficient for nitrifying organisms, g VSS/g VSS.d

$$b_{n,T} = (b_{n,20})\,\theta^{(T-20)} \quad (2\text{-}6)$$

$b_{n,20} = 0.17$ g/g.d (Adapted from U.S. EPA (2010)).

θ = Temperature Coefficient (1.029) (Adapted from U.S. EPA (2010)).

Y_H = heterotrophic bacteria synthesis yield coefficient, g VSS/g COD used

Y_n = synthesis yield coefficient, g VSS/g NH_4-N

f_d = fraction of biomass that remains as cell debris, g VSS/g biomass VSS depleted by decay

When nitrification is included in the process, the oxygen required for oxidizing ammonia and nitrite needs to be included in the equation as follows:

$$R_0 = Q(S_0\text{-}S) - 1.42P_{x,bio} + 4.57\,Q(NO_x) \quad (2\text{-}7)$$

1.42 = respiration oxygen demand of MLVSS, g O_2/g MLVSS

4.57 = Oxygen demand to oxidize TKN, g O_2/g N oxidized

Based on the assumption that biomass ($C_5H_7NO_2$) contains 0.12 g N/g biomass NO_x concertation is derived as follows:

$$Q(NO_x) = Q\,(TKN_0) - QN_e - 0.12P_{x,bio} \quad (2\text{-}8)$$

Where TKN_0 = influent TKN concentration, mgl^{-1}

N_e = effluent NO_3-N concentration, mgl^{-1}

When denitrification is included in the process, the oxygen credit needs to be included in the equation to account for the amount of oxygen supplied by nitrate reduction as follows:

$$R_0 = Q\,(S_0\text{-}S) - 1.42P_{x,bio} + 4.57\,Q\,(NO_x) - OC \quad (2\text{-}9)$$

Where: OC = oxygen credit, kgh^{-1}

$$OC = 2.86\,Q\,(NO_x - Ne) \quad (2\text{-}10)$$

2.86: g O_2/g NO_3-N

The following nitrogen mass balance determines how much nitrate is produced in aeration zone and what Internal Recycle (IR) must be used to meet the desired effluent nitrate concentration:

$$Q\,(NO_x) = N_e\,[Q + (IR)\,Q + (R)\,Q] \quad (2\text{-}11)$$

$$IR = NO_x/Ne - 1.0 - R \quad (2\text{-}12)$$

Where:

IR = internal recycle ratio

R = RAS recycle ratio

2.3 ASP Aeration Submodel

2.3.1 Background

Aeration models are external submodels to biokinetic ASM family models to predict air requirements for ASP.

The aeration system design for the ASP must be adequate to satisfy the oxygen demand for the biological oxidation of the bCOD, endogenous respiration of the biomass, and biological nitrification in the influent wastewater. Additionally, the aeration system design must be able to provide adequate mixing, and maintain the desired DO concentration throughout the aeration tank (Metcalf, & Eddy, Inc, 2014).

Calculating oxygen transfer efficiencies in ASP aeration systems involves adjusting clean water oxygen transfer performance data for the effect of process water operating conditions (Metcalf, & Eddy, Inc, 2014). The oxygen transfer efficiency can be defined as follows:

$$\mathrm{OTE} = \frac{(\mathrm{O_{2,in}} - \mathrm{O_{2,out}})}{(\mathrm{O_{2,in}})} \qquad (2\text{-}13)$$

Where:

$\mathrm{O_{2,in}}$ and $\mathrm{O_{2,out}}$ = mass fluxes of input and output oxygen.

Standard oxygen transfer efficiency (SOTE) is resulted from normalizing OTE to standard conditions (20^{o}C, zero DO and salinity, 1 atm) (ASCE 1992; ASCE 1997, ASCE 2006).

The alpha factor is defined as the ratio of the oxygen transfer rate in process water to that in clean water. The alpha factor of process water is less than 1 due to the adverse effect of organic contaminants, surfactants, and viscosity.

$$\alpha = \frac{K_L a \text{ of Process Water}}{K_L a \text{ of Clean Water}} \quad (2\text{-}14)$$

Where:

$K_L a$= Volumetric mass transfer coefficient ($time^{-1}$)

The α-factor can be determined as follows:

$$\alpha = \frac{\alpha SOTE}{SOTE} \quad (2\text{-}15)$$

Where:

SOTE = Standardized OTE in clean water

α.SOTE = Standardized OTE in process water

α.SOTE is directly proportional to mean cell retention time (MCRT), diffuser submergence, number of the diffusers, and surface area while inversely proportional to air flow rate (AFR) (U.S. EPA, 1989; Rosso et al., 2005).

2.3.2 Air Requirements and Oxygen Transfer Calculation

Oxygen transfer rate under process condition can be estimated by Equation 2-16 as follows:

$$OTR_f = \left[\frac{(\tau\beta\Omega C^*_{\backsim 20} - C)}{C^*_{\backsim 20}}\right][(\theta)^{t-20}](\alpha)(F) \qquad (2\text{-}16)$$

Where:

OTR_f = field oxygen transfer rate estimated for the system operating under process conditions at an average DO concentration, C, and temperature, T, kg O_2h^{-1}.

SOTR = oxygen transfer rate under standard conditions (20 ^oC, 1 atm, C = 0 mgl^{-1}), kg O_2h^{-1}

τ = temperature correction factor = C^*_{st}/C^*_{20}

C^*_{st} = dissolved oxygen surface saturation concentration at operating temperature, mgl^{-1}

C^*_{s20} = dissolved oxygen surface saturation concentration at standard temperature (20 ^oC), mgl^{-1}

β = relative DO saturation to clean water, typically 0.95 – 0.98 = $C^*_{\backsim}$ (wastewater)/ $C^*_{\backsim}$ (tap water)

$C^*_{\backsim}$ = steady-state DO saturation concentration obtained from nonlinear regression analysis of clean water test results.

Ω = pressure correction factor = P_b/P_s

P_b = barometric pressure at test site, m, kP_a

Ps = Standard barometric pressure (1.00 atm)

Barometric formula for an isothermal ideal gas:

$$\Omega = \text{Exp}[\frac{-\text{Mg z}}{\text{RT}}] \quad (2\text{-}17)$$

M = molecular weight of dry air, 28.97 kg(kmol)$^{-1}$

R = universal gas constant for air, 8.314 J(mole.K)$^{-1}$

Z = height above sea level, m

$C^*_{\backsim, 20}$ = saturated DO value at sea level and standard temperature (20 ^{o}C) for diffused aeration, mgl^{-1}. It is higher than C_{st} as it is affected by oxygen transfer from bubbles under pressure in water column. The values of $C^*_{\backsim, 20}$ can be estimated using the following equation (U.S. EPA, 1989):

$$C^*_{\backsim 20} = [1 + d_e \left(\frac{D_f}{P_s}\right)] \quad (2\text{-}18)$$

d_e = mid-depth correction factor; may vary from 0.25-0.45

D_f = depth of diffusers in basin, m

C = Average dissolved oxygen concentration within the entire process water volume, mgl^{-1}

θ = empirical temperature correction factor, typically 1.024

T = field temperature, ^{o}C

T_s = Standard temperature, ^{o}C

α = relative oxygen transfer rate in process water vs clean water = K_{Laf20} (wastewater)/K_{La20} (tap water)

F = fouling factor, typically 0.65-0.9

Fine-bubble diffusers have replaced coarse-bubble diffusers to achieve significant power savings. Rosso and Stenstrom (2006a) quantified the consequences of aging

processes on fine-pore diffusers and showed that the performance of diffusers critically affects the wastewater treatment plant economics. Datasets from 94 field measurements were analyzed and showed a clear pattern of performance decline with time in operation.

Oxygen transfer efficiency declines rapidly during the first 24 months of operation. Cleaning the diffusers restores efficiency, and reduces plant's energy expenditure. Periodic cleaning prolongs the economically viable lifespan for the aeration system (Rosso and Stenstrom 2006a).

Figures 2.1 and 2.2 illustrate the best-fit linear regressions analysis for various diffuser groups (new, aged, old, and cleaned) by Rosso and Stenstrom (2006a). The regression analysis indicates that the oxygen transfer efficiency decreases drastically over time with higher rates of decline in the first 24 months of operation and lower rates of decline after 24 months. Diffuser cleaning restores transfer efficiency significantly, for both α and α.SOTE. Diffuser cleaning does not result in complete restoration of transfer efficiency due to the irreversibility of certain fouling, scaling, and especially material aging processes.

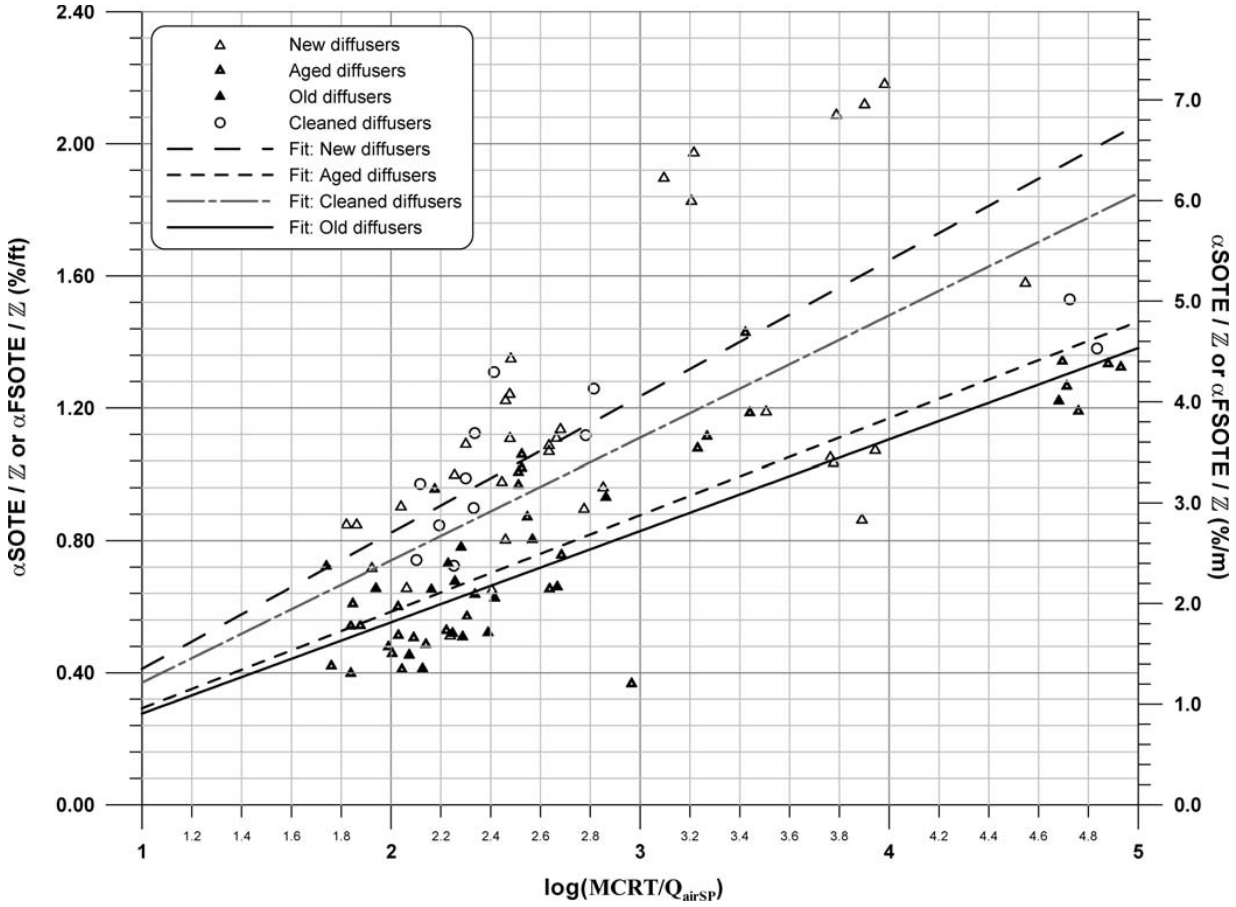

Figure 2.1. SOTE per unit depth versus plant operative parameters (Rosso and Stenstrom 2006a). (Q_{airSP}=airflow rate per total diffuser active area)

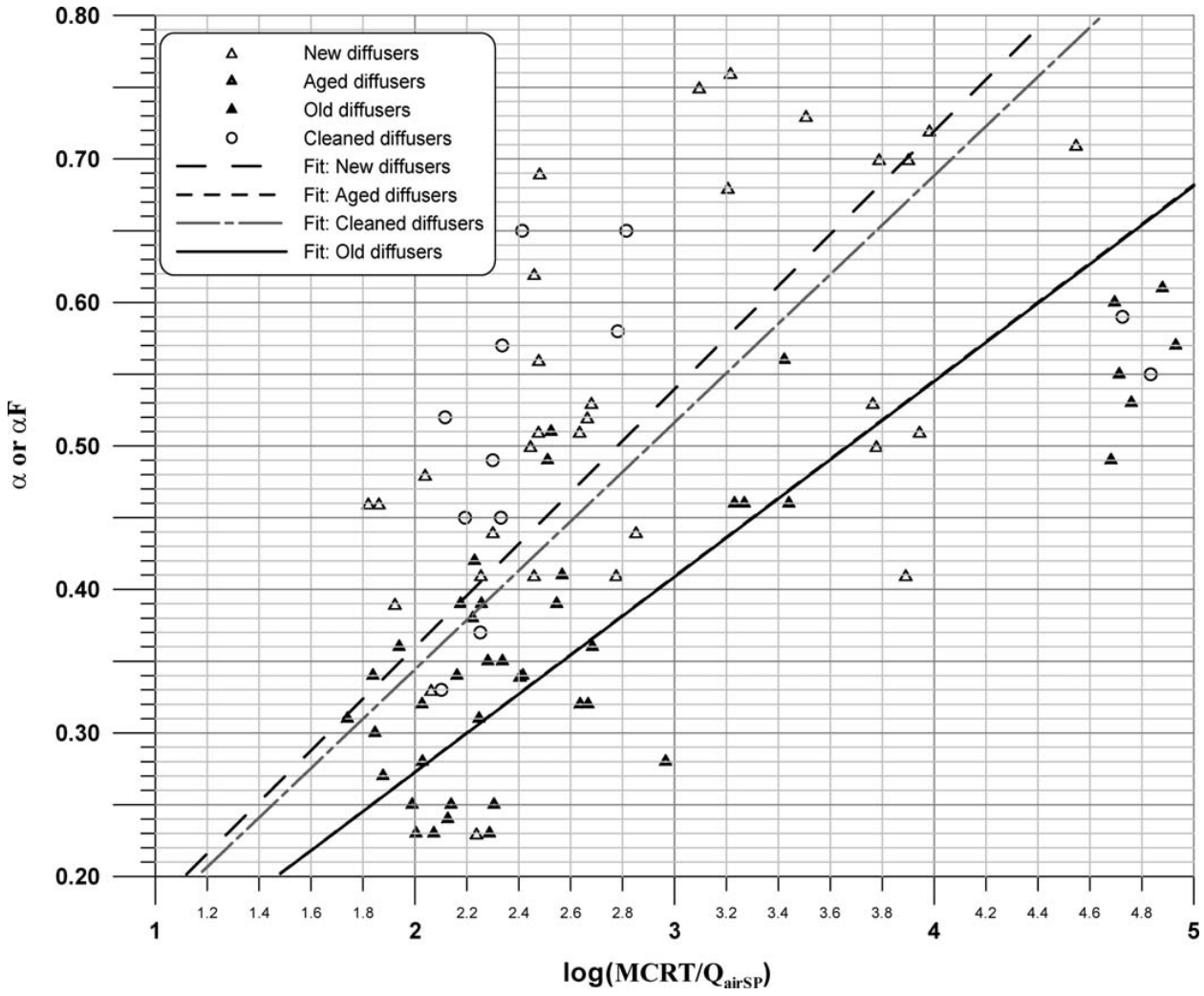

Figure 2.2. Water quality parameter a versus plant operative parameters (Rosso and Stenstrom 2006a). (Q_{airSP}=airflow rate per total diffuser active area)

Figure 2.3 shows that the transfer efficiency declines over time without cleaning. The new diffusers transfer efficiency exceeds those of aged or old diffusers. The decline in efficiency over time is attributed to the formation of larger bubbles or coalescence as a result of the biofilm coating of the diffuser surface.

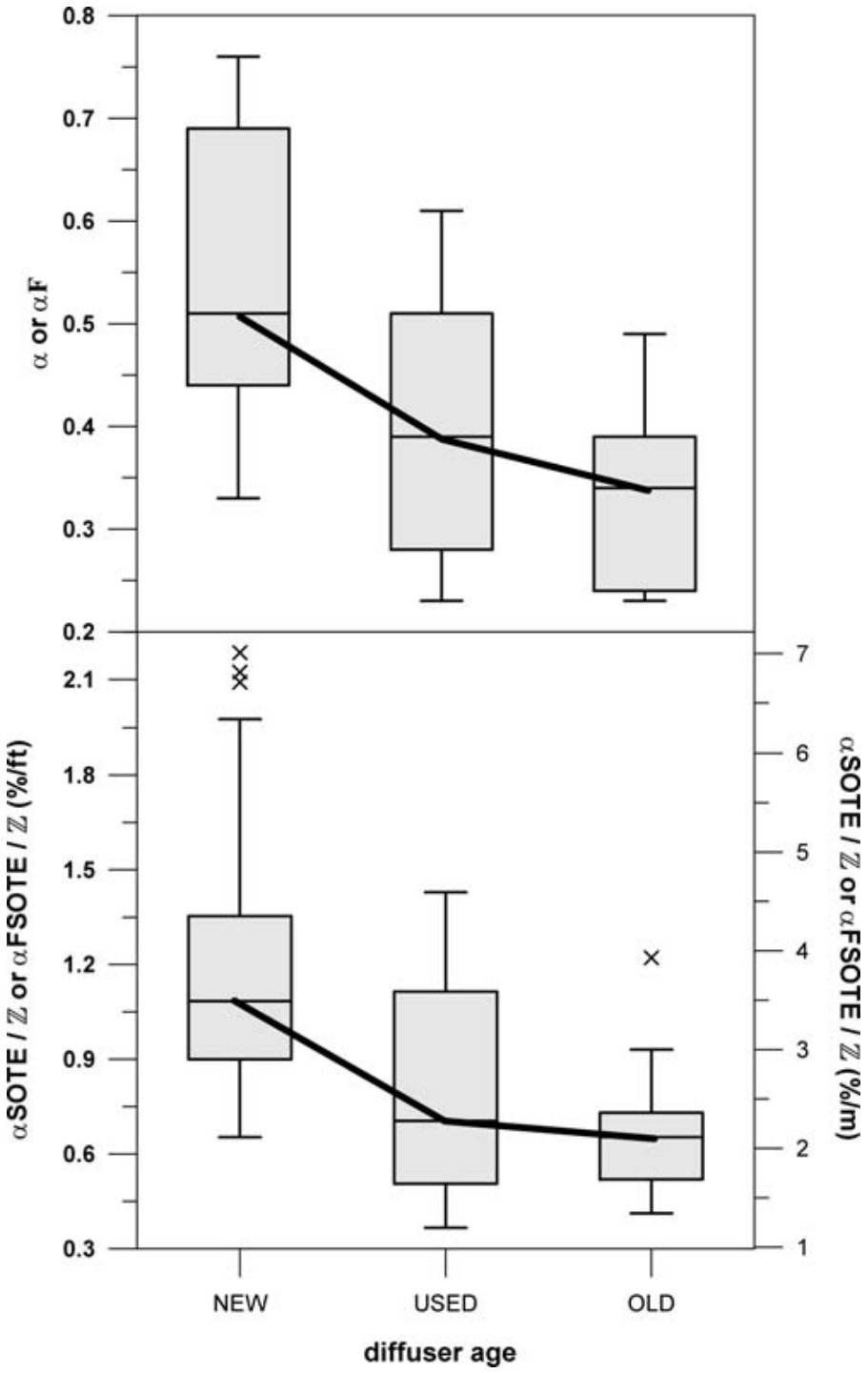

Figure 2.3. Efficiency decrease versus time in operation (Rosso and Stenstrom 2006a).

Additionally, Rosso and Stenstrom (2006a) quantified the economic implications of diffuser fouling and cleaning frequency with a net-present-value calculation tool. The tool consists of an iterative algorithm that calculates the net-present values of power cost, power overhead resulting from decreased oxygen transfer efficiency and increased diffuser pressure drop, and cleaning frequency. The cleaning frequency is based on the cleaning cost and cumulative power overhead.

Cleaning is recommended when the wasted power exceeds the cleaning cost. ‘‘wasted power’’ is defined as the difference between the actual power cost at a given time and the initial power cost. Figure 2.4 plots the evolution of the power waste over time, and the shaded rectangle shows a cleaning event.

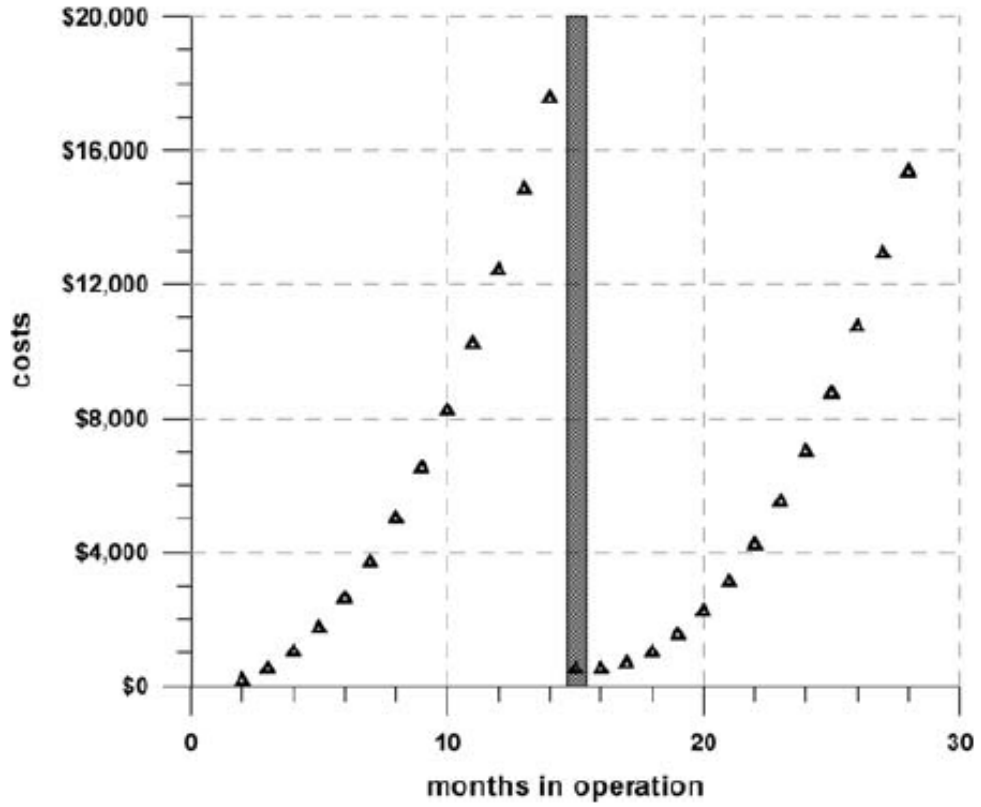

Figure 2.4. Power waste cost versus time in operation (Rosso and Stenstrom 2006a).

Oxygen transfer efficiencies were integrated into the model using a regression analysis developed by Rosso el al (2005) to establish correlations for α and α.SOTE as a function of diffuser type, tank geometry, airflow rates, and MCRT. The regression analysis is based on off-gas transfer efficiency analysis on fine-bubble diffusers. The dataset includes 30 plants nationwide and 372 different flux-averaged off-gas analyses.

The off-gas analysis is a technique developed by Redmon et al. (1983) to estimate the oxygen transfer efficiency in process water. Off-gas analysis estimates the oxygen transfer efficiency by performing a mass balance on oxygen in off-gas and ambient air.

The correlations were established as follows:

$$\alpha.\mathrm{SOTE} = 5.717.\log\chi - 6.815 \quad (2\text{-}19)$$

$$\alpha = 0.172.\log\chi - 0.131 \quad (2\text{-}20)$$

$$Q_N = \frac{\mathrm{AFR}}{\mathrm{a.ND.z}} \quad (2\text{-}21)$$

$$\chi = \frac{\mathrm{MCRT}}{\mathrm{QN}} \quad (2\text{-}22)$$

Where:

Q_N = normalized air flux, s^{-1}

AFR = airflow rate, m^3s^{-1}

a = diffuser specific area, m^2

ND = total diffuser number

Z = diffuser submergence, m

MCRT = Mean Cell Residual Time, d

χ = Plant characteristic number, T^2

Figure 2.5 shows efficiency parameters versus the plant characteristic group, χ. The ellipses in Figure 2.5 represent 90% confidence. Regression analyses were performed to estimate both α and α.SOTE as linear functions of log χ.

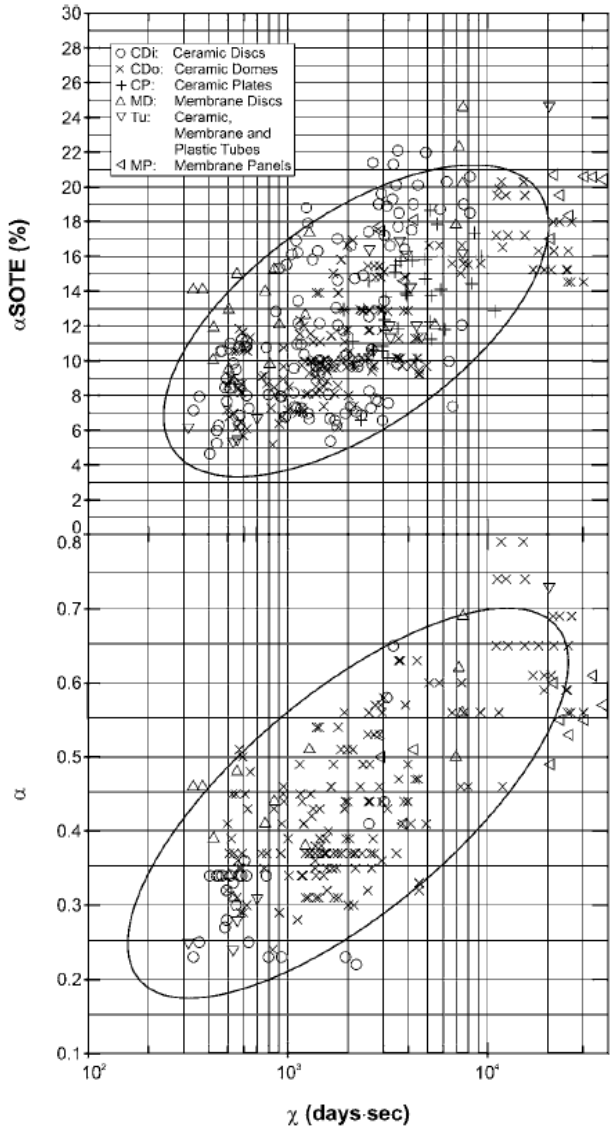

Figure 2.5. α and α.SOTE versus plant characteristic number χ.

Figure 2.6 shows the α.SOTE as a function of MCRT, with contours showing α.SOTE (Equation 2-19) for equal, normalized air fluxes. Transfer efficiency increases at higher MCRTs and lower air fluxes as expected.

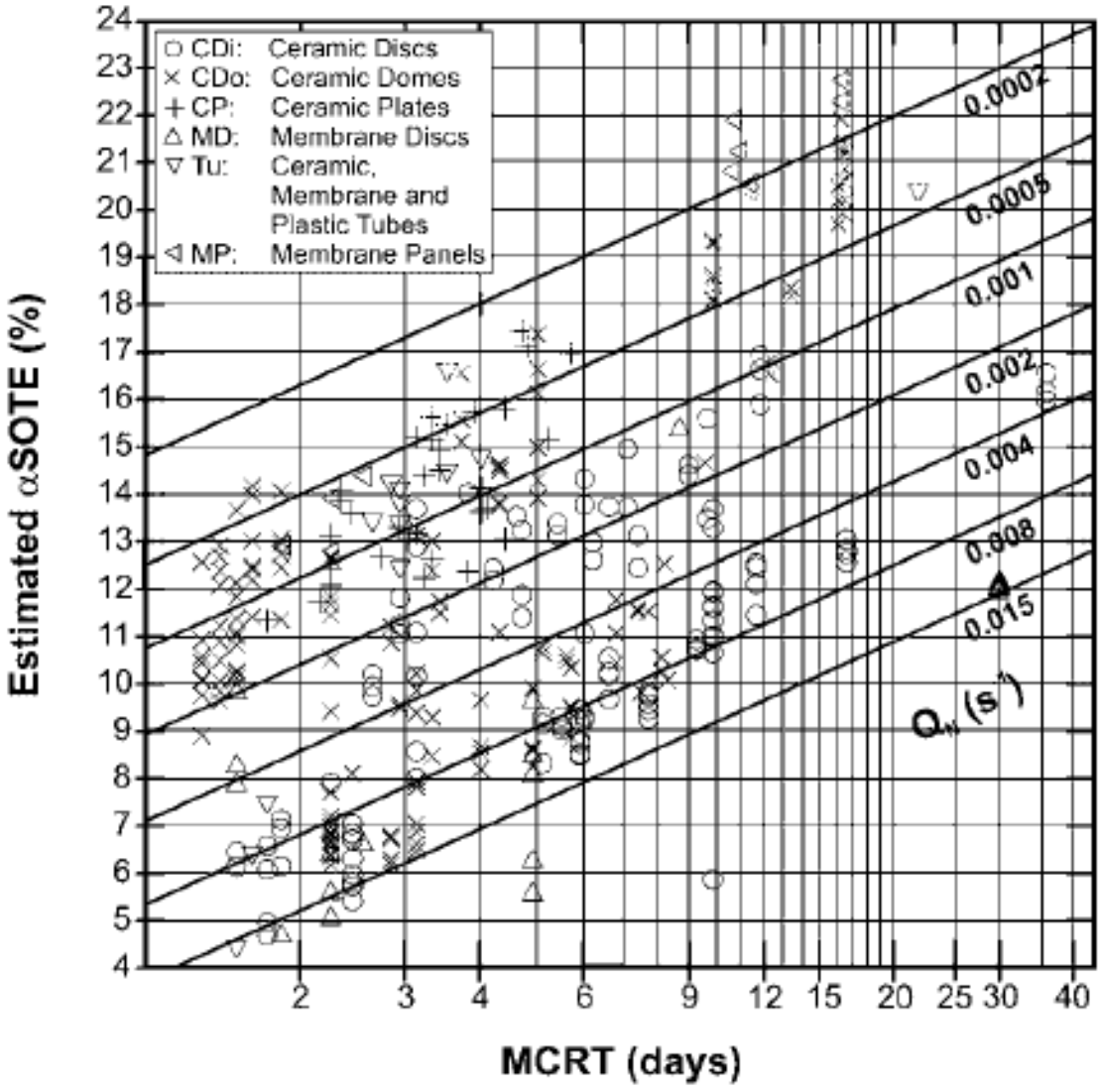

Figure 2.6. α.SOTE vs MCRT; QN is expressed as contours, eq. 2-19 (Rosso et al., 2005)

Similarly, Figure 2.7 shows the α factor vs MCRT. Contour lines on Figure 2.6 and 2.7 show the effect of MCRT on transfer efficiency. Vertical direction on contours shows the overall effect of specific air flux.

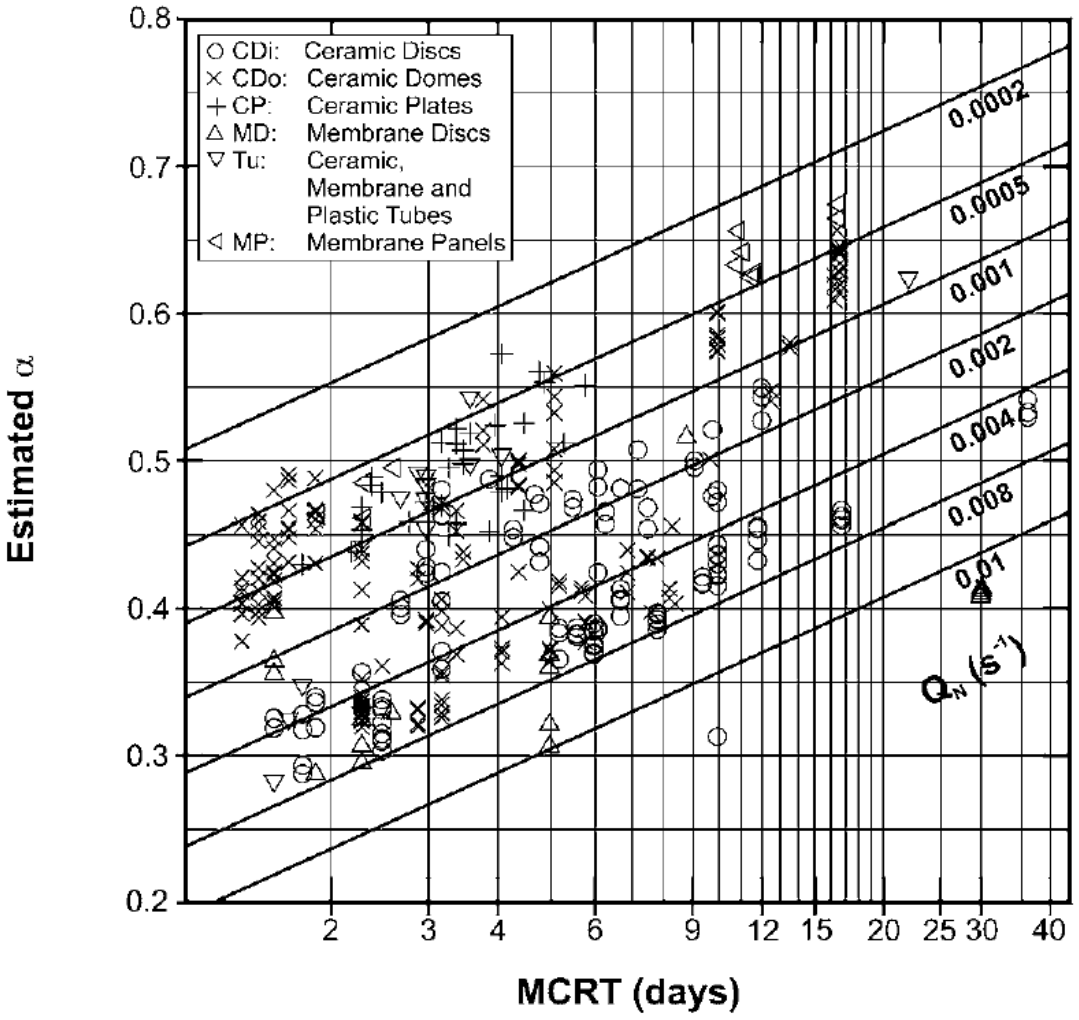

Figure 2.7. α vs. MCRT; QN is expressed as contours, eq. 2-20 (Rosso et al., 2005)

2.4 Power Requirements for ASP Aeration

Aeration blowers must be selected to have adequate capacity for hot summer days. The power requirement for adiabatic compression is given in Equation 2-23 (Metcalf, & Eddy, Inc, 2014).

$$P_w = \frac{wRT_1}{28.97\ n\ e}\left[\left(\frac{p_2}{p_1}\right)^n - 1\right] \quad (2\text{-}23)$$

Where:

Pw = Blower's Power Requirement, kW

w = weight of air flow rate, kgs^{-1}

R = universal gas constant for air, 8.314 J/mole.K

T_1 = absolute inlet temperature, k

p_1 = absolute inlet pressure, atm

p_2 = absolute outlet pressure, atm

n = (k-1)/k where k is the specific heat ratio (1.395 for dry air)

28.97 = molecular weight of dry air, $kg(kmol)^{-1}$

2.5 Temporal and Spatial Variations in CO_2 Emission Intensity

The indirect marginal emissions of electrical demand vary spatially and temporally across the United States (Zivin et al., 2014). Figure 2.8 provides a general overview of the US electrical grid with an illustration of how the United States is partitioned into three interconnections (Western, ERCOT, and Eastern).

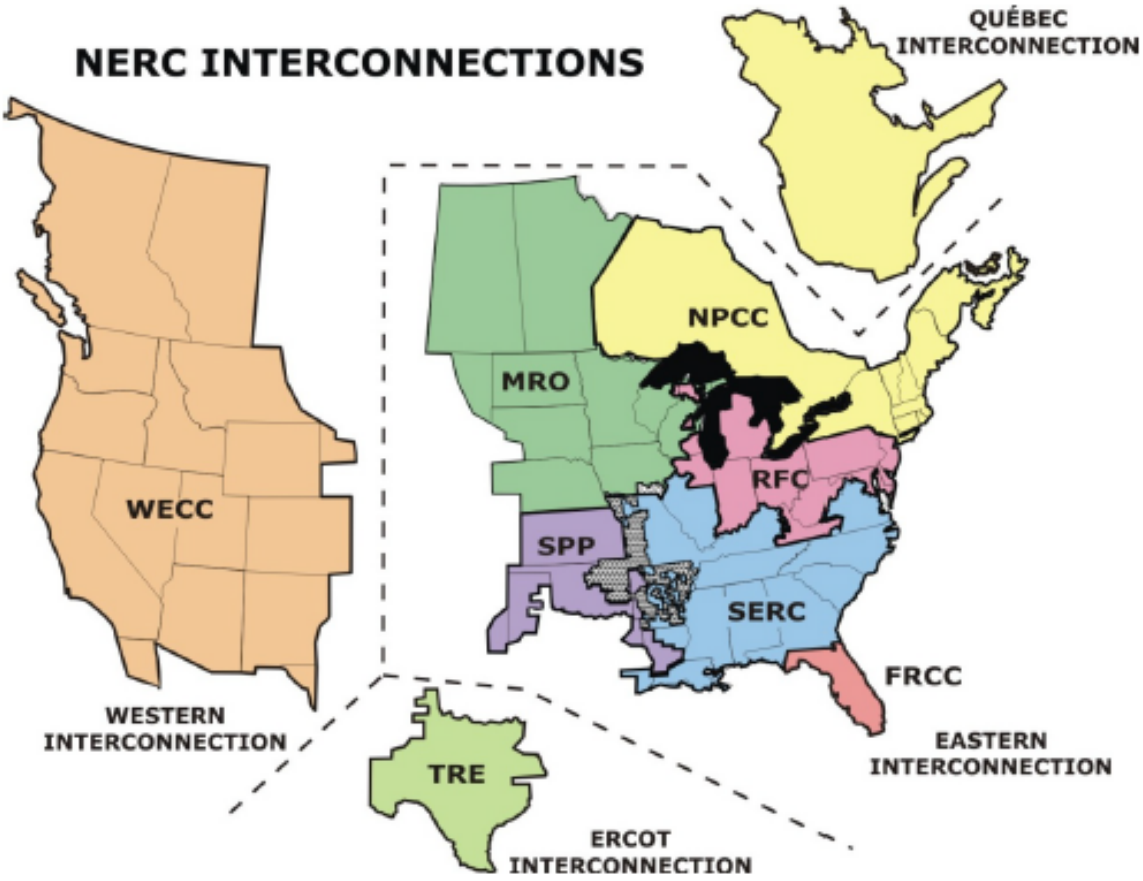

Figure 2.8. Grid interconnections (source: NERC website at www.nerc.com)

It should be noted that the direct CO_2 emissions from WRRF ASP are considered short-cycle and do not represent a net flux to the atmosphere. ASP direct CO_2 emissions are of biogenic origin and are not accounted in the Intergovernmental Panel on Climate Change (IPCC) Guidelines (IPCC 2006).

Zivin et al. (2014) has developed a regression model to quantify spatial and temporal marginal $CO_{2,eq}$ emission intensities for the electrical demand. The model accounts for the generation mix within interconnected electricity markets and shifting diurnal load profiles, with a focus on carbon dioxide.

Table 2.1 tabulates the regression results of marginal CO_2 emissions ($kg(kWh)^{-1}$) by interconnection.

Table 2.1. Regression results of marginal CO_2 emissions ($kg(kWh)^{-1}$) by interconnection

	Interconnection		
Hour	WECC	ERCOT	Eastern
1:00 AM	0.38	0.49	0.66
2:00 AM	0.38	0.50	0.67
3:00 AM	0.38	0.51	0.67
4:00 AM	0.36	0.51	0.67
5:00 AM	0.35	0.49	0.65
6:00 AM	0.32	0.45	0.62
7:00 AM	0.30	0.43	0.57
8:00 AM	0.31	0.43	0.55
9:00 AM	0.35	0.43	0.56
10:00 AM	0.39	0.42	0.57
11:00 AM	0.40	0.42	0.58
12:00 PM	0.40	0.41	0.58
1:00 PM	0.39	0.42	0.57
2:00 PM	0.38	0.42	0.55
3:00 PM	0.37	0.42	0.54
4:00 PM	0.36	0.42	0.54
5:00 PM	0.36	0.41	0.54
6:00 PM	0.36	0.41	0.54
7:00 PM	0.36	0.41	0.54
8:00 PM	0.37	0.40	0.54
9:00 PM	0.36	0.40	0.54
10:00 PM	0.37	0.41	0.56
11:00 PM	0.37	0.43	0.59
12:00 AM	0.38	0.46	0.63
R2	0.95	0.97	0.99

Figure 2.9 illustrates the mean 95-percent confidence interval temporal variations in marginal $CO_{2,eq}$ emissions for the Western Electricity Coordinating Council (WECC), Electric Reliability Council of Texas (ERCOT), and Eastern electricity interconnections across the United States.

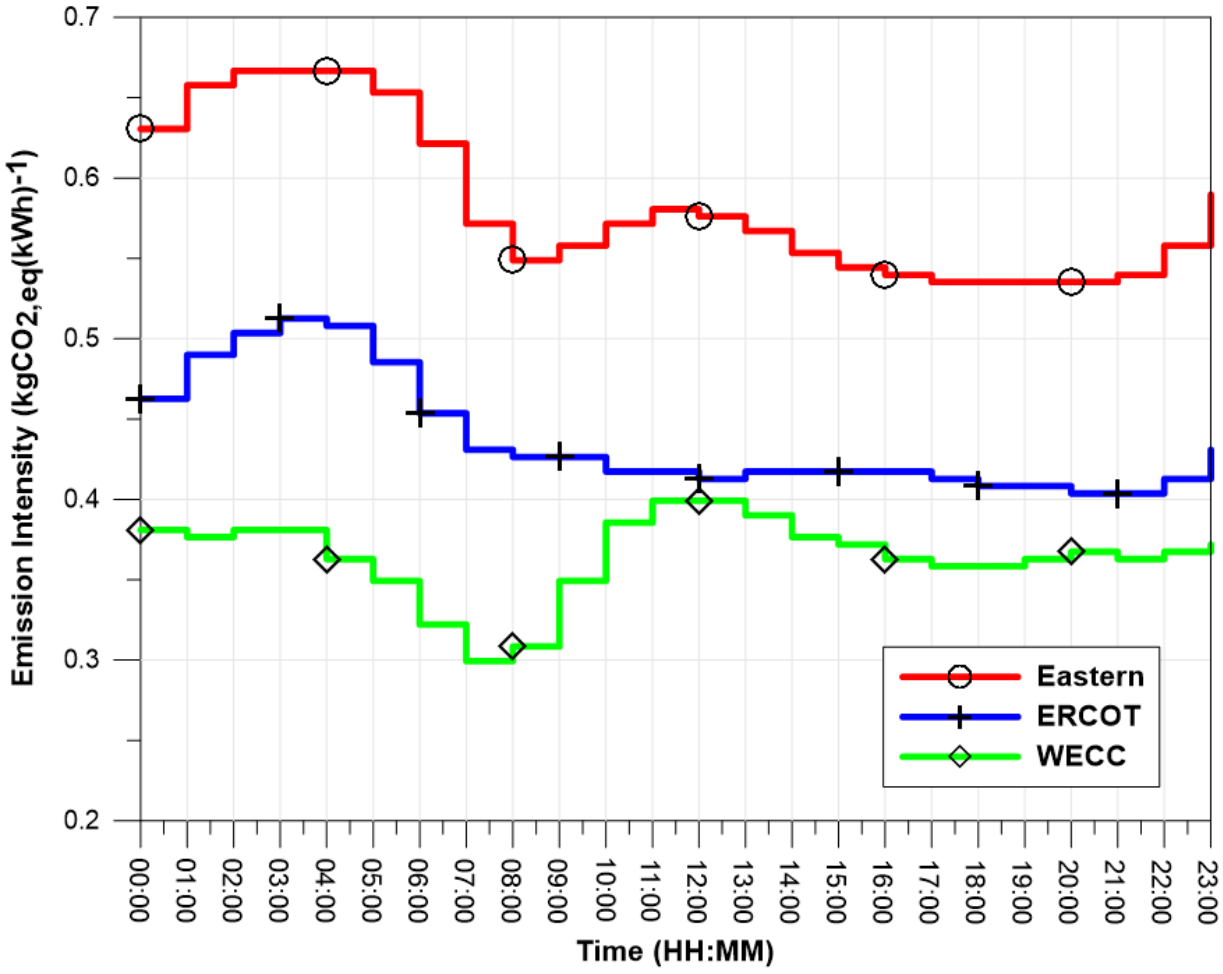

Figure 2.9. Temporal and spatial variations in $CO_{2,eq}$ emission Intensity (Zivin et al., 2014)

2.6 Energy Consumption and TOU Economic Implications

Energy systems are strongly influenced by consumption patterns. DSM includes a portfolio of measures such as smart energy tariffs to improve energy efficiencies in ASP. While there is plenty of experience in optimizing energy generation and distribution, it is the demand side that is receiving increasing attention by research and industry (Palensky and Dietrich, 2011; Aymerich 2015).

Energy costs are site-specific and depend on local energy tariff structures applied at various water reclamation facilities (Aymerich et al., 2015). The ASP energy costs are strongly influenced by TOU charges and peak power demand penalties. Using average energy prices may lead to biased conclusions (Rieger et al., 2015).

2.7 Role of Extracellular Polymeric Substances (EPS) on Oxygen Transfer and Secondary Settling

Sludge volume index (SVI) is a test to monitor activated sludge settleability and compaction. Lower SVI values are normally associated with more efficient clarifier performance.

The SVI is determined by placing a mixed-liquor sample in a 1- to 2-L cylinder and measuring the settled volume after 30 minutes.

$$\text{SVI, mL/g} = \frac{\text{Settled volume of sludge,mL/L)(1000 mg/g)}}{\text{(suspended solids,mg/L)}} \quad (2\text{-}24)$$

A SVI value of 100 mL/g is often considered a good settling sludge. SVI values below 120 mL/g are typically desired. SVI values above 150 mL/g are normally associated with filamentous growth and poor settling (bulking) (Metcalf, & Eddy, Inc, 2014).

Lower dissolved oxygen levels in AS aeration tanks are desirable in terms of energy savings; however, if the DO concentration is too low, filamentous organisms could predominate, resulting in poor settling. In general, the dissolved oxygen concentration in all areas of the aeration tanks should be maintained at about 1.5 to 2.0 mgl^{-1} (Metcalf, & Eddy, Inc, 2014).

Extracellular polymeric substances (EPS) are crucial constituent of activated sludge and may account for 60–80% of the total biomass (Liu and Fang, 2003; Zhang et al., 2015). As most of the microorganisms in water resource recovery facilities (WRRFs) are present in the form of microbial aggregates (flocs), the entire treatment operation will be influenced by the bioflocculation characteristics of the process (More et al., 2014; Ni et al.,

2009; Sheng et al., 2010; Subramanian et al., 2010). EPS play essential roles in two of key processes in WRRFs: aeration and settling. However, it has been observed that the EPS characteristics that promote improved oxygen transfer efficiency differ from those required for enhanced sludge settling properties. A thorough analysis and understanding of the exact role of EPS and the best balance to achieve the benefits of both cases are of the upmost importance to optimize WRRFs operations.

The effects of EPS characteristics on oxygen transfer efficiency are being slowly understood. A plethora of studies have consistently shown that increasing SRT improves aeration efficiency (Kaliman et al., 2008; Rosso et al., 2008, 2005). Given a certain SRT, an improvement in oxygen transfer was attributed to denitrifiers that sorb and consume the organic compounds responsible for the reduction of oxygen transfer (Rosso and Stenstrom, 2007). Nevertheless, recent studies are suggesting that the role of EPS is the actual key in the increase of oxygen transfer efficiency. EPS is being pointed out as the main mechanism of removal, or deactivation, of those compounds depressing oxygen transfer, by adsorbing surfactants in systems with long SRT, or in BNR configurations.

BNR processes are characterized by longer SRT, lower food-to-mass ratio (F/M), and lower protein to polysaccharide content ratio, which results in close to starving conditions for microorganisms. The starving conditions drive the EPS to exhibit much lower negative surface charges. The absence of negative surface charges in EPS may avoid the repulsion of surfactants, promoting their adsorption in the EPS matrix (Van Winkle et al., 2017), strengthening the hypothesis that the adsorption is the main mechanism controlling the observed aeration improvement in longer SRT conditions. Similarly, Tomczak-Wandzel et al., (2009) demonstrated the importance of the adsorption capacity of

BNR sludge by showing an increase of absorption capacity when the presence of surfactants was decreased (Tomczak-Wandzel et al., 2009).

The role of EPS on the sludge settling performance is also being slowly elucidated. Recent studies have demonstrated that the quantity of the EPS has no clear influence on the settling performance (measured by the SVI) (Liao et al., 2001; Liu and Fang, 2003; Zhang et al., 2014). On the other hand, the quality of the EPS (composition, hydrophobicity, zeta potential, etc.), which is intrinsically related with the SRT, has the biggest impact. Therefore, as it has been recorded previously, SRT seems to have the most relevant impact, dictating EPS composition and characteristics, thus, concurrently controlling process stability (expressed as settling performance).

2.8 Flow Equalization

2.8.1 Description/Application of Flow Equalization

The inherent variations of the influent flow and carbonaceous/nitrogenous constituents' concentrations in the wastewater treatment plants can be dampened by utilizing flow equalization basins.

Figure 2.10 and Figure 2.11 illustrates the application of the flow equalization in wastewater treatment plants. In the in-line configuration (Figure 2.10), all of the flow passes through the equalization basin. This arrangement can be used to achieve a considerable amount of constituent concentration and flow dampening (Metcalf, & Eddy, Inc, 2014).

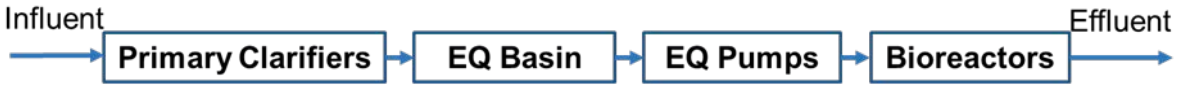

Figure 2.10. In-line equalization configuration

In the off-line configuration (Figure 2.11), only flow above some predetermined limit is diverted into the equalization basin. Although pumping requirements are minimized in this arrangement, the amount of constituent concentration dampening is considerably reduced. Off-line equalization is sometimes used to capture the firs flush from combined collection systems (Metcalf, & Eddy, Inc, 2014).

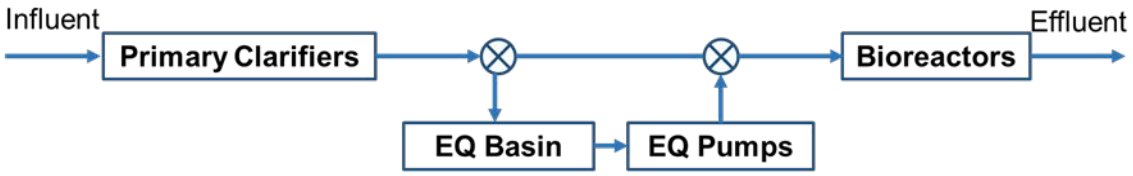

Figure 2.11. Off-line equalization configuration

2.8.2 The Benefits of Flow Equalization

Variations in influent flow and constituents' concentrations in the wastewater treatment plants may result in non-compliant effluent quality even in well-designed systems (Beler Baykal et al., 1994).

Several benefits have been attributed to the use of flow equalization in wastewater treatment plants (Foess et al., 1977).

- Dampens fluctuations in the organics and nutrients constituent concentration and fluxes in the influent wastewater, providing more stable retention periods and biomass concentrations in the bioreactors.
- Improves performance of primary and secondary clarifiers by leveling hydraulic variations and reducing peak flow rates; allowing for utilization of smaller clarifiers.
- Improves the settleability of wastewater.
- Simplifies manual and automated control of operations, such as chemical feeding, disinfection, and sludge recycle pumping.
- Mitigates shock loads to primary clarifiers, bioreactors, and secondary clarifiers by dampening concentrated waste streams.
- Allows for lowering energy costs by leveling power demand for pumping and aeration.

As discussed previously, ASP is an energy intensive process and is associated with the direct and indirect release of GHG. It requires higher rates of aeration during the peak flow and peak carbonaceous/nitrogenous constituent loadings to be able to maintain the DO set-points, and to meet the effluent water quality limits.

The literature review in the previous sections indicated that the ASP energy costs are strongly influenced by TOU charges and peak power demand penalties. Moreover, the indirect marginal emissions of electrical demand vary temporally. Flow equalization can reduce the energy cost and indirect marginal emissions of the electrical demand associated with the ASP by shifting the peak influent flow to the periods with lower TOU charges and marginal emissions.

Leu et al. (2009) showed that significant savings can be realized if the plant flow is shifted to diurnal periods associated with lower power rates. An operating strategy of limiting peak flows can saves up to 8% during the peak season, 5 to 6% during average winters and summers, and 6% on a yearly basis. If the flow can be adjusted to shift the low loading period, which ordinarily occurs at night, to the power rate peak hours in the afternoon, up to 31% of savings can occur in the peak season, or 16% on a yearly basis (Leu et al., 2009).

Application of the flow equalization in the wastewater treatment plants is limited due to the land requirements, capital costs, additional operation and maintenance, and nuisance problems.

2.8.3 Design Considerations

The design of flow equalization systems is concerned with the following considerations (Metcalf, & Eddy, Inc, 2014).

Optimal Location

The optimal location varies based on the wastewater influent characteristics, the treatment process, and land requirements and availability. The equalization basins can be sited upstream or downstream of the primary treatment systems. Equalization systems located downstream of the primary treatment causes fewer odor, solids settling, and scums issues.

If located upstream of primary treatment, sufficient mixing and aeration must be provided to prevent solids settling and odor problems.

Determination of Storage Volume Requirements

The required storage volume is determined by conducting an inflow cumulative analysis. In practice, the required storage volume will be larger than that theoretically determined to allow for continuous operation of the aeration and mixing equipment, to accommodate recycle streams, and to provide contingency for diurnal flow variations.

Configuration

For in-line equalization systems, it is important to use a geometry that allows for continuous-flow stirred-tank reactor.

Mixing and Air requirements

Proper mixing and aeration in equalization systems is crucial to prevent solids settling and preventing the wastewater from becoming septic and odorous.

The mixing requirements range from 0.004 to 0.008 kWm^{-3} for a medium strength municipal wastewater with a TSS of approximately 210 mgl^{-1}.

Aeration requirements range from 0.01 to 0.015 $m^3m^{-3}min^{-1}$ to maintain aerobic conditions.

2.9 Summary of the Literature Review

The available literature offers the theoretical basis required to develop a simplified equilibrium biokinetic model to study the dynamics of aeration systems in ASP including air, energy requirements, and their associated costs and GHG emissions.

The variations in influent carbonaceous/nitrogenous constituents follow the pattern of flow rate variations (Metcalf, & Eddy, Inc, 2014). Sobhani et al. (2013) showed how those variations amplify the energy consumption during the peak hours, and consequently cause higher energy costs and carbon emissions.

The indirect marginal emissions of electrical demand vary spatially and temporally across the United States (Zivin et al., 2014).

Energy systems are strongly influenced by consumption patterns. Demand Side Management includes a portfolio of measures such as smart energy tariffs to improve energy efficiencies. Energy costs are site-specific and depend on local energy tariff structures applied at various WRRF (Aymerich et al., 2015). The ASP energy costs are strongly influenced by time-of-use (TOU) charges and peak power demand penalties. Using average energy prices in lieu of energy tariff structures may lead to biased conclusions (Rieger et al., 2015).

The effects of EPS characteristics on oxygen transfer efficiency are being slowly understood. A plethora of studies have consistently shown that increasing solid retention time improves aeration efficiency. Recent studies are suggesting that the role of EPS is the actual key in the increase of oxygen transfer efficiency. EPS is being pointed out as the main mechanism of removal, or deactivation, of those compounds depressing oxygen transfer, by

adsorbing surfactants in systems with long SRT, or in biological nutrient removal configurations.

Application of flow equalization in wastewater treatment plants enhances the biological treatment, improves settleability in primary and secondary clarifiers, simplifies process control, mitigates shock loads to primary clarifiers, bioreactors, and secondary clarifiers, and allows for lowering energy costs and indirect marginal emissions of electrical demand.

Simulation of WRRF provides detailed insight into the ASP behavior. Biokinetic models are robust tools for process design, operational optimization, performance assessment, controller design, and model-based process control to respond effectively to these variations. Table 2.2 summarizes the review presented in this chapter.

Table2.2. Summary of Research

SUBJECT MATTER	AVAILABILITY	REFERENCE
Dynamic Simulation of ASP	Yes	Gori et al., 2013 Flores-Alsina et al. 2014 Caniani et al., 2015 Mannina et al., 2016a Henze et al., 1987, 2000 Rieger et al., 2015 Karpinska et al., 2016 Langergraber et al., 2004 Flores- Alsina et al., 2011 Corominas et al., 2012 Guo et al., 2012 Flores- Alsina et al., 2014
Aeration Efficiency	Yes	USEPA 1989 Rosso and Stenstrom, 2006b Leu et al 2009 Rosso et al., 2005 Rosso 2008 ASCE 1992 ASCE 1997 ASCE 2006 Krampe and Krauth, 2003
Energy Systems and their Associated Costs Demand Side Management	Yes	Reardon, 1995 Palensky and Dietrich, 2011 Aymerich 2015 Rieger et al., 2015 Rosso and Stenstrom, 2005 Rosso et al., 2008 WEF, 2009. Olsson, 2012b Amand et al., 2013 Olsson, 2012a
Spatial and Temporal Marginal CO_2 Emission Intensities for the Electrical	Yes	Zivin et al., 2014

Demand		
GHG Emissions	Yes	Monteith et al., 2005 de Haas et al., 2008 Kampschreur et al. 2009 Ahn et al., 2010 Foley et al., 2010 Park et al., 2010 Flores-Alsina et al. 2011 Corominas et al. 2012 Law et al., 2012 IPCC 2006 Flores- Alsina et al., 2011 Corominas et al., 2012 Guo et al., 2012 Flores- Alsina et al., 2014
Circadian Variations and Amplification of Energy Demand, Energy cost, and Carbon emission	Yes	Sobhani et al. 2013 Gori et al., 2011 Gori et al., 2013 Mannina et al., 2016b
Optimal Aeration Control	Yes	Olsson, 2012b Amand et al., 2013 Karpinska et al., 2015 Åmand and Carlsson, 2012 Karpinska et al., 2016 Langergraber et al., 2004
Cost Implications of the Stability of Aerated Processes	No	
Performance Analysis-Simplified Equilibrium Biokinetic Model with an Appropriate Aeration Submodel Structure vs Dynamic Biokinetic Model Coupled with an Aeration Submodel Lacking Appropriate Structure	No	

CHAPTER 3: METHODOLOGY

3.1 Wastewater Treatment Process Selected

The selected plant is an upstream satellite water reclamation plant operating in the Modified Ludzack-Ettinger (MLE) configuration with 8.30×10^4 $m^3 d^{-1}$ (22 MGD) capacity. When the sewage flows beyond its capacity, the outfall sewer carries the excess water to the downstream WRRF. The removed bio-mass is conveyed to the downstream treatment plant. The plant utilizes head works, influent pumping, primary treatment, ASP secondary treatment, secondary clarifiers, and tertiary treatment. The plant's secondary treatment employs six identical parallel MLE and secondary clarifier trains. Each process train utilizes three anoxic zones, three aerobic zones, and a rectangular secondary clarifier as shown in Figure 3.1. The volumes of anoxic and aerobic zones in each train are equal to 1,020 m^3 (36,000 ft^3) and 2,268 m^3 (80,100 ft^3), respectively. The submerged depth of each bioreactor is 4.9 m (16.1 ft). The surface area of each secondary clarifier is 632 m^2 (6,800 ft^2) with a submerged depth of 2.93 m (9.6 ft).

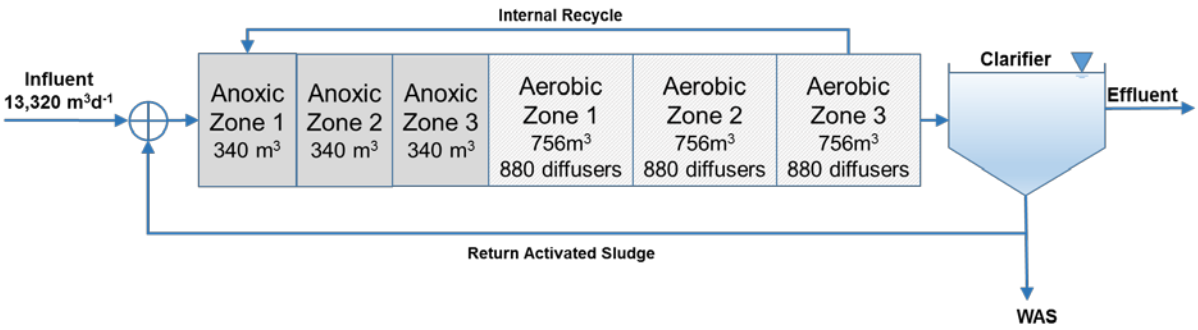

Figure 3.1. Process schematic at the selected plant for one of the six parallel trains

Primary effluent is equally distributed among the operating trains. Under normal dry-weather conditions, five process trains operate at a time and one is idling. The plant utilizes three 1,100 kW blowers, one operating at a time with a design capacity of 4.30×10^4 $Nm^3\,h^{-1}$ (27 kSCFM). Table 3.1 presents the average water quality at this plant.

Table 3.1. Average water quality at the benchmark plant for the period simulated

Plant Influent (Average Values)	
Flow (m^3d^{-1})	66.6×10^3 (17.6 MGD)
Secondary ASP (Average Values)	
BOD_{in} (mgl^{-1})	226
COD_{in} (mgl^{-1})	486
NH_4^+-N_{in} (mgl^{-1})	33.0
Organic-N_{in} (mgl^{-1})	8.3
WAS (m^3d^{-1})	2,195 (0.58 MGD)
RAS Ratio	120%
Recycle Ratio	400%
COD_{out} (mgl^{-1})	32.0
NH_4^+-N_{out} (mgl^{-1})	0.3
NO_2 + NO_3 (mgl^{-1})	4.9
MCRT (days)	4.6

3.2 Biokinetic Model and Aeration Submodel

Process simulation was conducted using a simplified equilibrium biokinetic model (ASM1) with circadian inputs of influent flow rates and constituent concentrations. ASP air requirements were simulated using process inputs and effluent water qualities identical to the benchmark plant. The effluent water quality meets the average monthly effluent limitation (AMEL) and average weekly effluent limitation (AWEL) set by State Water Resources Control Board (SWRCB) (Tentative Order R4-2017-00XX). Table 3.2 summarizes the ASP effluent water quality objectives.

Table 3.2. ASP effluent water quality objectives

BOD (mgl^{-1})	<20
TSS (mgl^{-1})	<15
Ammonia Nitrogen (as N) (mgl^{-1})	<3.7
NO_2+NO_3 (mgl^{-1})	<7.2

Oxygen transfer efficiencies were integrated into the model using a regression model developed by Rosso el al (2005) to determine α.SOTE as a function of diffuser type, tank geometry, airflow rates, and MCRT which was presented in Section 2.3.2.

3.3 Energy and CO_2 Emission Model

A model was developed to quantify the energy consumption (kWh), power demand (kW), and their associated indirect $CO_{2,eq}$ emissions ($kgCO_{2,eq}h^{-1}$). The model input includes ASP required air, temporal carbon emission intensities, system curve for the aeration

system, and local weather variables. Figure 3.2 illustrates the structure of the integrated process, energy, and CO_2 emissions model.

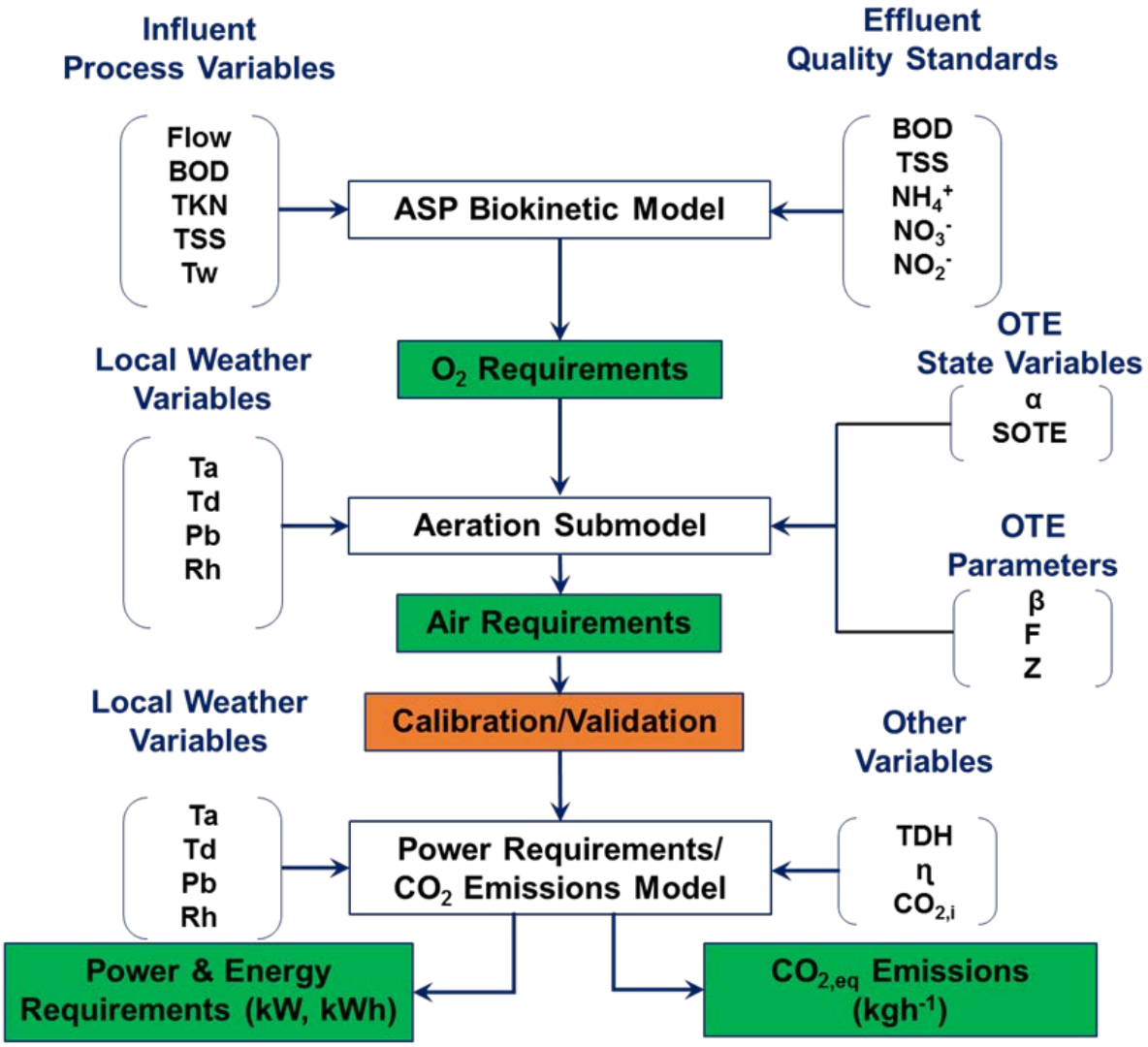

Figure 3.2. ASP integrated model structure and calibration

To quantify the energy-associated indirect $CO_{2,eq}$ emissions, the model utilizes the temporal marginal $CO_{2,eq}$ emission intensities for the electrical demand of the Western Electricity Coordinating Council (WECC) interconnection.

3.4 Circadian Amplification of Energy Consumption and TOU Economic Implications

Time-of-use electrical rates are based on the time in which customers use electricity. Energy rates vary seasonally and during off/mid/on peak hours. In this section the economic implications of the circadian amplification of energy consumption is demonstrated using a Southern California Edison tariff structure. It should be noted that the benchmark plant is not served by SCE and using this tariff is for demonstration purposes. The aim of this exercise is to demonstrate a typical case applicable to many WRRF while recognizing caveats and limitations.

The analysis was conducted using SCE 2017 TOU-8 industrial schedule rate (Option B, 2-50 kV) for summer season as the electrical rates vary drastically during summer (extreme case). Table 3.3 tabulates various charges and rates under SCE 2017 TOU-8.

Table 3.3. SCE energy charges and rates for the primary industrial customers (i.e., 2-50 kV) (SCE TOU-8, 2017)

	Delivery Service	**Generation**
Energy Charge ($/kWh/Month)		
Summer (On-Peak)	0.024	0.071
Summer (Mid-Peak)	0.024	0.047
Summer (Off-Peak	0.024	0.032
Winter (Mid-Peak)	0.024	0.046
Winter (Off-Peak)	0.024	0.036
Peak Demand Charge ($/kW/Meter/Month)		
Facilities Related	18.34	
Time Related		
Summer (On-Peak)		18.97
Summer (Mid-Peak)		3.58
Summer (Off-Peak		0
Winter (Mid-Peak)		0
Winter (Off-Peak)		0
Customer Charge ($/Meter/Month)	303.25	

3.5 Model Calibration and Verification

The model calibration involved comparison of the simulated air requirement values with the data extracted from the plant's SCADA system. During model calibration, the model was run with plant data collected from one dry-weather operation dataset (June 2016) under the steady-state condition.

The simulation was performed with the literature values of the kinetic, stoichiometric, and aeration parameters and then the results were compared with the observed field data. Discrepancies (expressed as root mean square error, RMSE) between the measured and simulated values of the output variables were minimized by adjusting ASP kinetic, stoichiometric, and aeration parameters. Four parameters (K_s, Y_H, b_H, b_n) were adjusted to calibrate the model. The selection of β and F was from usual literature values

(i.e., β = 0.98 from Metcalf, & Eddy, Inc (2014); F = 0.8 from EnviroSim Associates Ltd. User Manual for BioWin X.Y Hamilton, Ontario: EnviroSim Associates Ltd.). The values of the calibrated parameters for the steady-state simulation and literature values are compared in Table 3.4.

During validation, datasets on air flow from dry-weather operation (July 2016) were used for modelling and the results were compared and verified.

Table 3.4. Calibrated values of kinetic and stoichiometric parameters

Parameter	Unit	Literature Value	Calibrated Value
K_s	gm^{-3}	8[a]	8
b_H	d^{-1}	0.12[a]	0.12
Y_H	-	0.45[a]	0.5
b_n	d^{-1}	0.17[b]	0.17

a Henze et al. (1995); Barker and Dold (1997)
b U.S. EPA (2010)

3.6 Simulation Using a Biokinetic ASM Family Dynamic Model (BioWin)

Process simulation was conducted using the BioWin biokinetic model (ASM) with circadian inputs of influent flow rates and constituent concentrations. ASP air requirements were simulated using process inputs and effluent water qualities identical to the benchmark plant. The effluent water quality meets the average monthly effluent limitation (AMEL) and average weekly effluent limitation (AWEL) set by State Water Resources Control Board (SWRCB) (Tentative Order R4-2017-00XX) as summarized in Table 3.2. Figure 3.3 illustrates a schematic of process model developed using BioWin biokinetic dynamic model.

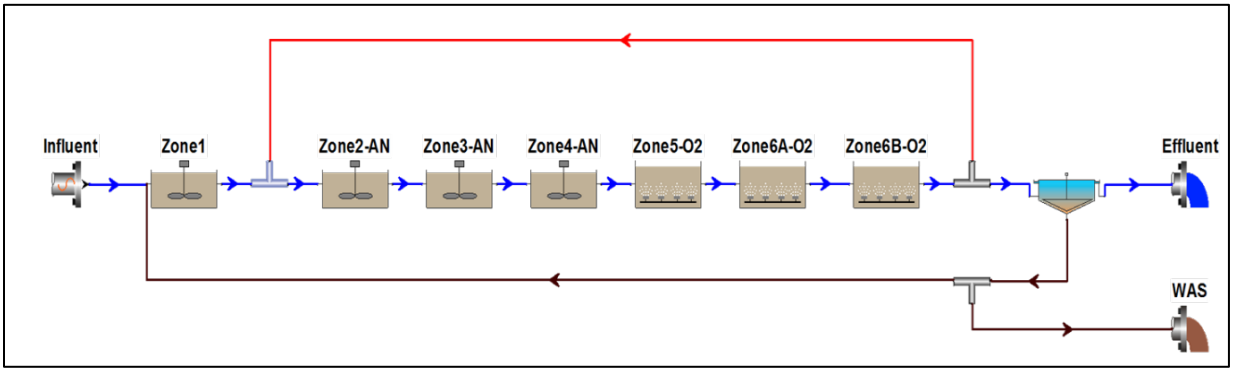

Figure 3.3. Schematic of model developed using BioWin biokinetic dynamic model

CHAPTER 4: RESEARCH PLAN

Hypothesis

The literature review and preliminary analysis from the previous chapters indicated that the simulation of the biokinetic and aeration dynamics in ASP is instrumental in understanding the intertwined relation among influent flow rates, constituent concentrations, GHG emission intensities, electrical rates, the effects on aeration/energy requirements and their associated costs and GHG emissions. The **central hypothesis** is that **using a simplified equilibrium biokinetic model with an appropriate aeration submodel structure yields a lower estimated error (expressed as RMSE) than a dynamic biokinetic model coupled with an aeration submodel lacking appropriate structure.**

The primary objective of this hypothesis is to demonstrate the significance of integrating appropriate aeration submodels into the ASM family biokinetic models to improve the performance of predictive dynamic models. We proposed completion of the following tasks to achieve the research goals:

Task 1 - Develop a simplified equilibrium biokinetic model

A simplified equilibrium biokinetic model was developed for the benchmark water resources recovery facility (WRRF) Activated Sludge Process (ASP) operating in the Modified Ludzack-Ettinger (MLE) configuration.

Task 2 - Develop an aeration submodel

An aeration submodel was developed and integrated into the abovementioned simplified equilibrium biokinetic model using a regression analysis developed by Rosso el al (2005) to determine α.SOTE as a function of diffuser type, tank geometry, airflow rates, and MCRT. The aeration parameters were further examined and fine-tuned toward developing the desired aeration submodel.

Task 3 - Calibrate/validate the developed models

The model calibration involved comparison of the simulated air requirement values with the data extracted from the plant's SCADA system. During model calibration, the model was run with plant data collected from one dry-weather operation dataset (June 2016) under the steady-state condition.

The simulation was performed with the literature values of the kinetic, stoichiometric, and aeration parameters and then the results were compared with the observed field data. Discrepancies (expressed as root mean square error, RMSE) between the measured and simulated values of the output variables were minimized by adjusting ASP kinetic, stoichiometric, and aeration parameters. Four parameters (K_s, Y_H, b_H, b_n) were adjusted to calibrate the model.

To validate the model, datasets on air flow from dry-weather operation (July 2016) were used for modelling and the results were compared and verified.

Task 4 - Simulate the process using a commercial dynamic model

Dynamic simulation was conducted using the BioWin biokinetic model (ASM) for the WRRF ASP operating in the MLE configuration.

Task 5 - Evaluate and compare the performance of the models

This task was the core of the proposed research. It involved assessing the performance of biokinetic models, integrating an appropriate aeration submodel.

Upon the completion of tasks 1 thru 4, further analysis was conducted to assess and compare the performance of ASM family dynamic models against the simplified equilibrium biokinetic model with an integrated aeration submodel that we developed.

Task 6 – Investigations over practical applications

As part of this complimentary research, we investigated practical applications such as the effects of flow equalizations on ASP energy and carbon footprint. The study was presented at the CWEA Annual Conference 2016. Additionally, we have initiated a study on the cost implications of the stability of aerated processes and the effects of extracellular polymeric substances (EPS) on oxygen transfer efficiency and secondary settling. Such cost implications include the additional costs associated with the inability of maintaining DO set points and the adverse effects on settling in secondary clarifiers. An abstract was submitted to WEFTEC Annual Conference, 2018.

CHAPTER 5: RESULTS AND DISCUSSION

5.1 Variations in ASP Influent Characteristics

The dry-weather (summer) data analysis indicates that the diurnal influent flow increases rapidly from a minimum of 4.46×10^3 $m^3 d^{-1}$ (1.2 MGD) at 6:00 to a near maximum of 15.25×10^3 $m^3 d^{-1}$ (4.0 MGD) at 12:00. The peak COD, ammonia (NH_4^+-N), and Total Kjeldahl Nitrogen (TKN) concentrations occur between 10:00 to 12:00 nearly coinciding with the peak flow. The concurrency of these circadian variations amplifies carbonaceous/nitrogenous constituent loadings into the process trains between 10:00 to 12:00 resulting in a peak air requirement that will be discussed later.

Figure 5.1 illustrates the circadian variations in flow and key ASP influent constituent concentrations (COD, NH_4^+-N, and TKN) in each process train during the summer dry-weather conditions.

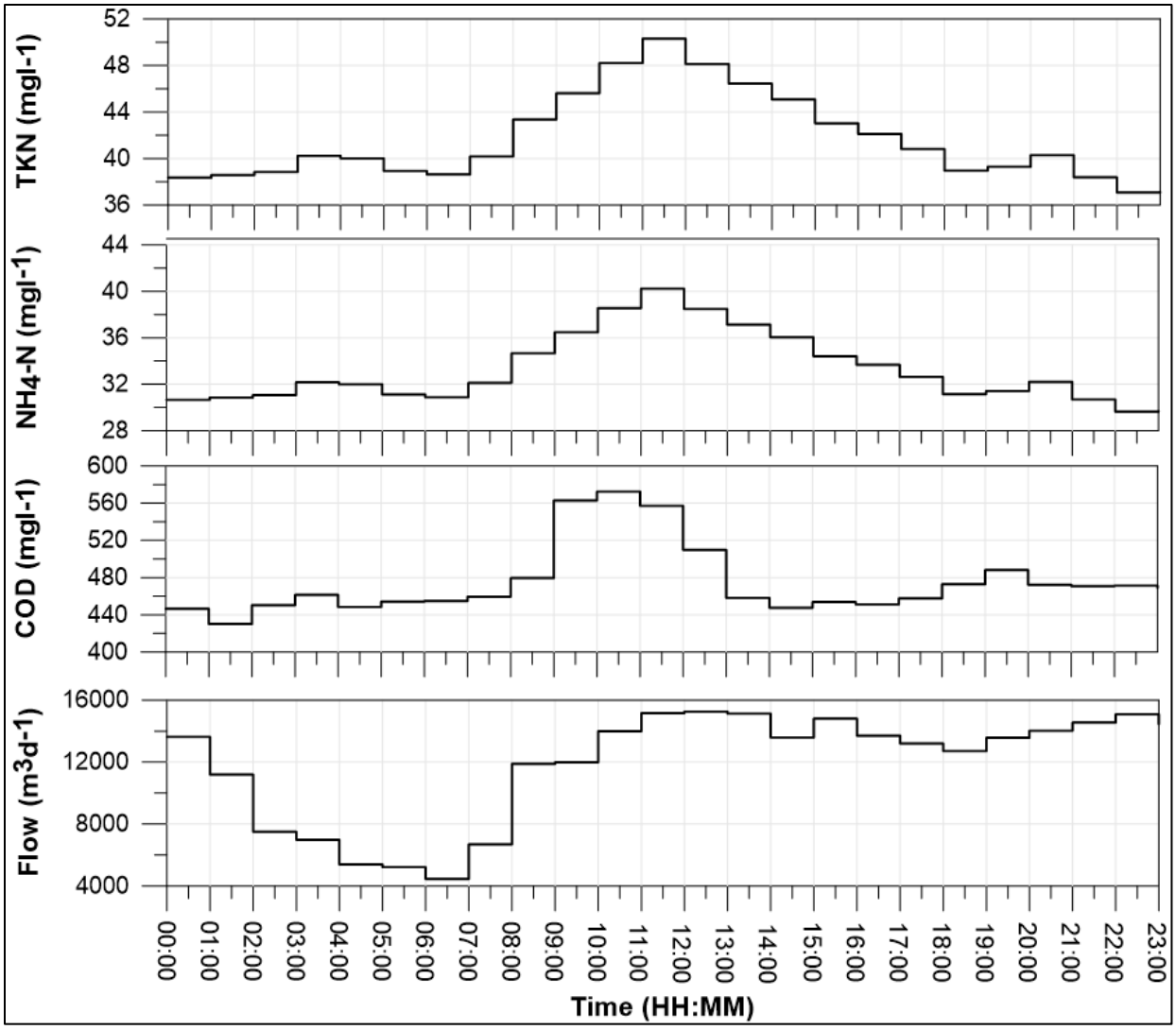

Figure 5.1. Circadian variations in ASP influent characteristics for each process train

5.2 Dynamic Simulation of ASP Air Requirements

The ASP was simulated with circadian inputs of flow rates and constituent concentrations with a DO set point of 2.0 mgl^{-1}. The model was calibrated by the comparison of its results with the observed data from the plant. Figure 5.2 compares the simulated air requirements (kscfm) with the observed plant data for each process train. The results indicate that from 19:00 to 2:00, the simulated and observed air discharges are fairly matched and DO levels are fairly sustained at 2.0 mgl^{-1} set point (Figure 5.2). As influent flow starts declining rapidly at 2:00, the observed air discharges from the plant exceed the simulated results. This is possibly an over-aeration condition due to a sudden decrease in air requirements and limitations associated with the turn down ranges of aeration blowers in throttling the supplied air. Both curves reach their troughs at around 6:00 and start to rise after that. Due to the over-aeration condition, the observed DO levels within this timeframe (2:00 to 8:00) exceed the set point (2.0 mgl^{-1}) with a peak DO of 2.8 mgl^{-1} at 7:00. In later hours, both datasets present a significant increase.

The increase in air requirements is attributed to the increase in influent flow rates and constituent loadings prompting aeration blowers to ramp up to maintain the DO set point. The observed air discharges from the plant are at lower levels in comparison to the simulated results during this timeframe (8:00 to 14:00). This is possibly an under-aeration condition due to a sudden increase in air requirements and limitations associated with the aeration blowers to ramp up the supplied air effectively. Correspondingly, the observed DO drops to 1.3 mgl^{-1} at 10:00 which is indicative of under-aeration condition.

The simulated air requirement starts declining from its peak at 11:00, 7.84×10^3 Nm^3h^{-1} (4.88 kscfm), as the influent flow rates and constituent loadings decrease. There are sporadic over and under-aeration between 15:00 to 1:00 possibly due to abrupt fluctuations in influent flow and the lag time associated with instrumentation & control (I&C) and aeration system in response.

The over- and under-aeration in ASP will result in excessive energy use and incompliance with effluent water quality standards, respectively. Effluent water quality limit exceedances are not observed in the benchmark plant as the under-aeration water qualities deficiencies are offset by over-aeration effluent qualities.

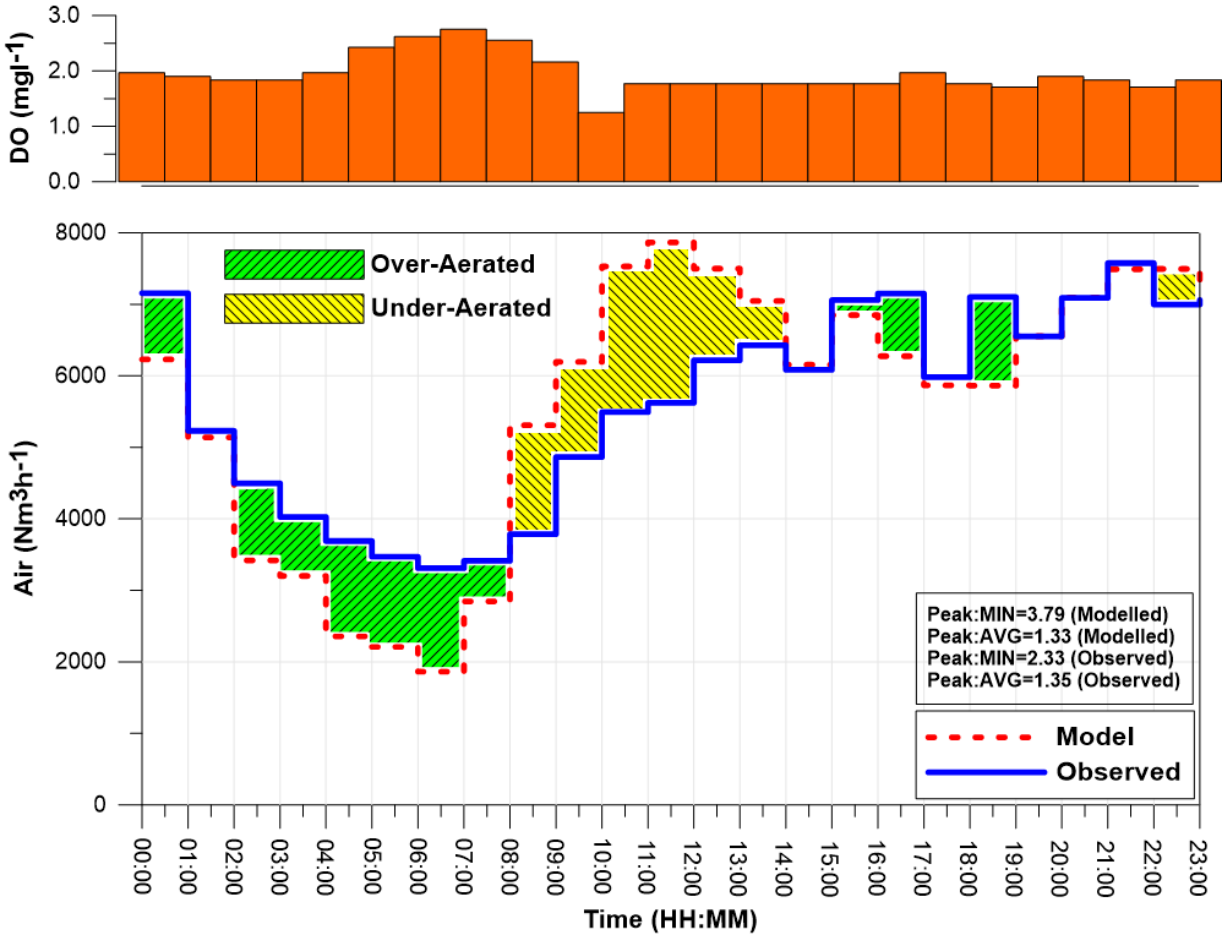

Figure 5.2. Comparison between the modelled air requirements and plant's data

As previously discussed, α.SOTE is a function of diffuser type, tank geometry, airflow rates, and MCRT (Rosso et al., 2005). Figure 5.3 shows that variations in α.SOTE are inversely proportional to air flow rate. The peak α.SOTE (0.116) and the trough of air requirements ($1.863x10^3$ Nm^3h^{-1}) occur concurrently. Similarly, the trough of α.SOTE (0.096) occurs during near peak air requirements at 21:00.

The plot in Figure 5.2 illustrates the discrepancy between the recorded air discharge and the modelled air required for discharge, a combination of the technological limits of the blower battery, the varying DO during the diurnal cycle, and the generalized correlation (Equation 2-20) used in our model to estimate alpha. The discrepancy in the two curves appears in the form of areas between the two curves, even though the peak/average ratios are consistent (1.33 and 1.35 for modelled and observed air, respectively). In fact, we modelled the diurnal cycle using the plant DO pattern and a constant pattern, and the results exhibited minor differences, leading to the conclusion that a combination of blower limitations and alpha estimation contributed to the discrepancy.

The issue of under- and over-aeration at this facility was confirmed through interviews with the operations personnel, who attributed the cause to the blower operations, limited in latitude of air flow discharge. At this point it is impossible to assign weight to the two causes of the discrepancy in Figure 5.2 (i.e., the contribution from blower limitations vs. the error committed in modelling through the use of Equation 2-20 instead of a site-specific correlation).

One of the goals of this work is to underline the importance of using modelling as a tool to quantify such site-specific issues and to assign a proper weight to the personnel

reports on operating limitations. More, the placement of flow meters and the compounding uncertainty of multiple metering units, may lead in general to conclude that the metered air flow at a full-scale facility should in fact be a bandwidth of possible flow rates, rather than a single point measurement. Finally, despite the regular calibration of the flow meters in this facility, in many others there could be no recent calibration of the metering units, leading to further uncertainty on the measured air discharge Alex et al (2016). For all the considerations above, the quantification of the diurnal variations of aeration energy and of the associated indirect CO_2 emission, presented below, is based on the modelled air flow. Hence, the results presented below would only change in absolute value by changing the basis of calculation (i.e., actual air flow vs. modelled air flow) but not in significance.

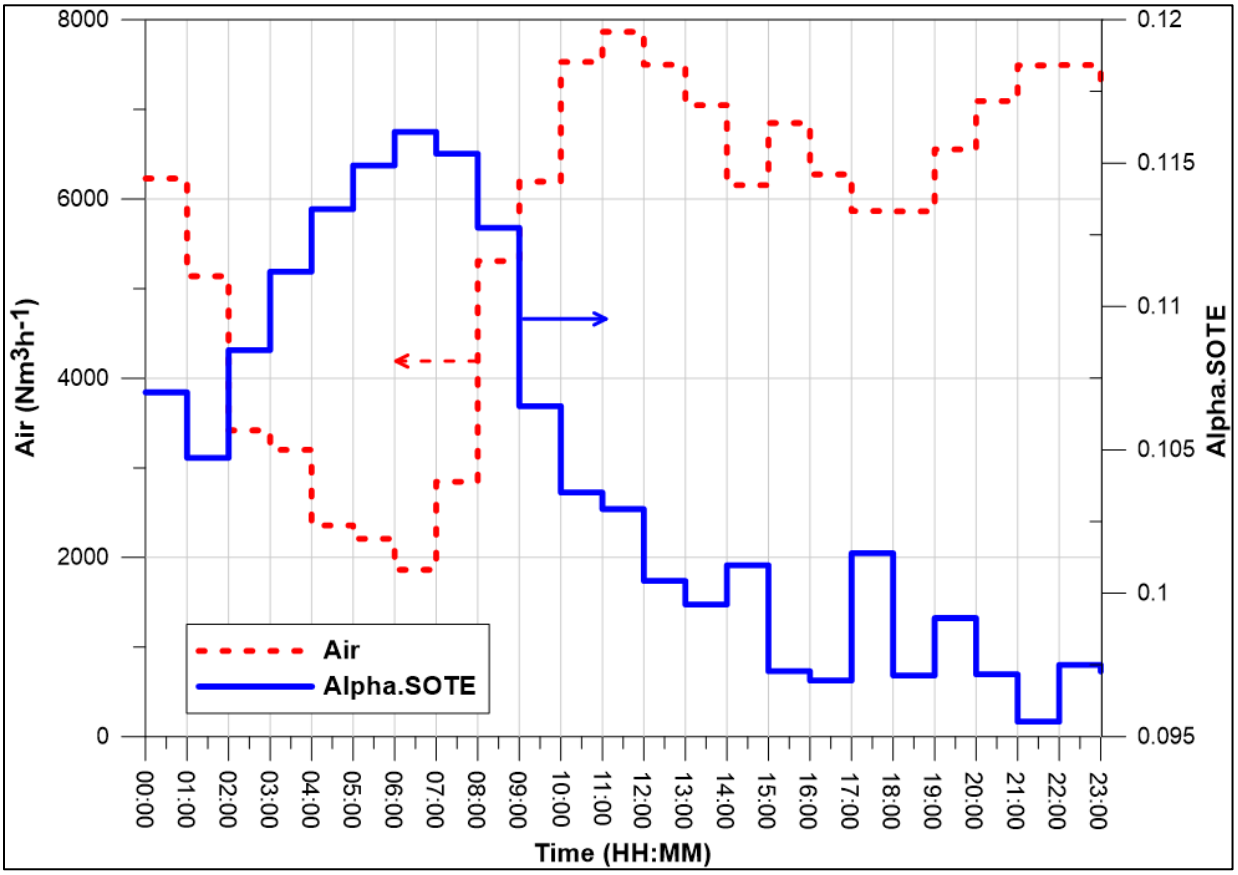

Figure 5.3. Evolution of α.SOTE vs modelled air flow during a diurnal cycle

5.3 Model Performance Evaluation

The performance of the calibrated model versus the observed air flow rates was assessed using statistical performance indices such as the root mean square error (RMSE) and coefficient of determination (R^2) as presented in Figure 5.4. A RMSE value of zero and R^2 value of unity represents an ideal model performance. The RMSE and R^2 values for the abovementioned modelling scenarios are fairly identical as shown in Figure 5.4.

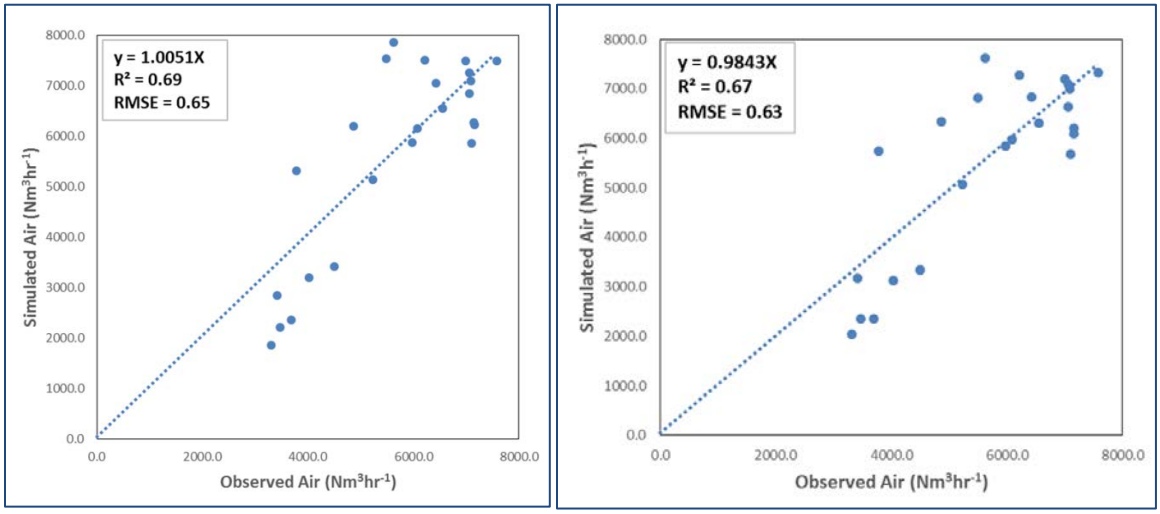

Figure 5.4 a. DO = 2mgl^{-1} Figure 5.4 b. DO as observed

Figure 5.4. Model performance evaluation

5.4 Circadian Amplification of Air Requirements

Circadian Amplification of Air Requirements

To demonstrate the amplification of air requirements in ASP, circadian variations in influent flow, COD, TKN, α.SOTE, and simulated air requirement are compared collectively as shown in Figure 5.5. To make the scale of variations comparable, variables have been normalized by dividing them by the daily average values. The results indicate that the normalized flow and COD concentration vary between 0.38 and 0.9 in their troughs, and 1.29 and 1.20 at their peaks, respectively. Normalized TKN concentration varies between 0.93 in its trough and 1.21 at its peak.

Figure 5.5 indicates that peak values for COD, TKN, and air requirements occur during influent peak flow rates. The peak air flow rate is fairly concurrent with peak COD with 1-hour lag time. The lag time could be attributed to the overarching effect of hydraulic retention time (HRT) and constituents' loadings.

Under normal conditions, low influent hydraulic loadings coincide with low constituent concentrations (e.g., BOD and NH_4). Conversely, high influent hydraulic loadings coincide with high constituent concentrations. The concurrency of these variations amplifies the alterations among the air requirements. The amplification in the air requirement is shown in Figure 5.5 with normalized air requirement fluctuating between 0.33 in its trough (6:00) and 1.39 at its peak (11:00).

The increase of bCOD can decrease the α value (Leu et al., 2009), and concurrently the increase of air flow has a similar impact on standard oxygen transfer efficiency (α.SOTE) (Rosso et al., 2005). Therefore, α.SOTE typically is expected to vary over the

diurnal cycle in a reciprocal pattern to the process load. The diurnal cycle of α.SOTE is presented in Figure 5.5. The peak normalized COD (1.2 at 10:00), and peak normalized air requirements (1.39 at 11:00) correspond with a normalized α.SOTE of 0.99. Conversely, peak normalized α.SOTE (1.12 at 6:00) fairly coincides with the trough of normalized COD (0.9 at 4:00), and trough of normalized air requirements (0.33 at 6:00).

The effect of amplification could be observed as the peak/minimum ratio increases from 3.4 to 4.2 for the influent flow and air requirements, respectively as illustrated in Figure 5.5.

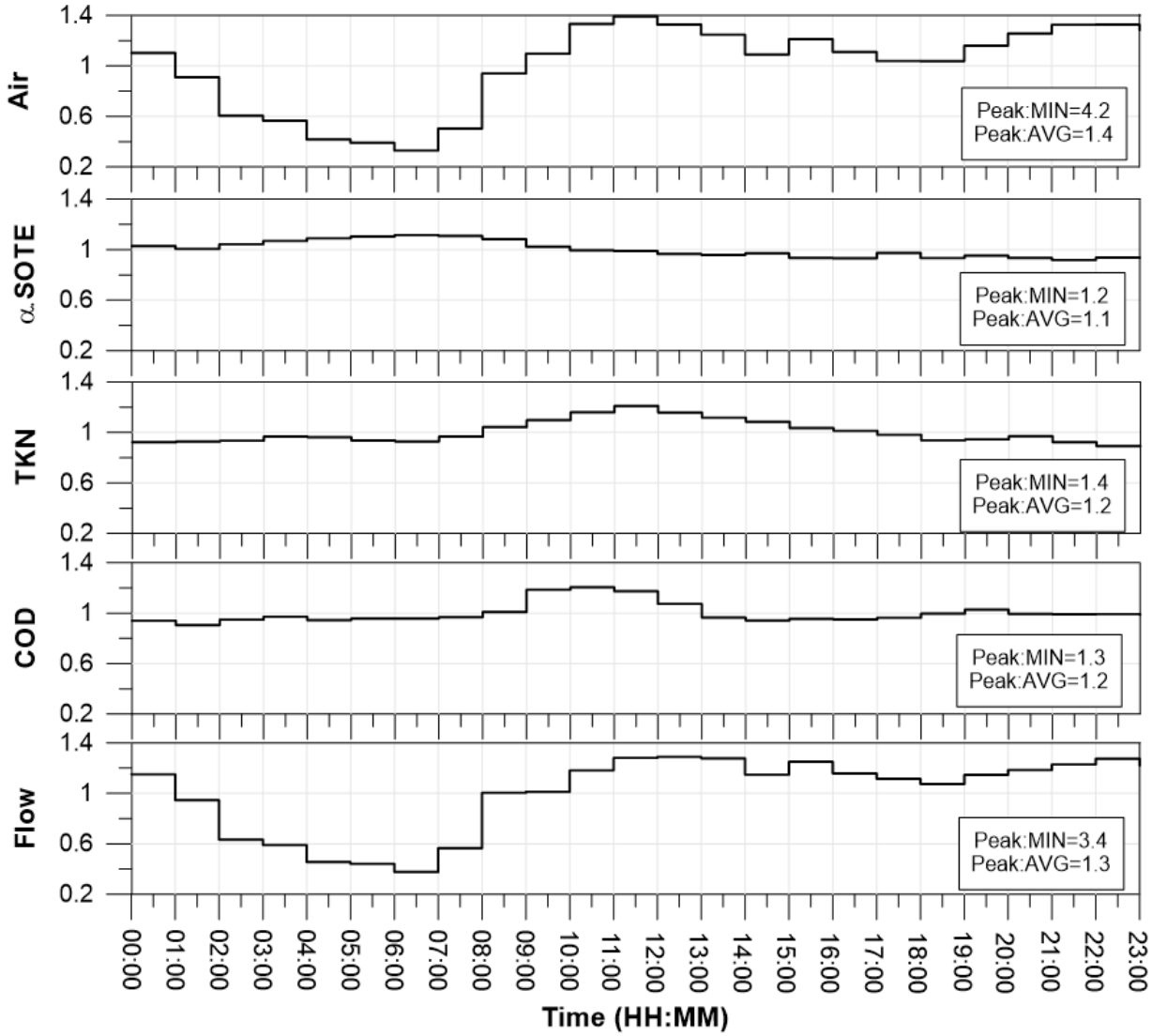

Figure 5.5. Normalized values of influent flow, BOD, TKN, oxygen transfer efficiency (α.SOTE) and modelled air flow vs. time

5.5 Circadian Amplifications of the Energy Demand and $CO_{2,eq}$ Emissions

The concurrency of ASP influent flow, COD and TKN peak values with the trough of α.SOTE induces an amplified circadian air requirements response which was presented in Figure 5.5. Accordingly, the ASP power demand and the associated indirect $CO_{2,eq}$ emissions follow the same pattern as our model indicates. The spatial and temporal variations in carbon emission intensities [$kgCO_{2,eq}(kWh)^{-1}$] suggested by the regression model (Zivin et al) were discussed earlier. The concurrency of the circadian variations in $CO_{2,eq}$ emission intensities with the influent flow and energy demand is significant. It further amplifies the circadian variations in $CO_{2,eq}$ emissions as illustrated in Figure 5.6.

Peak influent flow of $15.0x10^3$ m^3d^{-1} (4.0 MGD), and peak $CO_{2,eq}$ emission intensity [0.4 $kgCO_{2,eq}(kWh)^{-1}$] occur at 11:00 corresponding to peak $CO_{2,eq}$ emission of 64.0 $kgCO_{2,eq}h^{-1}$ and peak energy demand of 160 kWh. Figure 5.6 also indicates that the troughs of ASP influent flow, $4.46x10^3$ m^3d^{-1} (1.18 MGD) at 6:00, and $CO_{2,eq}$ emission intensity [0.3 $kgCO_{2,eq}(kWh)^{-1}$ at 7:00] are fairly concurrent (1-hour lag time). Correspondingly, the troughs of energy demand (37.9 kWh) and $CO_{2,eq}$ Emission (12.2 $kgCO_{2,eq}h^{-1}$) at 6:00 are concurrent. Circadian amplification of $CO_{2,eq}$ emissions is more pronounced due to the combined effect of emission intensities and energy demand as shown in Figure 5.6.

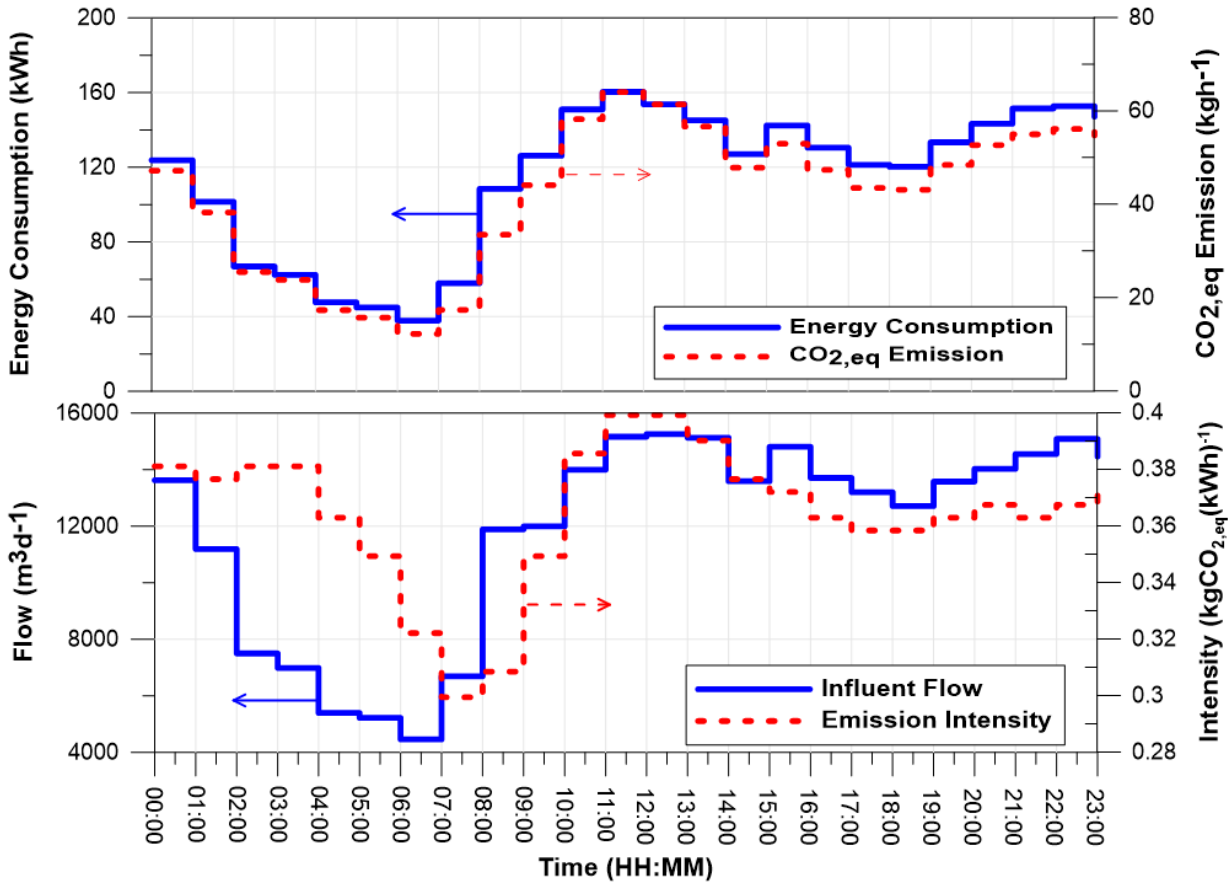

Figure 5.6. Circadian amplification of indirect $CO_{2,eq}$ emissions

To make the scale of variations comparable, all variables were normalized by their daily average values. The results indicate that the normalized energy consumption varies between 0.33 and 1.4 while the normalized $CO_{2,eq}$ emission varies between 0.29 and 1.51. The observed amplification effect is due to the concurrency of variations in energy consumption and emission intensities. Figure 5.7 illustrates the variations in normalized variables, indicating amplification in $CO_{2,eq}$ emissions. The amplification effect could be observed as the peak/minimum ratio increases from 3.4 to 4.2 and then 5.2 for the influent flow, hourly energy consumption, and hourly emission rates, respectively as illustrated in Figure 5.7.

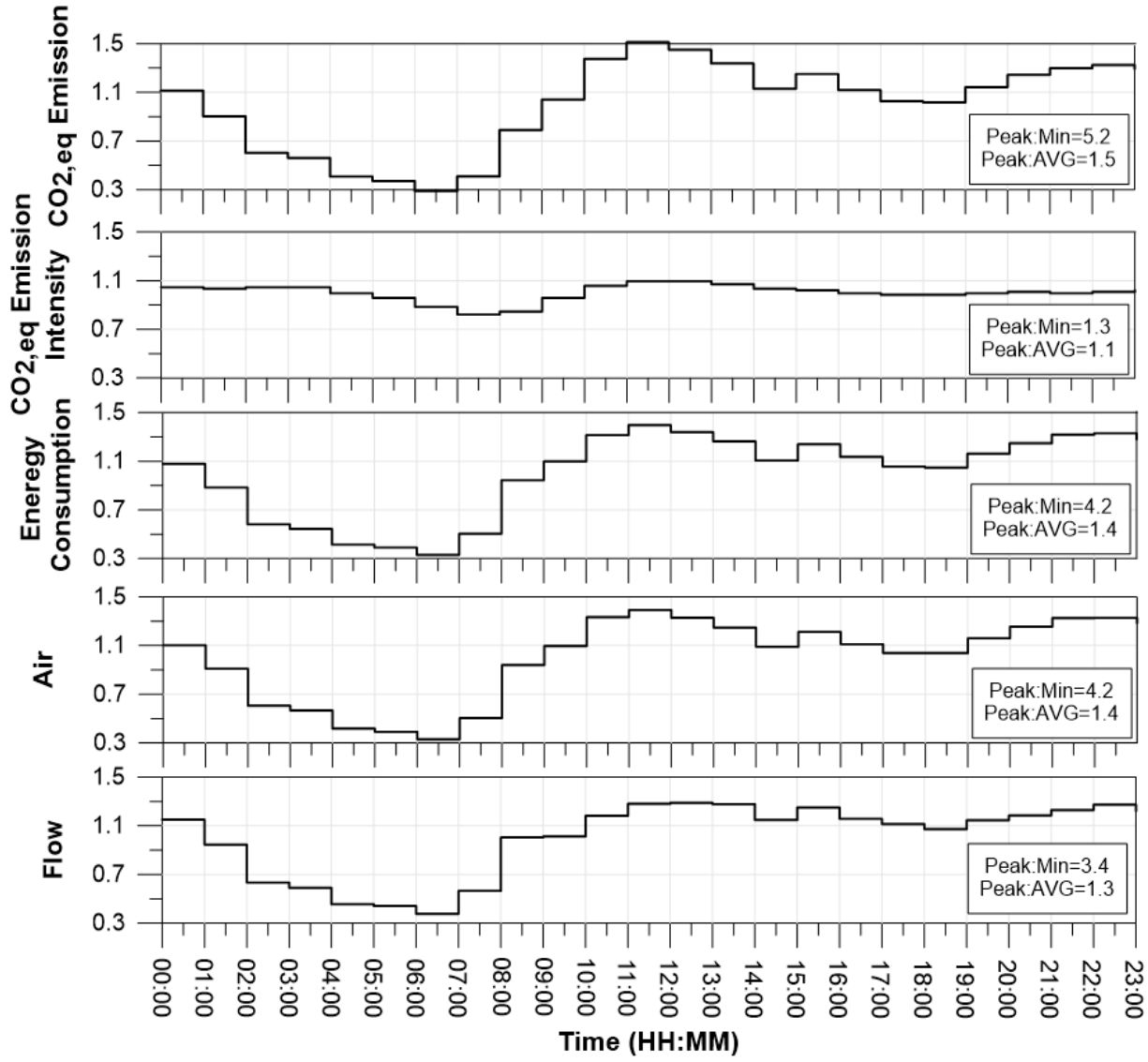

Figure 5.7. Normalized circadian variation in flow, air, energy consumption & $CO_{2,eq}$ emissions

5.6 TOU Energy Consumption and Economic Implications

The results of our analysis present a circadian amplification in hourly energy costs of ASP as shown in Figure 5.8. The peak electrical consumption (160 kWh) occurs during the Mid-Peak period rates ($0.071/kWh) while the trough of energy consumption (37.9 kWh) falls within Off-peak rates ($0.056/kWh). It is expected that by including monthly peak demand charges, energy costs will be further amplified. Our analysis indicates that energy tariff structures can drastically impact the operating energy costs of ASP.

Our analysis also indicates that the peak $CO_{2,eq}$ emissions occur during the peak hours as illustrated in Figure 5.8. The effect of amplification could be observed as the peak/minimum ratio increases from 4.2 to 5.2 for the hourly energy consumption (kWh) and hourly emission rates ($kgCO_{2,eq}h^{-1}$), respectively as illustrated in Figure 5.8.

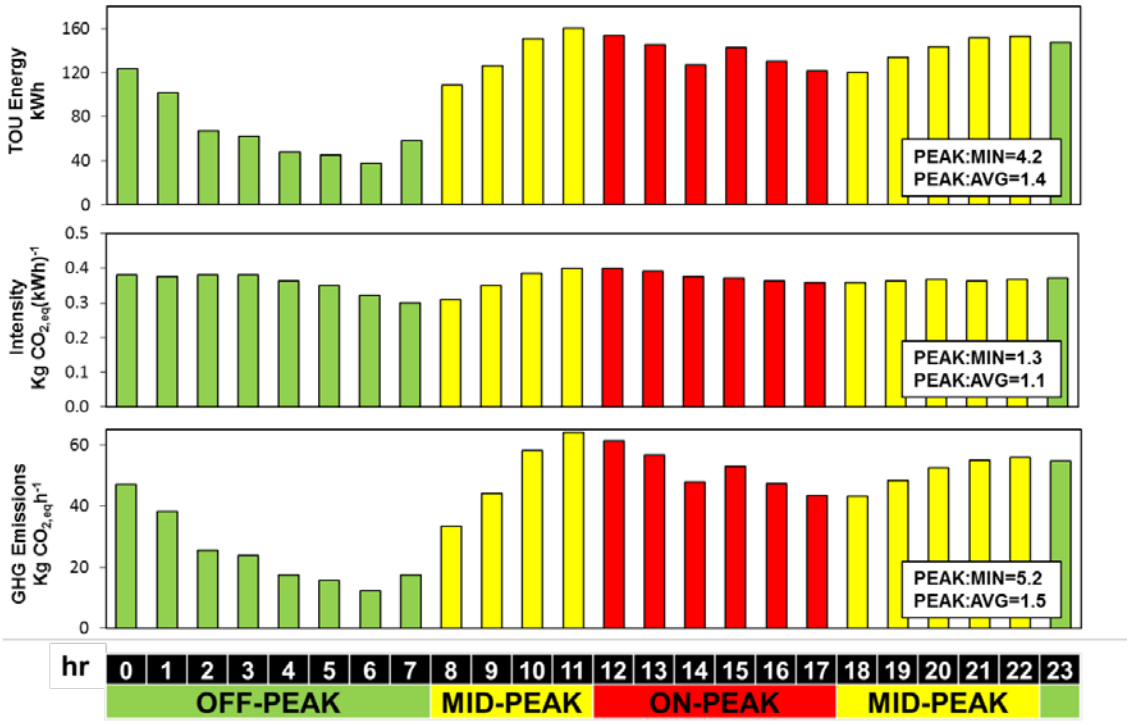

Figure 5.8. Circadian amplification of time of use energy (kWh), carbon emission intensity [$kgCO_{2,eq}(kWh)^{-1}$], and indirect greenhouse gas emissions ($kgCO_{2,eq}\,h^{-1}$)

5.7 Performance Analysis of Dynamic Model (BioWin) vs Simplified Model

The performance of the calibrated simplified equilibrium biokinetic model (with appropriate aeration submodel) and calibrated BioWin ASM family biokinetic dynamic model were assessed and compared against the observed air flow rates using statistical performance indices such as the root mean square error (RMSE) and coefficient of determination (R^2) as presented in Figure 5.9. A RMSE value of zero and R^2 value of unity represents an ideal model performance. The performance analysis indicates that the performance of simplified equilibrium biokinetic model with an integrated aeration submodel (R^2 = 0.69 & RMSE = 0.65) exceeds the performance of the BioWin biokinetic dynamic model (R^2 = 0.41 & RMSE = 0.86) as shown in Figure 5.9.

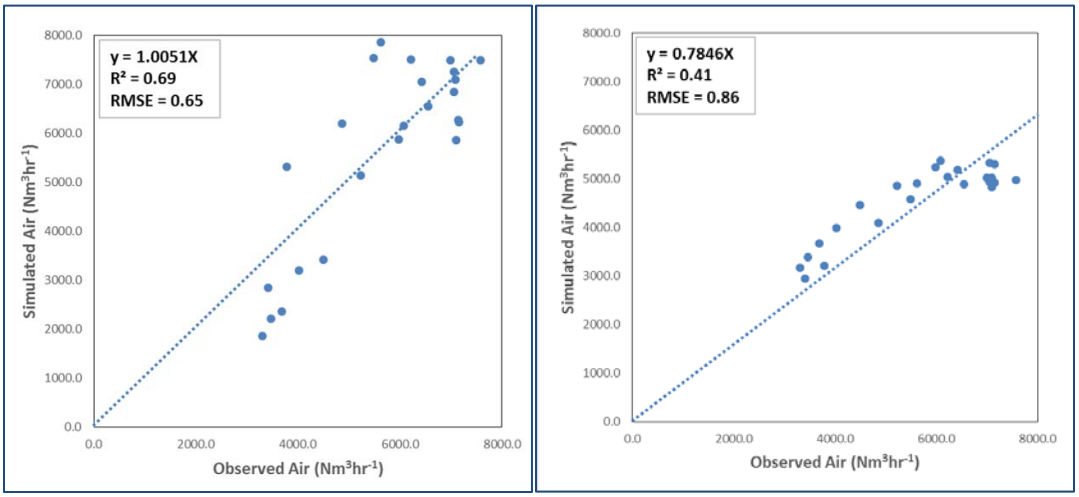

Figure 5.9 a. Simplified Equilibrium Model Figure 5.9 b. BioWin Dynamic Model

Figure 5.9. Model performance evaluation (Simplified equilibrium vs BioWin)

CHAPTER 6: SUMMARY AND CONCLUSIONS

We developed a simplified equilibrium biokinetic model for the benchmark water resources recovery facility (WRRF) Activated Sludge Process (ASP) operating in the Modified Ludzack-Ettinger (MLE) configuration.

Additionally, we developed an aeration submodel which was integrated into the abovementioned simplified equilibrium biokinetic model, using a regression analysis developed by Rosso el al (2005) to determine α.SOTE as a function of diffuser type, tank geometry, airflow rates, and MCRT. The aeration parameters were further examined and fine-tuned toward developing the desired aeration submodel.

The simplified equilibrium biokinetic model with the integrated aeration submodel was calibrated by comparing the simulated air requirement values with the data extracted from the plant's SCADA system. To validate the model, different datasets on air flow were used for modelling and the results were compared and verified.

Dynamic simulation was conducted using the BioWin biokinetic model (ASM). The performance of the ASM dynamic model was compared against the simplified equilibrium biokinetic model with an integrated aeration submodel that we developed.

Our analysis indicates that circadian variations in influent flow and constituents' concentrations substantially affect the dynamics of air requirements, energy consumption and their associated energy costs and GHG emissions in ASP as depicted in Figure 6.1.

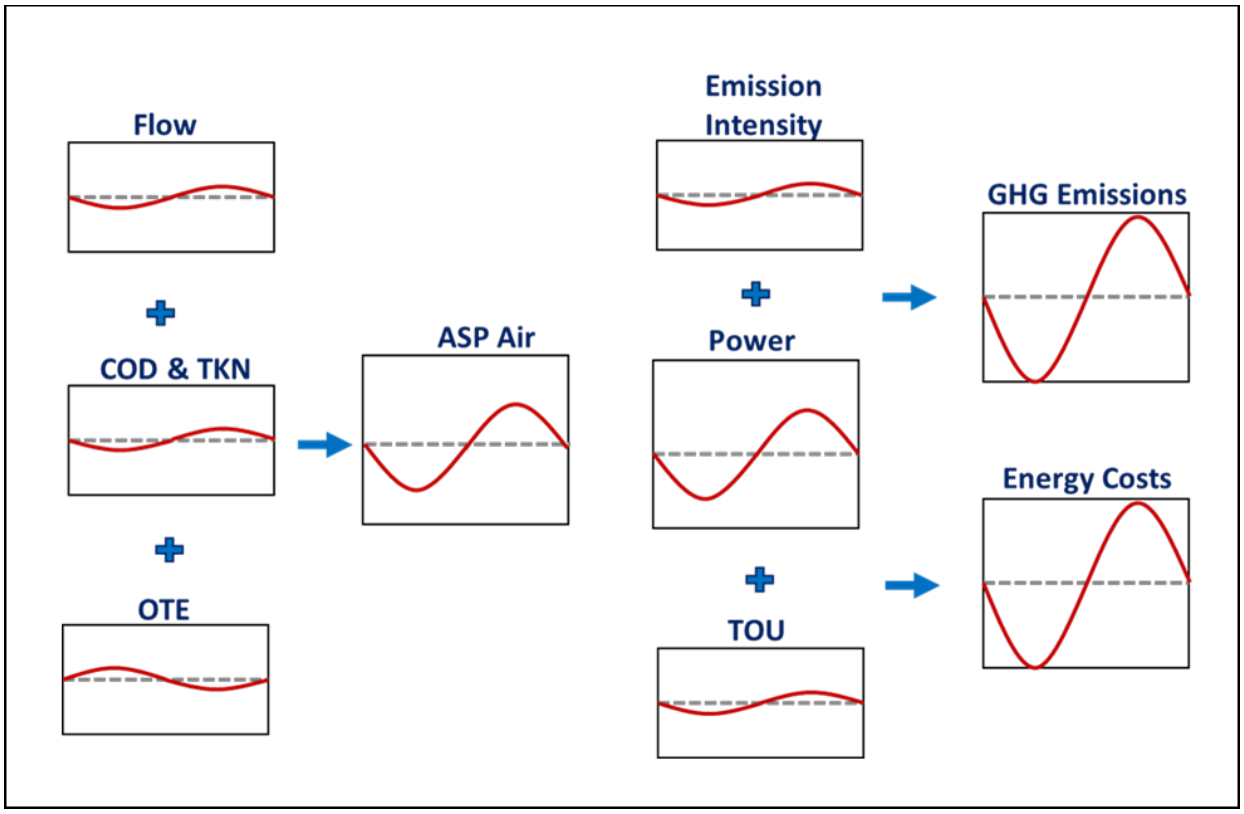

Figure 6.1. Graphical depiction of circadian amplification in ASP

We have analyzed the effects of circadian variations in influent flow and carbonaceous/nitrogenous constituent concentration on the aeration requirement and the associated energy consumption, energy costs, and carbon emissions in an ASP operating in the MLE configuration.

The spatial and temporal variations in marginal carbon emissions were quantified, using carbon emission intensities from the regression model developed by Zivin et al. (2014).

The economic implications of the TOU energy consumption associated with ASP aeration was also demonstrated using a Southern California Edison tariff structure.

The results indicate that the concurrency of the circadian variations in flow and constituent concentrations amplifies the loadings into the process trains, and causes amplification in air requirements. Meanwhile, circadian variations in influent bCOD and air requirements induce a reciprocal response in α.SOTE which further amplifies the air requirements by reducing OTE during high BOD loadings.

The variations in air requirement induce a circadian amplification response in energy consumption, occurring during the TOU electrical peak hours with high electrical rates. The concurrency of energy consumption and TOU electrical rates further amplifies the aeration energy associated costs.

The temporal variations in carbon emission intensities overlap with those of energy consumption. The concurrency of circadian variations in energy consumption and carbon emission intensities further exacerbates the ASP carbon emissions.

The analysis also indicates that the performance of simplified equilibrium biokinetic model with an integrated aeration submodel exceeds the performance of the BioWin biokinetic dynamic model.

Understanding the intertwined relation among influent flow rates, constituent concentrations, GHGs emission intensities, TOU electrical rates, and aeration parameters is instrumental for the successful implementation of ASP energy and cost efficiency measures. Mechanistic dynamic models are essential tools to optimize design and operation of WRRF and to develop strategies aimed at reducing energy consumption and GHG emissions.

CHAPTER 7: IMPLICATIONS ON FULL-SCALE FACILITIES

7.1 Effects of Flow Equalization on ASP Energy and Carbon Footprint

Description/Application of Flow Equalization

The inherent variations of the influent flow and carbonaceous/nitrogenous constituents' concentrations in the wastewater treatment plants can be dampened by utilizing flow equalization basins.

Figure 7.1.1 and Figure 7.1.2 illustrates the application of the flow equalization in wastewater treatment plants. In the in-line configuration (Figure 7.1.1), all of the flow passes through the equalization basin. This arrangement can be used to achieve a considerable amount of constituent concentration and flow dampening (Metcalf, & Eddy, Inc, 2014).

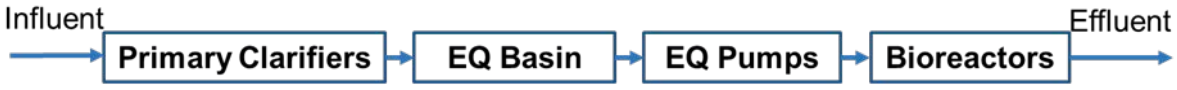

Figure 7.1.1. In-line equalization configuration

In the off-line configuration (Figure 7.1.2), only flow above some predetermined limit is diverted into the equalization basin. Although pumping requirements are minimized in this arrangement, the amount of constituent concentration dampening is considerably reduced. Off-line equalization is sometimes used to capture the firs flush from combined collection systems (Metcalf, & Eddy, Inc, 2014).

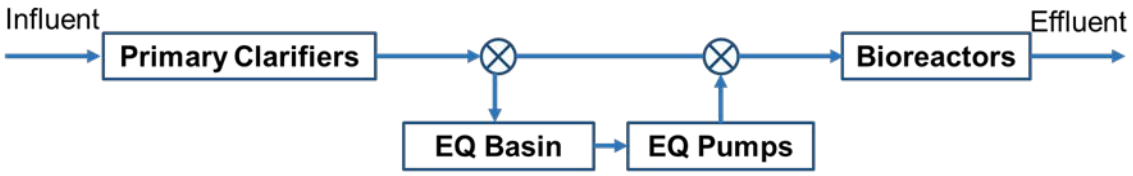

Figure 7.1.2. Off-line equalization configuration

The Benefits of Flow Equalization

Variations in influent flow and constituents' concentrations in the wastewater treatment plants may result in non-compliant effluent quality even in well-designed systems (Beler Baykal et al., 1994).

Several benefits have been attributed to the use of flow equalization in wastewater treatment plants (Foess et al., 1977).

- Dampens fluctuations in the organics and nutrients constituent concentration and fluxes in the influent wastewater, providing more stable retention periods and biomass concentrations in the bioreactors.
- Improves performance of primary and secondary clarifiers by leveling hydraulic variations and reducing peak flow rates; allowing for utilization of smaller clarifiers.
- Improves the settleability of wastewater.
- Simplifies manual and automated control of operations, such as chemical feeding, disinfection, and sludge recycle pumping.
- Mitigates shock loads to primary clarifiers, bioreactors, and secondary clarifiers by dampening concentrated waste streams.
- Allows for lowering energy costs by leveling power demand for pumping and aeration.

As discussed previously, ASP is an energy intensive process and is associated with the direct and indirect release of GHG. It requires higher rates of aeration during the peak flow and peak carbonaceous/nitrogenous constituent loadings to be able to maintain the DO set-points, and to meet the effluent water quality limits.

The literature review in the previous sections indicated that the ASP energy costs are strongly influenced by TOU charges and peak power demand penalties. Moreover, the indirect marginal emissions of electrical demand vary temporally. Flow equalization can reduce the energy cost and indirect marginal emissions of the electrical demand associated with the ASP by shifting the peak influent flow to the periods with lower TOU charges and marginal emissions.

Leu et al. (2009) showed that significant savings can be realized if the plant flow is shifted to diurnal periods associated with lower power rates. An operating strategy of limiting peak flows can saves up to 8% during the peak season, 5 to 6% during average winters and summers, and 6% on a yearly basis. If the flow can be adjusted to shift the low loading period, which ordinarily occurs at night, to the power rate peak hours in the afternoon, up to 31% of savings can occur in the peak season, or 16% on a yearly basis (Leu et al., 2009).

Application of the flow equalization in the wastewater treatment plants is limited due to the land requirements, capital costs, additional operation and maintenance, and nuisance problems.

Design Considerations

The design of flow equalization systems is concerned with the following considerations (Metcalf, & Eddy, Inc, 2014).

Optimal Location

The optimal location varies based on the wastewater influent characteristics, the treatment process, and land requirements and availability. The equalization basins can be sited upstream or downstream of the primary treatment systems. Equalization systems located downstream of the primary treatment causes fewer odor, solids settling, and scums issues.

If located upstream of primary treatment, sufficient mixing and aeration must be provided to prevent solids settling and odor problems.

Determination of Storage Volume Requirements

The required storage volume is determined by conducting an inflow cumulative analysis. In practice, the required storage volume will be larger than that theoretically determined to allow for continuous operation of the aeration and mixing equipment, to accommodate recycle streams, and to provide contingency for diurnal flow variations.

Configuration

For in-line equalization systems, it is important to use a geometry that allows for continuous-flow stirred-tank reactor.

Mixing and Air requirements

Proper mixing and aeration in equalization systems is crucial to prevent solids settling and preventing the wastewater from becoming septic and odorous.

The mixing requirements range from 0.004 to 0.008 kWm^{-3} for a medium strength municipal wastewater with a TSS of approximately 210 mgl^{-1}.

Aeration requirements range from 0.01 to 0.015 $m^3m^{-3}min^{-1}$ to maintain aerobic conditions.

Using the BioWin (ASM) model, four in-line equalization scenarios were simulated: (1) Referenced scenario without flow equalization; (2) operation with an integrated equalization basin with equalization system aeration and mixing not required; (3) operation with an integrated equalization basin with equalization system aeration required and mechanical mixing not required, and (4) operation with an integrated equalization basin with both aeration and mechanical mixing required for equalization system.

Figure 7.1.3 illustrates a schematic of the process model developed using BioWin with an integrated flow equalization system.

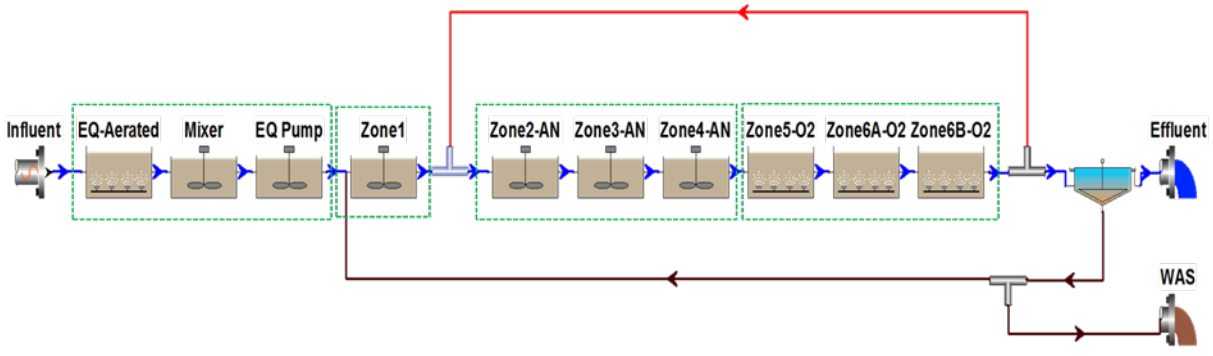

Figure 7.1.3. Schematic of the model developed with an integrated flow equalization system

The required equalization basin storage volume was determined by conducting an inflow cumulative analysis as shown in Figure 7.1.4. The analysis indicates that 1,703 m^3 (0.45 million gallons) is required for the equalization basin storage volume.

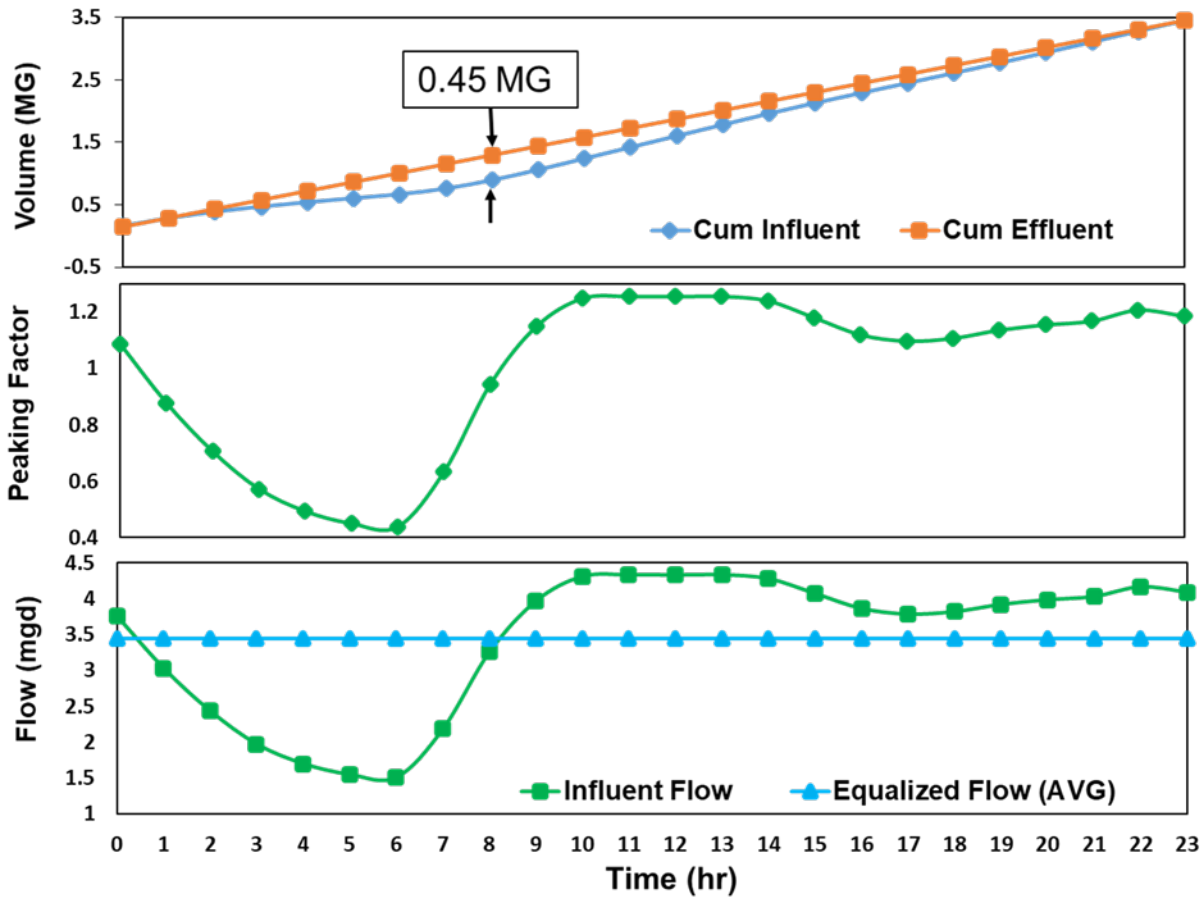

Figure 7.1.4. Schematic mass diagram for the determination of the required equalization basin storage volume

The power requirements were calculated based on the ASP aeration and flow equalization system pumping, aeration, and mixing combined power requirements for each modelling scenario.

Table 7.1.1 summarizes the average power requirements and the potential savings for each modelling scenario. The results show significant savings (25%) for the best-case scenario (Scenario No.2, operation with an integrated equalization basin with aeration and mixing not required for equalization system).

Table 7.1.1. Summary of the power requirements and potential savings

Operation Scenarios	**AVG Power Requirements (kW)**	**AVG Savings**
1. Current operation-No equalization	100	-
2. Flow equalization-no aeration, no mixing	75	+25%
3. Flow equalization with aeration, no mixing	100	0
4. Flow equalization with aeration and mixing	106	-6%

The analysis demonstrated that operation under Scenario No. 3, operation with an integrated equalization basin with equalization system aeration required and mechanical mixing not required, will not achieve any power savings.

Scenario No.4, operation with an integrated equalization basin with both aeration and mechanical mixing required for equalization system, presents the worst-case scenario in terms of power requirements. The power requirements increases by 6% in this scenario due to the power demand for equalization system's aeration and mechanical mixing. Figure 7.1.5 illustrates the power requirements break-down for each scenario.

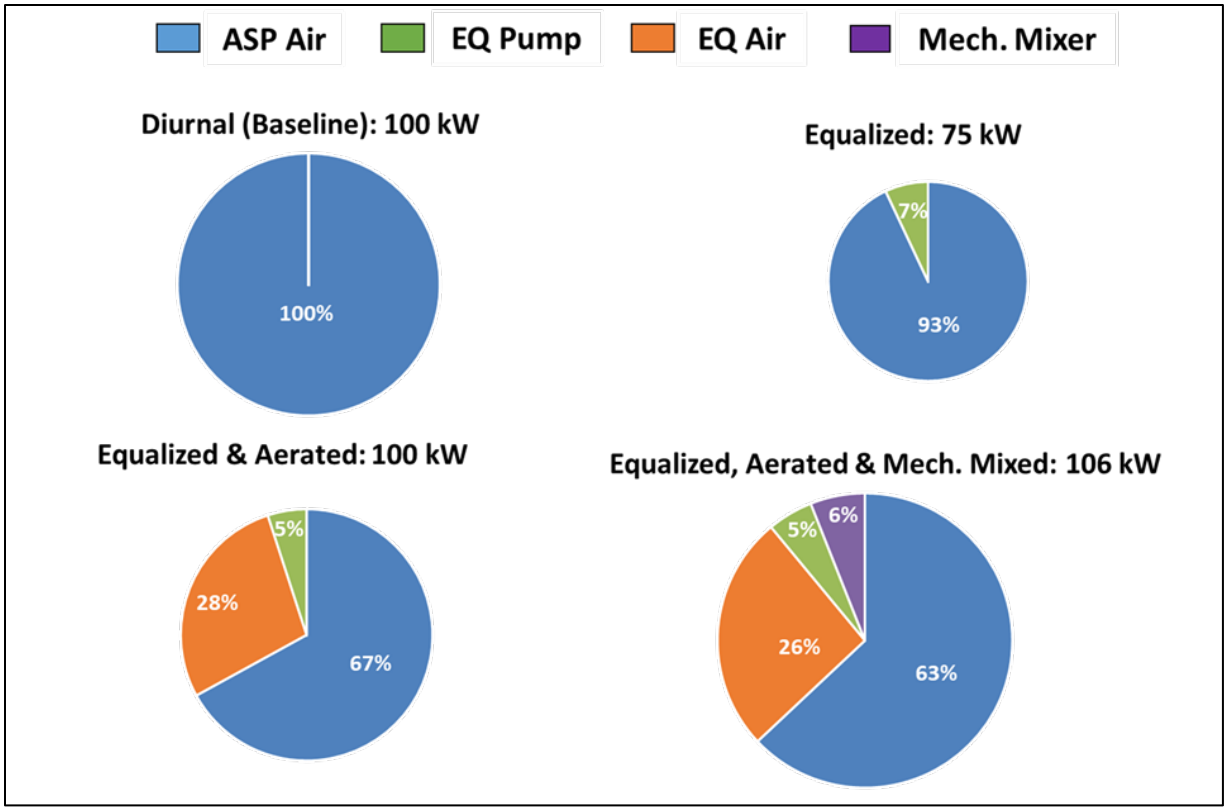

Figure 7.1.5. Comparison of equalized and non-equalized power requirements

The flow equalization has an additional advantage for reducing greenhouse gas emissions. As discussed previously, the indirect marginal emissions of electrical demand vary temporally. Flow equalization can reduce the energy cost and indirect marginal emissions of the electrical demand associated with the ASP by shifting the peak influent flow to the periods with lower TOU charges and marginal emissions.

The average marginal $CO_{2,eq}$ emissions were calculated based on the power requirements calculated previously for each modelling scenario and the indirect marginal emission intensities of electrical demand for WECC (Zivin et al., 2014).

Table 7.1.2 summarizes the average indirect marginal $CO_{2,eq}$ emissions and the potential reductions for each modelling scenario. The results show significant reductions

(19%) for the best-case scenario (Scenario No.2, operation with an integrated equalization basin with aeration and mixing not required for equalization system).

The analysis demonstrated that operation under Scenario No. 3, operation with an integrated equalization basin with equalization system aeration required and mechanical mixing not required, will slightly reduce the marginal $CO_{2,eq}$ emissions (2.7%).

Scenario No.4, operation with an integrated equalization basin with both aeration and mechanical mixing required for equalization system, presents the worst-case scenario in terms of marginal $CO_{2,eq}$ emissions generated. Under this scenario, the marginal $CO_{2,eq}$ emissions increased by 5.4% due to the power demand for equalization system's aeration and mechanical mixing.

Table 7.1.2. Summary of the $CO_{2,eq}$ emissions and potential reductions

Operation Scenario	**AVG $CO_{2,eq}$ Emission (kgh^{-1})**	**AVG Reductions**
1. Current operation-No equalization	37	-
2. Flow equalization-no aeration, no mixing	30	+19%
3. Flow equalization with aeration, no mixing	36	+2.7%
4. Flow equalization with aeration and mixing	39	-5.4%

Figure 7.1.6 illustrates the diurnal variations in power requirements (kW) for each modelling scenario. It shows drastic diurnal variations in power requirements for Scenario No. 1 (reference) and dampening effect of the flow equalization in other scenarios.

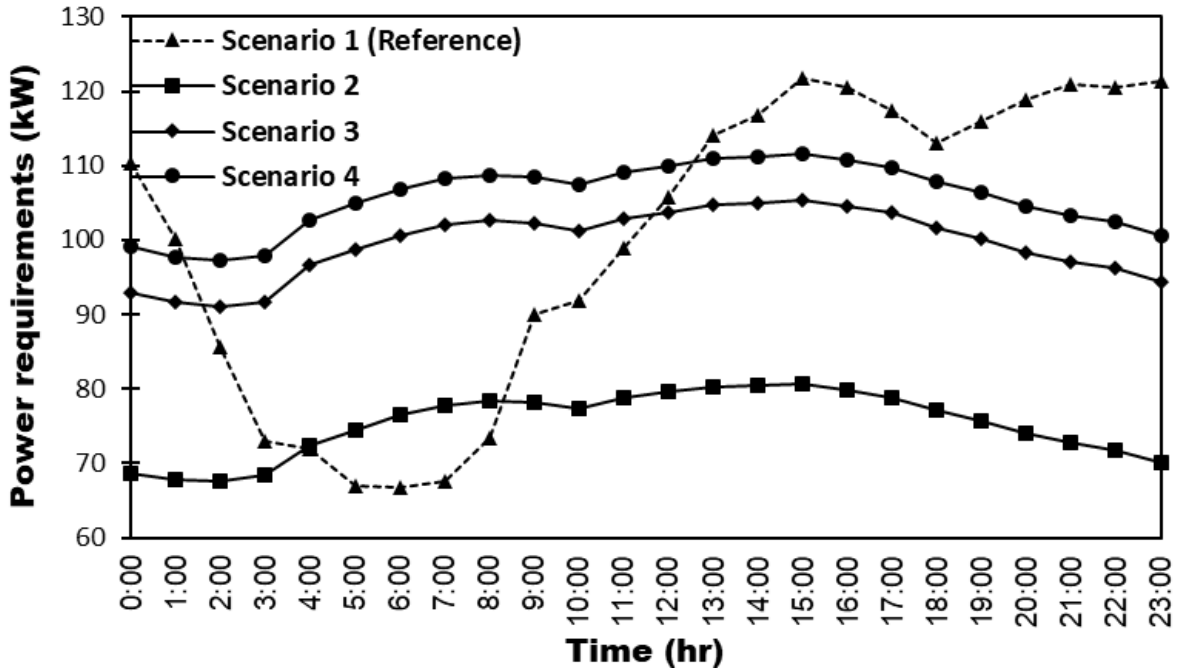

Figure 7.1.6. Diurnal variations in power requirements

Figure 7.1.7 illustrates the diurnal variations in indirect $CO_{2,eq}$ emissions (kgh^{-1}) for each modelling scenario. It shows drastic diurnal variations in $CO_{2,eq}$ emissions for Scenario No. 1 (reference) and dampening effect of the flow equalization in other scenarios.

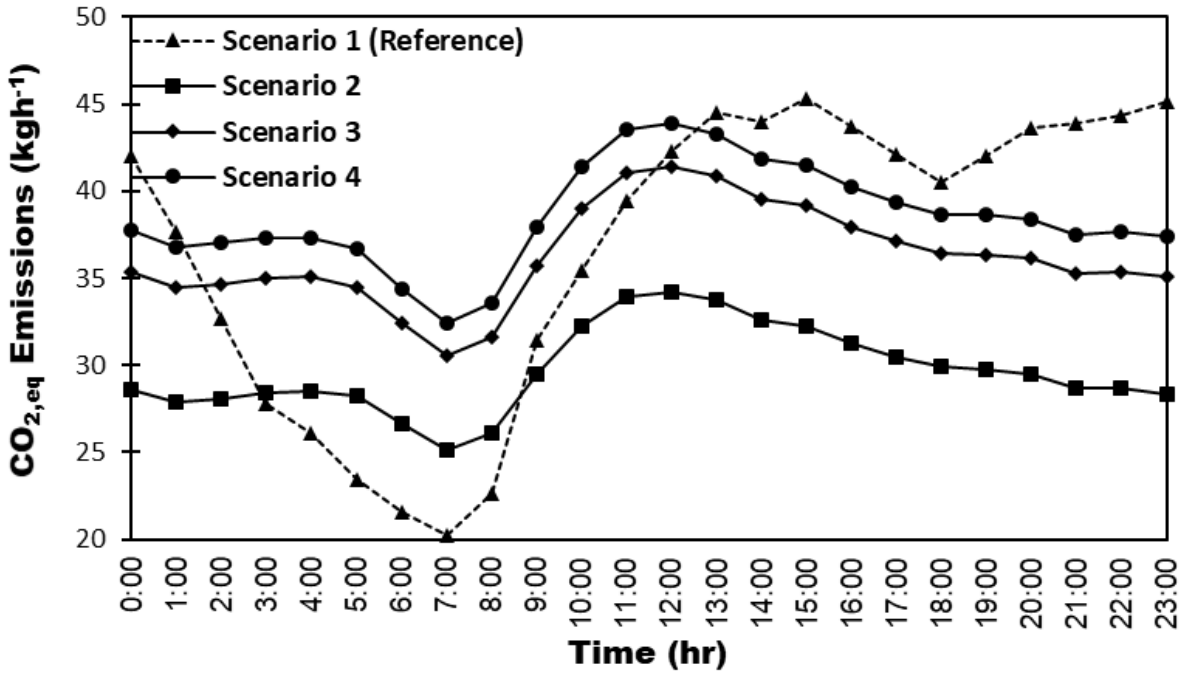

Figure 7.1.7. Diurnal variations in $CO_{2,eq}$ emissions

As part of this ongoing research, an abstract was submitted to CWEA Annual Conference, 2016. Further analysis will be conducted using BioWin biokinetic model with the aeration submodel developed as part of this effort to explore the cost implications of the flow equalization in WRRF.

7.2 Carbon Capture and Management Strategies: Role of Extracellular Polymeric Substances (EPS) on Oxygen Transfer and Secondary Settling

BNR processes are characterized by longer SRT, lower food-to-mass ratio (F/M), and lower protein to polysaccharide content ratio, which results in close to starving conditions for microorganisms. The starving conditions drive the EPS to exhibit much lower negative surface charges. The absence of negative surface charges in EPS may avoid the repulsion of surfactants, promoting their adsorption in the EPS matrix (Van Winkle et al., 2017), strengthening the hypothesis that the adsorption is the main mechanism controlling the observed aeration improvement in longer SRT conditions. Similarly, Tomczak-Wandzel et al., (2009) demonstrated the importance of the adsorption capacity of BNR sludge by showing an increase of absorption capacity when the presence of surfactants was decreased (Tomczak-Wandzel et al., 2009).

The role of EPS on the sludge settling performance is also being slowly elucidated. Recent studies have demonstrated that the quantity of the EPS has no clear influence on the settling performance (measured by the SVI) (Liao et al., 2001; Liu and Fang, 2003; Zhang et al., 2014). On the other hand, the quality of the EPS (composition, hydrophobicity, zeta potential, etc.), which is intrinsically related with the SRT, has the biggest impact. Therefore, as it has been recorded previously, SRT seems to have the most relevant impact, dictating EPS composition and characteristics, thus, concurrently controlling process stability (expressed as settling performance).

It is the aim of this study to identify the best balance between operational conditions promoting the best composition of EPS for both aeration efficiency, which could be

improved nearly 50% when nitrifying configurations are used, and settling performance, which may be maximized at shorter SRT.

Full-scale studies. Bioaugmented (Receiving nitrifying waste AS sludge) and non-bioaugmented secondary reactors are installed and operated in parallel with a residual DO of 0.5 to 1.0 mg/L. 100 % of waste activated sludge (WAS) from the biological nutrient removal (BNR) stage is recycled to the bioaugmented reactor, while the non bioaugmented reactor operates normally without receiving any WAS recycling.

Off-gas analysis. Oxygen transfer in process conditions in both full-scale studies was measured using the off-gas technique according to the ASCE testing protocol (ASCE, 1997). Off-gas measurements were taken in triplicates along the 140m in length, with a total of 15 sampling locations.

Data base library. The dataset is based on more than 20 plants nationwide and different flux-averaged off-gas measurements. All the plants were treating municipal wastewater, and wide range of diffuser ages and models (ceramic discs, domes and plates, membrane discs, tubes, and panels) was encountered.

Discussion. Figure 7.2.1 illustrates the results collected from more than 40 WRRFs in the US to show a comprehensive representation of the relationship between SVI and SRT. From the populated data, two distinct zones can be differentiated. Both zones seem to be strictly dependent on the EPS quality and corresponding process stage phases. The first zone, corresponding to low SRT values, shows the progressive improvement of the SVI with the increase in SRT.

The progressive production of EPS creates stronger flocs and facilitates the bioflocculation, EPS production will not be restricted since soluble COD is still available in the influent. Also, the rate at which the EPS is produced seems to generate two zones within SRTs values lower than 10 days. SRT values lower than 1.5 days deliver a low performance settling velocities (>120 mg/L SVI), which may be related the incapacity to generate a stronger and stable EPS due to the limited short time bacteria are in the system. On the other hand, an SRT between 1.5 to 5 days seems to be the most effective range to promote good EPS characteristics and enhance solid separation. However, as the SRT increases, an almost linear decrease on the settling properties of the sludge is observed. This second zone which ranges from excellent settling conditions (80) to bulking potential (150), shows how increasing EPS exposure time to starved bacteria promotes the progressive endogenous hydrolysis of the EPS. Increasing SRT may also promote the increase of those bacteria able to sustain themselves with less biodegradable substrates (EPS), by metabolizing EPS instead of soluble COD. Ramadani et al 2010 also suggested that longer SRT may favor the proliferation of endogenous bacteria instead of ordinary heterotrophic ones.

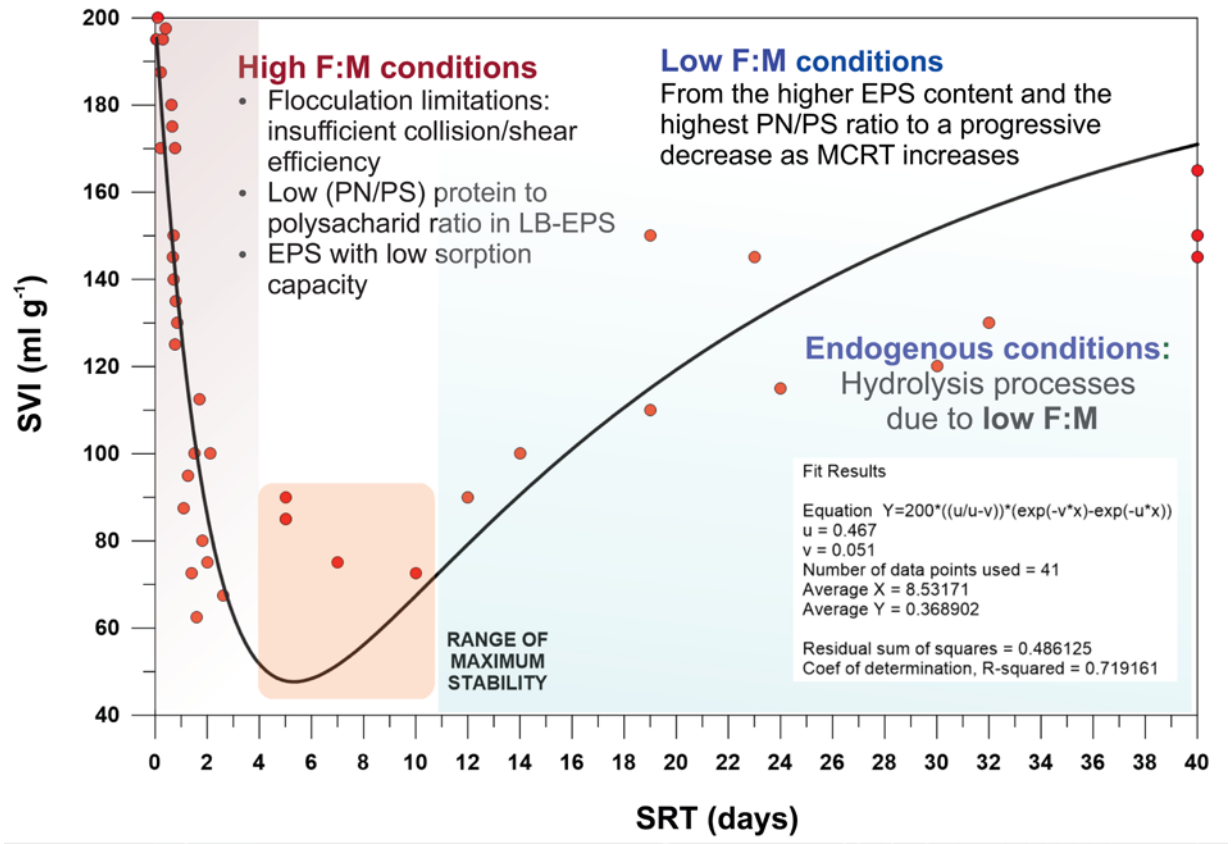

Figure 7.2.1. Observed correlation between SRT and settling volume index (SVI). Two differentiate zones with their corresponding trends depending on the EPS (phase) can be identified (Garrido-Baserba et al, 2018 submitted to WEFTEC Annual Conference).

On the other hand, the effect of using nitrifying sludge (EPS with distinct characteristics) on the oxygen transfer efficiency was also studied in two different full-scale studies (Figure 7.2.2).

Figure 7.2.2 shows the difference in α values between those reactor passes also receiving nitrifying sludge (i.e., bioaugmented) and those without (i.e., receiving only non-nitrifying sludge). A significant improvement in oxygen transfer efficiency can be observed when nitrifying sludge was used. An approximately 30-38% improvement in aeration efficiency indicators can be observed for the bioaugmented passes in comparison to non-

bioaugmented ones. The improvement is hypothesized by the increase of the EPS adsorption capacity and the concurrent removal of surfactants. The findings on the limitations and operational balance between the best EPS characteristics for each process will be further detailed on the full paper.

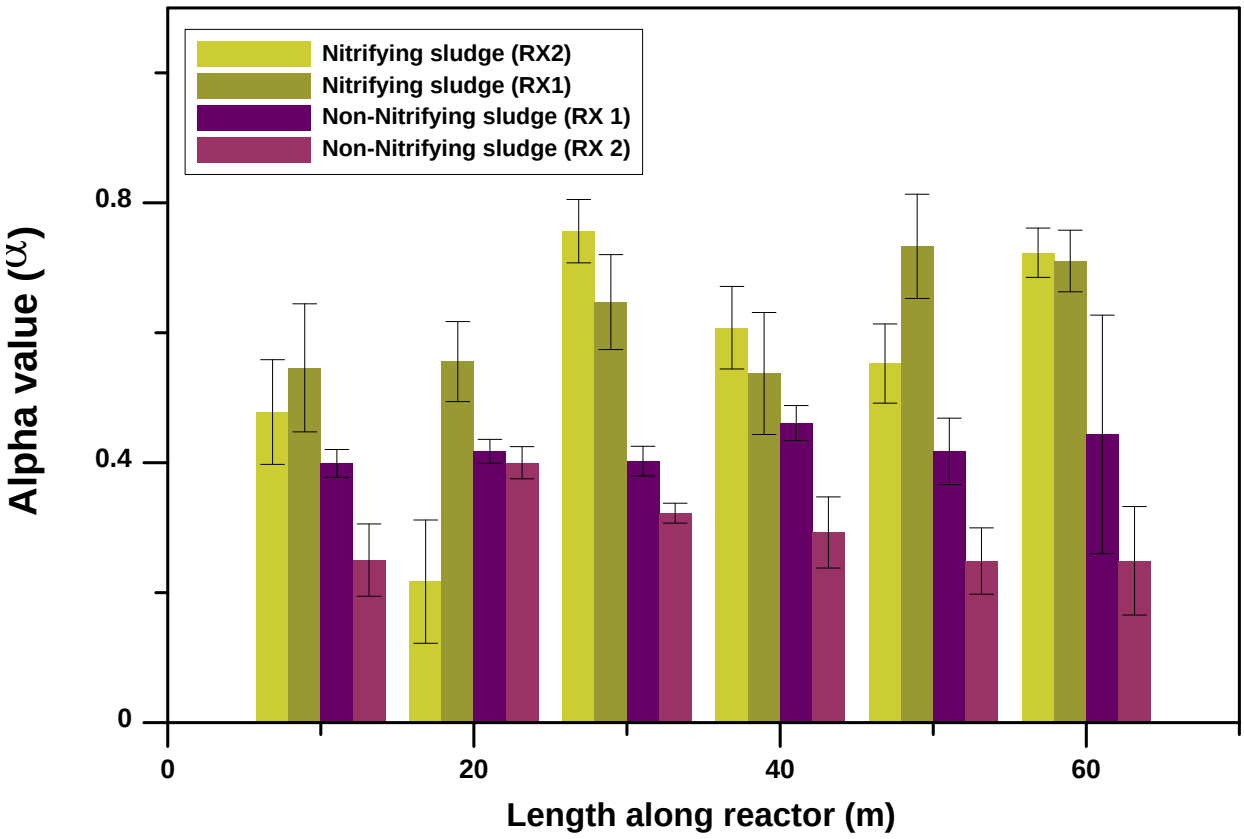

Figure 7.2.2. Comparison of oxygen transfer efficiency in secondary systems with and without sludge with nitrifying characteristics at full-scale. Alpha (α) values were measured at different locations along four different channel (green-like bars represent addition of nitrifying sludge and purple-like two non- nitrifying) (Garrido-Baserba et al, 2018 submitted to WEFTEC Annual Conference).

CHAPTER 8: REFERENCES

Abu-Orf, M., Bowden, G., Pfrang, W., & Metcalf & Eddy. (2014). *Wastewater engineering: treatment and Resource recovery*. G. Tchobanoglous, H. D. Stensel, R. Tsuchihashi, & F. Burton (Eds.). McGraw Hill Education.

Ahn, J. H., Kim, S., Park, H., Rahm, B., Pagilla, K., & Chandran, K. (2010). N2O emissions from activated sludge processes, 2008– 2009: results of a national monitoring survey in the United States. *Environmental Science & Technology*, *44*(12), 4505-4511.

Alex, J., Rieger, L., Schraa, O. (2016) Comparison of Advanced Fine-Bubble Aeration Control with Respect to Energy Efficiency and Robustness, *Proc. WEFTEC Conference*, New Orleans, LA.

Åmand, L., Olsson, G., & Carlsson, B. (2013). Aeration control–a review. *Water Science and Technology*, *67*(11), 2374-2398.

Åmand, L., & Carlsson, B. (2012). Optimal aeration control in a nitrifying activated sludge process. *Water research*, *46*(7), 2101-2110.

American Society of Civil Engineers - ASCE (1984, 1991, 2006). *Measurement of Oxygen Transfer in Clean Water*. ASCE 2-91, American Society of Civil Engineers, New York

ASCE (1997) Standard Guidelines for In-Process Oxygen Transfer Testing, ASCE 18-96, 345 E. 47th St, New York, NY

ASCE (2007) *Measurement of Oxygen Transfer in Clean Water.* ASCE 2-07, American Society of Civil Engineers, New York

Aymerich, I., Rieger, L., Sobhani, R., Rosso, D., & Corominas, L. (2015). The difference between energy consumption and energy cost: Modelling energy tariff structures for water resource recovery facilities. *water research*, *81*, 113-123.

Beler Baykal B. and Sekoulov I. (1993) Upgrading wastewater treatment plants using filters with biological activity. *Second Int. Spec. Conf. on Upgrading of Wastewater Treatment Plants*, Technische Universit/it Berlin, Germany.

BioWin. EnviroSim Associates Ltd. developers of BioWin dynamic wastewater treatment process modeling simulation and optimization software. Available at: http://www.envirosim.com/products/biowin

California Regional Water Quality Control Board (Tentative Order R4-2017-00XX). Available at: http://www.waterboards.ca.gov/losangeles/

Caniani, D., Esposito, G., Gori, R., & Mannina, G. (2015). Towards a new decision support system for design, management and operation of wastewater treatment plants for the reduction of greenhouse gases emission. *Water*, *7*(10), 5599-5616.

Corominas, L., Flores-Alsina, X., Snip, L., & Vanrolleghem, P. A. (2012). Comparison of different modeling approaches to better evaluate greenhouse gas emissions from whole wastewater treatment plants. *Biotechnology and bioengineering*, *109*(11), 2854-2863.

Haas, D. D., Foley, J., & Barr, K. (2008). Greenhouse gas inventories from WWTPs–the trade-off with nutrient removal. *Proceedings of the Water Environment Federation*, *2008*(6), 264-285.

Flores-Alsina, X., Arnell, M., Amerlinck, Y., Corominas, L., Gernaey, K. V., Guo, L., ... & Snip, L. (2014). Balancing effluent quality, economic cost and greenhouse gas emissions during the evaluation of (plant-wide) control/operational strategies in WWTPs. *Science of the Total Environment*, *466*, 616-624.

Flores-Alsina, X., Corominas, L., Snip, L., & Vanrolleghem, P. A. (2011). Including greenhouse gas emissions during benchmarking of wastewater treatment plant control strategies. *water research*, *45*(16), 4700-4710.

Foess, G., Meenahan, J., & Blough, D. (1977). Evaluation of In-Line and Side-Line Flow Equalization Systems. *Journal (Water Pollution Control Federation)*, 49(1), 120-130.

Foley, J., De Haas, D., Yuan, Z., & Lant, P. (2010). Nitrous oxide generation in full-scale biological nutrient removal wastewater treatment plants. *water research*, *44*(3), 831-844.

Gillot, S., and Heduit, A. (2008) Prediction of alpha factor values for fine pore aeration systems, Wat. Sci. Technol. 57(8) 1265-1270

Gori, R., Jiang, L. M., Sobhani, R., & Rosso, D. (2011). Effects of soluble and particulate substrate on the carbon and energy footprint of wastewater treatment processes. *water research*, *45*(18), 5858-5872.

Gori, R., Giaccherini, F., Jiang, L. M., Sobhani, R., & Rosso, D. (2013). Role of primary sedimentation on plant-wide energy recovery and carbon footprint. *Water Science and Technology*, *68*(4), 870-878.

Guo, L., Porro, J., Sharma, K. R., Amerlinck, Y., Benedetti, L., Nopens, I., ... & Vanrolleghem, P. A. (2012). Towards a benchmarking tool for minimizing wastewater utility greenhouse gas footprints. *Water Science and Technology*, *66*(11), 2483-2495.

Henze, M., Gujer, W., Mino, T., & Van Loosdrecht, M. C. M. (2000). *Activated sludge models ASM1, ASM2, ASM2d and ASM3*. IWA publishing.

Henze, M. (1987). Activated sludge model No. 1. *IAWPRC Scientific and technical Reports*, *1*.

Intergovernmental Panel on Climate Change (IPCC), 2006. Guidelines for National Greenhouse Gas Inventories. Intergovernmental panel on Climate Change. Available at: http://www.ipccnggip.iges.or.jp/public/2006gl/index.html.

Jiang, L.-M., Garrido-Baserba, M., Nolasco, D., Al-Omari, A., de Clippeleir, H., Murthy, S., Rosso, D. (2017) Modelling oxygen transfer using dynamic alpha factors, *Water research,* 124, 139-148.

Kaliman, A., Rosso, D., Leu, S.S.Y., Stenstrom, M.M.K., 2008. Fine-pore aeration diffusers: Accelerated membrane ageing studies. Water Res. 42, 467–475.

Kampschreur, M. J., Temmink, H., Kleerebezem, R., Jetten, M. S., & van Loosdrecht, M. C. (2009). Nitrous oxide emission during wastewater treatment. *Water research*, *43*(17), 4093-4103.

Karpinska, A. M., & Bridgeman, J. (2016). CFD-aided modelling of activated sludge systems–A critical review. *Water research*, *88*, 861-879.

Krampe, J., & Krauth, K. (2003). Oxygen transfer into activated sludge with high MLSS concentrations. *Water Science and Technology, 47*, 297-303.

Langergraber, G., Rieger, L., Winkler, S., Alex, J., Wiese, J., Owerdieck, C., ... & Maurer, M. (2004). A guideline for simulation studies of wastewater treatment plants. *Water Science and Technology*, *50*(7), 131-138.

Law, Y., Ye, L., Pan, Y., & Yuan, Z. (2012). Nitrous oxide emissions from wastewater treatment processes. *Phil. Trans. R. Soc. B*, *367*(1593), 1265-1277.

Leu, S. Y., Rosso, D., Larson, L. E., & Stenstrom, M. K. (2009). Real-time aeration efficiency monitoring in the activated sludge process and methods to reduce energy consumption and operating costs. *Water Environment Research*, *81*(12), 2471-2481.

Liao, B.Q., Allen, D.G., Droppo, I.G., Leppard, G.G., Liss, S.N., 2001. Surface properties of sludge and their role in bioflocculation and settleability. Water Res. 35, 339–350. doi:10.1016/S0043-1354(00)00277-3

Liu, Y., Fang, H.H.P., 2003. Influences of Extracellular Polymeric Substances (EPS) on Flocculation, Settling, and Dewatering of Activated Sludge. Crit. Rev. Environ. Sci. Technol. 33, 237–273. doi:10.1080/10643380390814479

Mannina, G., Cosenza, A., Gori, R., Garrido-Baserbac, M., Sobhani, R., & Rosso, D. (2016). Greenhouse Gas Emissions from Wastewater Treatment Plants on a Plantwide Scale: Sensitivity and Uncertainty Analysis. *Journal of Environmental Engineering*, *142*(6), 04016017.

Mannina, G., Ekama, G., Caniani, D., Cosenza, A., Esposito, G., Gori, R., ... & Olsson, G. (2016). Greenhouse gases from wastewater treatment—A review of modelling tools. *Science of the Total Environment*, *551*, 254-270.

Monteith, H. D., Sahely, H. R., MacLean, H. L., & Bagley, D. M. (2005). A rational procedure for estimation of greenhouse-gas emissions from municipal wastewater treatment plants. *Water Environment Research*, *77*(4), 390-403.

More, T.T., Yadav, J.S.S., Yan, S., Tyagi, R.D., Surampalli, R.Y., 2014. Extracellular polymeric substances of bacteria and their potential environmental applications. *J. Environ. Manage. 144*, 1–25.

Ni, B.-J., Fang, F., Xie, W.-M., Sun, M., Sheng, G.-P., Li, W.-H., Yu, H.-Q., 2009. Characterization of extracellular polymeric substances produced by mixed microorganisms in activated sludge with gel-permeating chromatography, excitation–emission matrix fluorescence spectroscopy measurement and kinetic modeling. *Water Res. 43*, 1350–1358.

Olsson, G. (2015). *Water and energy: threats and opportunities*. IWA publishing.

Olsson, G. (2012). ICA and me–a subjective review. *Water Research*, *46*(6), 1585-1624.

Palensky, P., & Dietrich, D. (2011). Demand side management: Demand response, intelligent energy systems, and smart loads. *IEEE transactions on industrial informatics*, *7*(3), 381-388.

Park, H. D., Lee, Y. H., Kim, H. B., Moon, J., Ahn, C. H., Kim, K. T., & Kang, M. S. (2010). Reduction of membrane fouling by simultaneous upward and downward air sparging in a pilot-scale submerged membrane bioreactor treating municipal wastewater. *Desalination*, *251*(1), 75-82.

Reardon, D.J., 1995. Turning down the power. *Civ. Eng. 65* (8), 54-56.

Redmon, D. T.; Boyle, W. C.; and Ewing, L. (1983). Oxygen Transfer Efficiency Measurements in Mixed Liquor using Off-gas Techniques. *J. Water Pollut. Control Fed., 55*, 1338–1347.

Rieger, L., Aymerich, I., Sobhani, R., Rosso, D., Schraa, O., & Corominas, L. (2015). Lower Energy Consumption but Higher Energy Bills? The Impact of Energy Tariffs on WRRF Operating Costs. In *Proceedings-Water Environment Association of Ontario Annual Conference*.

Rosso, D., Larson, L. E., & Stenstrom, M. K. (2008). Aeration of large-scale municipal wastewater treatment plants: state of the art. *Water Science and Technology*, *57*(7), 973-978.

Rosso, D., Stenstrom, M.K., 2007. Energy-saving benefits of denitrification. *Environ. Eng.*

Appl. Res. Pract. Environ. Eng. Appl. Res. Pract. 3.

Rosso, D.; Stenstrom, M. K. (2006a) Economic implications of fine pore diffuser aging. *Wat. Environ. Res., 78*, 810–815.

Rosso, D., & Stenstrom, M. K. (2006b). Surfactant effects on α-factors in aeration systems. *Water research*, *40*(7), 1397-1404.

Rosso, D., & Stenstrom, M. K. (2005). Comparative economic analysis of the impacts of mean cell retention time and denitrification on aeration systems. *Water research*, *39*(16), 3773-3780.

Rosso, D., Iranpour, R., & Stenstrom, M. K. (2005). Fifteen years of offgas transfer efficiency measurements on fine-pore aerators: key role of sludge age and normalized air flux. *Water Environment Research*, *77*(3), 266-273.

Sheng, G.-P., Yu, H.-Q., Li, X.-Y., 2010. Extracellular polymeric substances (EPS) of microbial aggregates in biological wastewater treatment systems: A review. *Biotechnol. Adv. 28*, 882–894.

Sobhani, R., Larson, L. E., & Rosso, D. (2013). Peak amplification of energy demand, energy cost, and carbon emission in water reclamation and purification processes during diurnal cycles. *Proceedings of the Water Environment Federation*, *2013*(3), 143-152.

Subramanian, B.S., Yan, S., Tyagi, R.D., Surampalli, R.Y., 2010. Extracellular polymeric substances (EPS) producing bacterial strains of municipal wastewater sludge: Isolation, molecular identification, EPS characterization and performance for sludge settling and dewatering. *Water Res. 44*, 2253–2266.

TOU-8 (2014) Southern California Edison (SCE), Schedule TOU-8, Time-of-use rates for large industrial customers.

Tomczak-Wandzel, R., Dereszewska, A., Cytawa, S., Medrzycka, K., Swarzewo, W.T.P., 2009. The effect of attractants on activated sludge process.

U.S. Environmental Protection Agency – USEPA (1989) *Fine Pore (Fine Bubble) Aeration Systems*, EPA/625/1-89/023; U.S. Environmental Protection Agency: Cincinnati, Ohio.

Water Environment Federation-WEF, 2009. Energy Conservation in Water and Wastewater Facilities (MOP 32). WEF Publishing, Alexandria, VA, USA.

Zhang, W., Peng, S., Xiao, P., He, J., Yang, P., Xu, S., Wang, D., 2015. Understanding the evolution of stratified extracellular polymeric substances in full-scale activated sludges in relation to dewaterability. *RSC Adv. 5*, 1282–1294.

Zhang, X., Li, X., Zhang, Q., Peng, Q., Zhang, W., Gao, F., 2014. New insight into the biological treatment by activated sludge: the role of adsorption process. Bioresour. Technol. 153,

160–4. doi:10.1016/j.biortech.2013.11.084

Zivin, J. S. G., Kotchen, M. J., & Mansur, E. T. (2014). Spatial and temporal heterogeneity of marginal emissions: Implications for electric cars and other electricity-shifting policies. *Journal of Economic Behavior & Organization*, *107*, 248-268.

APPENDIX A: NOMENCLATURE

a, Diffuser specific area [m^2]; $CO_{2,eq,}$ equivalent carbon emission [kgh^{-1}]; $CO_{2,i,}$ carbon emission intensity [kg/kWh]; $N_{D,}$ total diffuser number; $P_{b,}$ barometric pressure [psi]; $Q_{N,}$ normalized air flux [s^{-1}]; $R_{h,}$ relative humidity [-]; $T_{a,}$ ambient temperature [K]; $T_{d,}$ dew point temperature [K]; $T_{w,}$ water temperature [F]; z, diffuser submergence [m]

Greek letters

α, alpha factor, ratio of process-to clean-water mass transfer [-]; η, blower efficiency [-]; χ, plant characteristic number [s^{-2}]

Indices

a, refers to ambient; b, refers to barometric; d, refers to dew point; eq, refers to equivalent; h, refers to humidity; i, refers to intensity; in, refers to influent; N, refers to normalized; w, refers to water

Abbreviations

AFR, Air Flow Rate; AMEL, Average Monthly Effluent Limitation; ASM, Activated Sludge Model; ASP, Activated Sludge Process; AWEL, Average Weekly Effluent Limitation; BOD, Biological Oxygen Demand; COD, Chemical Oxygen Demand; DO, Dissolved Oxygen; DSM, Demand Side Management; EPS, Extracellular Polymeric Substances; ERCOT, Electric Reliability Council of Texas; ft, foot; GHG, Greenhouse Gas; HRT, Hydraulic Retention Time; I&C, Instrumentation & Control; IPCC, Intergovernmental Panel on Climate Change; IWA, International Water Association; m, meter; MCRT, Mean Cell Residence Time; MGD, Million Gallons per Day; MLE, Modified Ludzack-Ettinger; OTE, Oxygen Transfer Efficiency; RAS, Return Activated Sludge; RMSE, Root Mean Square Error; SCADA, Supervisory Control and Data Acquisition; SCE, Southern California Edison; SOTE, Standard Oxygen Transfer Efficiency; SWRCB, State Water Resources Control Board; TDH, Total Dynamic Head; TKN,

Total Kjeldahl Nitrogen; TOU, Time of Use; TSS, Total Suspended Solids; WAS, Waste Activated Sludge; WECC, Western Electricity Coordinating Council; WEF, Water Environment Federation; WRRF, Water Resources Recovery Facilities

APPENDIX B: SUPPLEMENTAL DATA

Table B.1 - Observed air discharge rates from the plant (kscfm)

HOUR	MON	TUE	WED	THU	FRI	MON	TUE	WED
	6/13/16	6/14/16	6/15/16	6/16/16	6/17/16	6/20/16	6/21/16	6/22/16
0:00	3.3	3.9	3.7	3.8	4.3	3.2	4.3	4.2
1:00	2.7	2.9	2.9	2.9	3.5	3.2	3.4	3.4
2:00	2.6	2.6	2.6	2.6	2.5	2.6	2.8	2.6
3:00	2.2	2.4	2.4	2.2	4.2	2.3	2.4	2.4
4:00	1.9	1.8	2.0	2.0	1.7	2.1	2.1	2.2
5:00	1.9	1.8	1.8	1.9	1.7	2.0	2.1	2.1
6:00	1.8	1.8	1.7	1.8	1.7	1.8	2.0	1.8
7:00	1.9	1.7	1.7	1.8	1.7	2.1	2.0	2.1
8:00	1.9	1.7	1.8	1.9	2.1	2.5	2.5	2.7
9:00	2.4	2.6	2.9	2.8	2.7	3.4	3.0	3.3
10:00	2.7	3.0	2.8	3.4	3.4	3.5	3.5	3.4
11:00	2.7	3.1	3.0	3.0	3.2	3.3	3.3	3.4
12:00	2.8	3.4	3.2	3.4	3.3	3.6	3.2	3.5
13:00	3.1	3.5	3.4	3.4	3.2	3.7	3.1	3.6
14:00	3.0	3.3	3.0	3.7	3.2	3.4	3.3	3.8
15:00	3.1	3.6	3.5	3.7	3.7	3.3	3.4	3.6
16:00	3.4	3.6	3.4	4.1	3.4	3.7	3.5	3.5
17:00	3.5	3.5	3.7	3.7	3.3	3.5	3.5	3.7
18:00	3.0	3.3	3.6	3.6	3.6	3.3	3.7	3.4
19:00	3.5	3.4	3.5	3.8	3.7	3.4	3.4	3.4
20:00	3.4	3.6	3.5	3.8	3.6	3.7	3.6	3.8
21:00	3.6	3.6	3.8	3.6	3.5	3.3	3.7	3.8
22:00	3.6	3.7	3.8	3.7	3.4	4.0	4.1	3.9
23:00	3.7	3.5	3.7	3.9	3.5	3.8	3.8	3.8

Table B.1 - Observed air discharge rates from the plant (kscfm)

HOUR	WED	THU	FRI	MON	TUE	WED	THU
	6/22/16	6/23/16	6/24/16	6/27/16	6/28/16	6/29/16	6/30/16
0:00	4.2	3.7	4.0	4.0	4.3	4.7	4.4
1:00	3.4	3.4	3.5	3.3	3.5	3.3	3.2
2:00	2.6	2.8	2.8	2.9	3.0	3.1	2.8
3:00	2.4	2.4	2.5	2.4	2.8	2.6	2.5
4:00	2.2	2.2	2.2	2.2	2.3	1.9	2.3
5:00	2.1	2.2	2.4	2.1	2.1	2.1	2.2
6:00	1.8	2.0	1.9	1.8	2.1	1.8	2.1
7:00	2.1	2.3	1.9	2.1	2.2	2.0	2.1
8:00	2.7	2.4	2.4	2.6	2.6	2.6	2.4
9:00	3.3	3.1	3.2	3.0	2.9	3.2	3.0
10:00	3.4	3.6	3.6	3.2	3.1	3.4	3.4
11:00	3.4	3.5	3.4	3.1	3.3	3.3	3.5
12:00	3.5	3.6	3.3	3.2	3.5	3.3	3.9
13:00	3.6	3.4	3.6	3.5	3.7	3.5	4.0
14:00	3.8	3.7	3.3	3.4	3.7	3.7	3.8
15:00	3.6	4.0	3.8	3.2	3.8	3.7	4.4
16:00	3.5	4.6	3.8	3.7	3.6	4.3	4.4
17:00	3.7	4.2	3.9	3.7	3.6	3.8	3.7
18:00	3.4	3.9	3.5	3.5	3.7	3.5	4.4
19:00	3.4	4.1	3.8	3.7	3.5	3.7	4.1
20:00	3.8	3.5	3.6	3.9	3.9	4.2	4.4
21:00	3.8	4.3	3.4	3.8	4.1	4.6	4.7
22:00	3.9	3.8	3.5	3.9	4.3	4.7	4.3
23:00	3.8	4.1	3.7	4.1	4.5	4.6	4.4

Table B.1 - Observed air discharge rates from the plant (kscfm)

HOUR	MON	TUE	WED	THU	FRI	MON	TUE
	7/11/16	7/12/16	7/13/16	7/14/16	7/15/16	7/18/16	7/19/16
0:00	3.3	3.9	3.7	4.0	4.2	3.8	4.6
1:00	3.1	3.2	3.2	3.7	3.3	3.6	3.5
2:00	2.4	2.6	2.5	2.8	2.9	2.9	3.1
3:00	2.1	2.2	2.2	3.0	2.7	2.5	2.7
4:00	1.9	2.1	2.0	2.6	2.3	2.4	2.3
5:00	2.0	2.0	1.9	2.4	2.3	2.4	2.1
6:00	1.7	1.8	1.9	2.2	2.1	2.2	2.0
7:00	1.8	1.8	1.9	2.3	2.3	2.2	2.0
8:00	2.4	2.5	2.2	2.8	2.5	2.4	2.4
9:00	2.7	2.8	3.0	3.4	2.8	2.9	2.9
10:00	2.9	2.8	3.1	3.6	3.4	3.4	3.2
11:00	2.9	2.8	3.2	3.9	3.3	3.4	3.1
12:00	3.4	3.0	3.7	3.9	3.3	3.7	3.5
13:00	3.8	3.3	3.4	4.0	3.6	3.8	3.7
14:00	3.9	3.0	3.2	3.7	3.5	3.8	3.6
15:00	3.7	3.3	3.6	4.2	3.7	4.0	3.9
16:00	3.5	3.8	4.0	3.9	3.9	3.9	4.3
17:00	3.5	3.5	3.8	4.0	3.5	4.2	3.8
18:00	3.4	3.5	3.6	3.6	3.5	3.9	3.9
19:00	3.5	3.6	3.7	4.1	3.6	3.8	3.9
20:00	3.7	3.8	4.0	4.2	3.5	3.8	3.6
21:00	3.8	3.6	3.9	4.2	3.8	3.8	3.9
22:00	3.7	3.8	3.8	4.1	3.6	3.8	4.4
23:00	4.3	3.6	3.8	4.0	3.6	4.6	4.5

Table B.1 - Observed air discharge rates from the plant (kscfm)

HOUR	WED	THU	FRI	MON	WED	THU	FRI
	7/20/16	7/21/16	7/22/16	7/25/16	7/27/16	7/28/16	7/29/16
0:00	4.6	4.6	4.1	3.8	4.3	4.5	4.5
1:00	4.7	3.8	3.6	3.4	3.6	3.5	3.5
2:00	2.8	2.8	2.8	2.7	3.0	2.7	2.8
3:00	2.5	2.5	2.5	2.4	2.6	2.4	2.5
4:00	2.3	2.5	2.4	2.3	2.5	2.4	2.4
5:00	2.2	2.1	2.1	2.3	2.4	2.0	2.0
6:00	1.9	2.1	1.8	1.9	2.0	1.9	2.0
7:00	1.8	2.2	2.0	1.9	1.9	1.9	2.1
8:00	2.2	2.3	2.5	2.4	2.6	2.4	2.6
9:00	2.7	3.1	2.8	3.0	2.8	2.8	3.0
10:00	3.1	3.2	3.1	3.0	3.3	3.3	3.2
11:00	3.3	3.3	3.5	3.3	3.3	3.1	3.1
12:00	3.8	3.5	3.6	3.5	3.5	3.3	3.4
13:00	3.8	3.8	3.5	3.6	3.7	3.8	3.4
14:00	3.8	3.5	3.5	3.6	3.7	4.0	3.5
15:00	3.8	3.8	3.7	3.7	3.9	4.2	3.5
16:00	3.6	4.4	3.7	3.9	4.1	4.2	3.8
17:00	3.6	4.5	3.7	4.1	4.0	3.6	3.7
18:00	3.7	3.6	3.5	3.6	3.9	3.8	3.4
19:00	3.8	3.7	3.9	3.9	3.9	4.1	3.6
20:00	4.1	3.7	3.9	3.9	4.5	4.1	3.7
21:00	4.5	4.0	3.8	3.7	4.6	4.4	3.9
22:00	4.5	3.9	3.7	4.1	4.1	4.2	3.6
23:00	4.6	4.4	3.7	4.5	4.3	4.4	3.9

Table B.2 - Observed ASP influent flow rates (MGD)

HOUR	WED	FRI	MON	TUE	WED	FRI
	6/1/16	6/3/16	6/6/16	6/7/16	6/8/16	6/10/16
0:00	3.5	3.6	3.6	3.6	3.6	3.6
1:00	2.4	2.8	2.5	2.8	2.7	2.7
2:00	1.9	1.9	1.8	1.9	1.9	2.1
3:00	1.7	1.5	1.5	1.6	1.5	1.7
4:00	1.2	1.2	1.2	1.1	1.1	1.4
5:00	1.2	1.0	1.1	1.1	1.1	1.1
6:00	1.0	0.9	0.9	1.0	1.0	1.0
7:00	1.3	1.3	1.5	1.3	1.3	1.4
8:00	3.3	3.2	3.0	3.2	2.8	2.6
9:00	3.1	3.5	3.2	3.4	3.6	3.4
10:00	3.6	3.6	2.8	3.1	3.7	3.7
11:00	2.9	3.1	3.6	3.5	3.6	3.6
12:00	2.7	3.7	3.5	3.7	3.6	3.6
13:00	3.4	3.5	3.6	2.2	3.7	3.6
14:00	3.2	3.2	3.3	3.0	3.2	3.2
15:00	3.5	3.6	3.7	3.7	3.5	3.6
16:00	3.4	3.6	3.6	3.4	3.2	3.6
17:00	3.5	3.6	3.1	3.3	3.3	3.7
18:00	3.5	3.3	3.1	3.3	3.0	3.6
19:00	3.1	3.6	3.4	3.0	3.4	3.6
20:00	3.5	3.6	3.5	2.6	3.4	3.5
21:00	3.5	3.6	3.7	3.7	3.6	3.6
22:00	3.5	3.6	3.6	3.6	3.6	3.7
23:00	3.5	3.6	3.6	3.6	3.4	3.2

Table B.2 - Observed ASP influent flow rates (MGD)

HOUR	MON	TUE	WED	THU	FRI	MON
	6/13/16	6/14/16	6/15/16	6/16/16	6/17/16	6/20/16
0:00	3.6	3.7	3.3	3.1	3.1	3.3
1:00	2.6	2.4	2.7	2.6	2.3	2.7
2:00	2.1	1.9	1.9	1.9	2.1	2.0
3:00	1.7	1.5	1.5	1.5	1.6	1.6
4:00	1.4	1.1	1.2	1.2	1.3	1.3
5:00	1.3	1.0	1.0	1.0	1.2	1.1
6:00	1.1	1.1	1.0	1.0	1.0	1.0
7:00	1.5	1.2	1.2	1.2	1.3	1.3
8:00	2.9	2.5	3.2	2.7	2.8	3.9
9:00	3.4	3.1	2.6	3.4	3.6	3.4
10:00	3.3	3.3	3.2	3.4	3.6	3.6
11:00	2.9	2.6	3.6	3.6	3.5	3.5
12:00	3.6	3.6	3.6	3.1	3.1	3.5
13:00	3.6	3.6	3.6	3.6	3.6	3.6
14:00	3.2	3.2	3.2	3.2	3.2	3.2
15:00	3.6	3.6	3.6	3.7	3.3	3.6
16:00	3.6	3.5	3.2	3.7	3.6	3.2
17:00	3.6	3.3	3.2	3.6	3.3	3.5
18:00	3.2	3.1	3.2	3.3	2.8	2.9
19:00	3.2	3.6	3.4	3.6	3.4	3.2
20:00	3.5	3.4	3.4	3.6	3.4	3.5
21:00	3.7	3.6	3.6	3.6	3.4	3.6
22:00	3.6	3.6	3.6	3.6	3.5	3.6
23:00	3.6	3.6	3.6	3.6	3.2	3.6

Table B.2 - Observed ASP influent flow rates (MGD)

HOUR	TUE	WED	THU	MON	TUE	WED	THU
	6/21/16	6/22/16	6/23/16	6/27/16	6/28/16	6/29/16	6/30/16
0:00	3.6	3.6	3.3	3.6	3.7	3.5	3.6
1:00	2.6	2.7	2.7	2.5	2.8	3.0	3.0
2:00	2.1	2.0	2.1	2.1	2.1	2.4	2.0
3:00	1.6	1.6	1.5	1.6	1.7	1.9	1.8
4:00	1.4	1.2	1.3	1.3	1.4	1.4	1.4
5:00	1.4	1.1	1.1	1.2	1.2	1.4	1.4
6:00	1.0	1.0	0.9	1.0	1.0	1.3	1.2
7:00	1.4	1.5	1.4	1.4	1.7	2.0	1.8
8:00	3.4	3.1	3.0	2.9	3.2	3.2	3.1
9:00	2.8	3.7	2.5	3.6	3.3	3.5	3.2
10:00	3.4	3.6	3.3	3.6	3.6	4.0	3.7
11:00	3.7	3.7	3.6	3.6	3.2	3.3	4.0
12:00	3.6	3.7	3.6	2.9	3.7	4.0	4.0
13:00	3.6	3.3	3.6	3.3	4.0	4.0	4.0
14:00	3.3	3.7	3.3	3.3	3.6	3.6	3.6
15:00	3.7	3.6	3.7	3.7	4.0	3.8	3.9
16:00	3.4	3.3	3.6	3.7	3.8	3.6	3.6
17:00	3.3	3.4	3.4	3.3	3.6	3.4	3.5
18:00	3.4	3.2	3.5	3.4	3.7	3.3	3.4
19:00	3.4	2.9	3.3	3.6	3.6	3.6	3.6
20:00	3.6	3.7	3.7	3.7	3.9	3.8	3.7
21:00	3.6	3.7	3.6	3.7	4.0	4.0	3.8
22:00	3.6	3.6	3.7	3.6	4.0	3.9	4.0
23:00	3.6	3.6	3.7	3.6	4.0	-	-

Table B.2 - Observed ASP influent flow rates (MGD)

HOUR	FRI	TUE	WED	THU	FRI	MON
	7/1/16	7/5/16	7/6/16	7/7/16	7/8/16	7/11/16
0:00	3.6	3.2	3.4	3.3	3.4	3.1
1:00	3.0	2.7	2.6	2.7	2.6	2.5
2:00	2.0	2.1	2.0	2.0	2.0	1.9
3:00	1.8	1.6	2.1	1.5	1.5	1.4
4:00	1.5	1.3	1.2	1.3	1.2	1.3
5:00	1.3	1.4	1.1	1.1	1.1	1.1
6:00	1.2	1.1	1.1	1.0	0.7	0.9
7:00	1.7	1.6	1.3	1.3	1.8	1.3
8:00	3.1	2.3	2.9	3.3	2.3	2.6
9:00	3.1	3.6	3.4	3.5	3.3	3.5
10:00	3.6	3.5	3.0	3.3	3.5	3.7
11:00	3.6	3.8	3.0	3.7	4.0	3.3
12:00	3.9	3.6	3.5	3.8	4.0	4.0
13:00	4.0	3.8	3.8	3.7	3.7	4.0
14:00	3.6	3.4	3.3	3.3	3.5	3.5
15:00	4.0	3.8	3.6	3.8	3.5	3.4
16:00	3.5	3.5	3.4	3.6	3.5	3.5
17:00	3.4	3.1	3.3	3.2	3.2	3.3
18:00	3.7	3.2	3.3	2.9	3.1	3.0
19:00	3.7	3.3	3.2	3.5	3.8	3.2
20:00	3.5	3.6	3.5	3.6	3.8	3.8
21:00	3.9	3.7	3.8	3.7	3.8	3.8
22:00	3.8	3.8	3.8	3.8	3.4	3.8
23:00	-	-	3.8	3.7	3.2	3.6

Table B.2 - Observed ASP influent flow rates (MGD)

HOUR	TUE	WED	THU	FRI	MON	TUE
	7/12/16	7/13/16	7/14/16	7/15/16	7/18/16	7/19/16
0:00	3.3	3.5	3.5	3.4	3.2	3.7
1:00	2.5	2.6	2.4	2.9	2.7	2.7
2:00	2.0	1.9	2.0	2.2	2.1	2.1
3:00	1.4	1.6	1.6	1.8	1.7	1.7
4:00	1.1	1.3	1.3	1.5	1.4	1.4
5:00	1.0	1.1	1.2	1.4	1.3	1.2
6:00	0.9	1.0	1.0	1.1	1.1	1.1
7:00	1.4	1.3	1.3	1.5	1.5	1.3
8:00	3.3	3.4	2.6	2.6	2.7	2.7
9:00	3.4	3.0	3.4	3.5	3.8	3.3
10:00	3.2	3.0	3.8	3.1	3.8	3.0
11:00	3.6	2.7	3.9	3.5	3.7	3.8
12:00	3.4	3.2	3.1	3.8	3.7	3.8
13:00	3.2	3.2	3.8	3.7	3.8	3.8
14:00	3.0	3.0	3.4	3.4	3.3	3.3
15:00	3.5	3.5	3.9	3.6	3.8	3.7
16:00	3.5	3.5	3.8	3.8	3.5	3.7
17:00	3.1	3.3	3.4	3.5	3.8	3.5
18:00	3.0	3.3	3.4	3.1	2.8	3.5
19:00	3.4	3.4	2.9	3.5	3.1	3.8
20:00	3.5	3.5	3.6	3.7	3.8	3.7
21:00	3.5	3.5	3.8	3.8	3.7	3.8
22:00	3.5	3.5	3.8	3.6	3.7	3.8
23:00	3.5	3.5	3.8	3.4	3.7	3.8

Table B.2 - Observed ASP influent flow rates (MGD)

HOUR	WED	THU	FRI	MON	WED	THU	FRI
	7/20/16	7/21/16	7/22/16	7/25/16	7/27/16	7/28/16	7/29/16
0:00	3.8	3.7	3.2	3.4	3.8	3.7	4.0
1:00	2.9	3.0	2.9	2.8	2.9	2.9	3.1
2:00	2.1	2.3	2.3	2.2	1.9	2.3	2.5
3:00	1.7	1.7	1.8	1.8	1.8	1.8	2.1
4:00	1.4	1.4	1.5	1.5	1.4	1.5	1.8
5:00	1.3	1.3	1.4	1.4	1.3	1.4	1.6
6:00	1.1	1.1	1.1	1.1	1.0	1.2	1.5
7:00	1.4	1.5	1.6	1.5	1.6	1.6	1.9
8:00	2.8	3.9	2.8	2.9	2.8	2.8	3.8
9:00	3.6	3.8	3.5	3.6	3.5	3.5	4.0
10:00	3.7	3.1	3.6	3.6	3.7	3.8	4.0
11:00	3.7	3.0	3.5	3.2	3.8	3.1	4.0
12:00	3.7	3.6	3.8	3.7	3.2	3.6	4.0
13:00	3.8	3.7	3.7	3.8	3.7	4.0	3.8
14:00	3.3	3.3	3.3	3.3	3.3	3.6	3.6
15:00	3.7	3.7	3.7	3.7	3.7	4.1	4.0
16:00	3.6	3.8	3.4	3.8	3.5	3.8	4.0
17:00	3.3	3.4	3.5	3.4	3.3	3.6	3.5
18:00	3.2	3.5	3.2	3.1	3.0	3.4	3.7
19:00	2.8	3.5	3.2	3.5	3.5	3.4	3.7
20:00	3.2	3.5	2.9	3.7	3.7	3.9	4.0
21:00	3.6	3.8	3.7	3.8	3.7	4.0	4.0
22:00	3.7	3.8	3.6	3.8	3.7	3.9	4.0
23:00	3.8	3.8	3.5	3.8	3.8	4.0	3.6

Table B.3 - ASP influent characteristics and observed DO (mgl^{-1})

HOUR	bCOD	NH3-N	O-N	TKN	DO[1]
0:00	216.5	30.7	7.7	38.3	2.0
1:00	208.6	30.9	7.7	38.6	1.9
2:00	218.4	31.1	7.8	38.8	1.8
3:00	223.7	32.2	8.1	40.2	1.8
4:00	217.5	32.0	8.0	40.0	2.0
5:00	220.2	31.1	7.8	38.9	2.4
6:00	220.6	30.9	7.7	38.6	2.6
7:00	222.8	32.1	8.0	40.2	2.8
8:00	232.5	34.7	8.7	43.4	2.6
9:00	273.0	36.5	9.1	45.6	2.2
10:00	277.6	38.6	9.7	48.2	1.3
11:00	270.2	40.2	10.1	50.3	1.8
12:00	247.2	38.5	9.6	48.1	1.8
13:00	222.2	37.1	9.3	46.4	1.8
14:00	217.0	36.1	9.0	45.1	1.8
15:00	220.0	34.4	8.6	43.0	1.8
16:00	218.8	33.7	8.4	42.1	1.8
17:00	221.9	32.6	8.2	40.8	2.0
18:00	229.3	31.2	7.8	39.0	1.8
19:00	236.7	31.4	7.9	39.3	1.7
20:00	229.0	32.2	8.1	40.3	1.9
21:00	228.3	30.7	7.7	38.4	1.8
22:00	228.6	29.6	7.4	37.1	1.7
23:00	227.4	29.7	7.4	37.1	1.8

1- Average DO in aerobic zones

Table B.4 - Temporal and spatial variations in CO_2 emission Intensity [$kgCO_{2,eq}(kWh)^{-1}$] (Zivin et al., 2014)

HOUR	WECC	ERCOT	EASTERN
0:00	0.38	0.46	0.63
1:00	0.38	0.49	0.66
2:00	0.38	0.50	0.67
3:00	0.38	0.51	0.67
4:00	0.36	0.51	0.67
5:00	0.35	0.49	0.65
6:00	0.32	0.45	0.62
7:00	0.30	0.43	0.57
8:00	0.31	0.43	0.55
9:00	0.35	0.43	0.56
10:00	0.39	0.42	0.57
11:00	0.40	0.42	0.58
12:00	0.40	0.41	0.58
13:00	0.39	0.42	0.57
14:00	0.38	0.42	0.55
15:00	0.37	0.42	0.54
16:00	0.36	0.42	0.54
17:00	0.36	0.41	0.54
18:00	0.36	0.41	0.54
19:00	0.36	0.41	0.54
20:00	0.37	0.40	0.54
21:00	0.36	0.40	0.54
22:00	0.37	0.41	0.56
23:00	0.37	0.43	0.59